SONNE-Berichte

NAPTRAM - Plastiktransportmechanismen, Senken und Interaktionen mit Biota im Nordatlantik

NAPTRAM - North Atlantic plastic transport mechanisms, sinks, and interactions with biota

Cruise No. SO279

Emden (Germany) – Emden (Germany)
04.12.2020 – 05.01.2021

Authors: Aaron Beck, with contributions from Erik Borchert, Louise Delaigue, Feifei Deng, Sonia Gueroun, Thea Hamm, Oliver Jacob, Mikael Kaandorp, Hashan Kokuhennadige, Elke Kossel, Sarah-Marie Kröger, Rebecka Molitor, André Mutzberg, Ulrike Panknin, Gabriella Pantó, Annalisa Sambolino, Rui Shen, Tristan Zimmermann

Chief Scientist: Aaron Beck

GEOMAR Helmholtz Centre for Ocean Research Kiel

2021

Table of Contents

1 Cruise Summary

1.1 Summary in English

The coastal and open oceans represent a major, but yet unconstrained, sink for plastics. It is likely that plastic-biota interactions are a key driver for the fragmentation, aggregation, and vertical transport of plastic litter from surface waters to sedimentary sinks. Cruise SO279 conducted sampling to address core questions of microplastic distribution in the open ocean water column, biota, and sediments. Seven stations were sampled between the outer Bay of Biscay and the primary working area south of the Azores. Additional samples were collected from surface waters along the cruise track to link European coastal and shelf waters with the open ocean gyre. Microplastic samples coupled with geochemical tracer analyses will build a mechanistic understanding of MP transport and its biological impact reaching from coastal seas to the central gyre water column and sinks at the seabed. Furthermore, floating plastics were sampled for microbial community and genetic analyses to investigate potential enzymatic degradation pathways. Cruise SO279 served as the third cruise of a number of connected research cruises to build an understanding of the transport pathways of plastic and microplastic debris in the North Atlantic from the input through rivers and air across coastal seas into the accumulation spots in the North Atlantic gyre and the vertical export to its sink at the seabed. The cruise was an international effort as part of the JPI Oceans project HOTMIC ("HOrizontal and vertical oceanic distribution, Transport, and impact of MICroplastics") and the BMBF funded project PLASTISEA ('Harvesting the marine Plastisphere for novel cleaning concepts'), and formed a joint effort of HOTMIC and PLASTISEA researchers from a range of countries and institutes.

1.2 Zusammenfassung

Die Küstengewässer und die offenen Ozeane sind wichtige, aber noch nicht begrenzte Senke für Kunststoffe. Es ist wahrscheinlich, dass die Wechselwirkungen zwischen Kunststoffen und Biota ein wesentlicher Faktor für die Fragmentierung, Aggregation und den vertikalen Transport von Plasticmüll aus den Oberflächengewässern in die Tiefseesendimente sind. Während der Ausfahrt SO279 wurden Proben genommen, um die wichtigsten Fragen zur Verteilung von Mikroplastik in der Wassersäule des offenen Ozeans, in Biota und Sedimenten zu klären. Sieben Stationen wurden zwischen dem äußeren Golf von Biskaya und dem Hauptarbeitsgebiet südlich der Azoren beprobt. Zusätzliche Proben wurden aus Oberflächengewässern entlang der Fahrtroute entnommen, um die europäischen Küsten- und Schelfgewässer mit dem offenen Ozeanwirbel zu verbinden. Mikroplastikproben in Verbindung mit geochemischen Tracer-Analysen werden ein mechanistisches Verständnis des MP-Transports und seiner biologischen Auswirkungen von den Küstenmeeren bis zur Wassersäule des zentralen Wirbel und den Senken am Meeresboden ermöglichen. Außerdem wurden schwimmende Plastikteile für mikrobielle Gemeinschaften und genetische Analysen beprobt, um mögliche enzymatische Abbauwege zu untersuchen. Die Fahrt SO279 war die dritte einer Reihe von zusammenhängenden Forschungsfahrten, die zum Ziel hatten, die Transportwege von Plastik- und Mikroplastikmüll im Nordatlantik vom Eintrag durch Flüsse und Luft über die Küstenmeere bis hin zu den Akkumulationsstellen im nordatlantischen Wirbel und dem vertikalen Export zu seiner Senke am Meeresboden zu verstehen. Die Fahrt war eine internationale Zusammenarbeit im Rahmen des JPI Oceans-Projekts HOTMIC ("HOrizontal and vertical oceanic distribution, Transport, and impact of MICroplastics") und des vom BMBF geförderten Projekts PLASTISEA ("Harvesting the marine Plastisphere for novel cleaning concepts") und bildete eine Zusammenarbeit von HOTMIC- und PLASTISEA-Forschern aus mehrere Ländern und Instituten.

2 Participants

2.1 Principal Investigators

Name	Institution
Achterberg, Eric, Prof. Dr.	GEOMAR
Beck, Aaron, Dr.	GEOMAR
Haeckel, Matthias, Dr.	GEOMAR
Hentschel-Humeida, Ute, Prof. Dr.	GEOMAR
Lenz, Mark, Dr.	GEOMAR

2.2 Scientific Party

Name	Discipline	Institution
Beck, Aaron	Fahrtleiter / Chief Scientist	GEOMAR
Borchert, Erik	Catamaran trawl and Multi-Net	GEOMAR
Delaigue, Louise	pH, nutrient, and carbon chemistry	NIOZ
Deng, Feifei	CTD and sediments	HZG
Fey, Vincent	CTD and in situ pumps	GEOMAR
Gueroun, Sonia	Catamaran trawl and Multi-Net	MARE
Hamisch, Stephan	CTD and in situ pumps	GEOMAR
Hamm, Thea	Catamaran trawl and Multi-Net	GEOMAR
Hoffmann, Jannes	Multi-core and box core	GEOMAR
Jacob, Oliver	CTD and sediments	IWC-TUM
Kaandorp, Mikael	Hyperspectral NIR plastics analysis	Utrecht
Kossel, Elke	Multi-core and box core	GEOMAR
Kröger, Sarah-Marie	Multi-core and box core	GEOMAR
Molitor, Rebecka	Catamaran trawl and Multi-Net	IMET - FZJ
Mutzberg, André	CTD and in situ pumps	GEOMAR
Panknin, Ulrike	Catamaran trawl and Multi-Net	GEOMAR
Pantó, Gabriella	Multi-core and box core	UGent
Reiner, Birgit	Data management and logistics support	GEOMAR
Sambolino, Annalisa	Catamaran trawl and Multi-Net	MARE
Schulz, Isabelle	Media and outreach coordination	GEOMAR
Shen, Rui	Per- and poly-fluorinated compounds	HZG
Zimmermann, Tristan	Underway microplastic sampling	HZG

2.3 Participating Institutions

GEOMAR	GEOMAR Helmholtz Zentrum für Ozeanforschung Kiel
IWC - TUM	Institute of Hydrochemistry (IWC), Technical University of Munich (TUM)
IMET - FZJ	Molekulare Enzymtechnologie (IMET), Heinrich Heine Universität Düsseldorf, Forschungszentrum Juelich GmbH (FZJ)
UGent	Ghent University
MARE	Marine and Environmental Sciences Centre (MARE), Agência Regional para o Desenvolvimento da Investigação Tecnologia e Inovação (ARDITI)
HZG	Helmholtz-Zentrum Geesthacht – Zentrum für Material- und Küstenforschung
NIOZ	Royal Netherlands Institute for Sea Research
Utrecht	Utrecht University

3 Research Program

3.1 Description of the Work Area

The NAPTRAM cruise supports the JPI Oceans project HOTMIC, which examines the plastic transport pathway between sources at Europe's west coast into the North Atlantic gyre. Some 20% of the global inventory of floating plastic debris is accumulated in the North Atlantic (Cózar et al., 2014; Eriksen et al., 2014). Most of this material is concentrated in the inner accumulation zone of the North Atlantic subtropical gyre (the North Atlantic "garbage patch"), between the Azores and Bermuda (Fig. 3.1; Cózar et al., 2014). Plastic inventories averaged 400 g km^{-2} within the inner accumulation zone, with maxima as high as 2500 g km^{-2} (Cózar et al., 2014). For the same sea area Eriksen et al. (2014), reported plastic particle densities of up to 10^6 km^{-2}. Plastic particles within the North Atlantic gyre comprise a wide range of compositions and sizes, including nanoplastics (ter Halle et al., 2017), and small size particles may comprise the major mass fraction in the region (Poulain et al., 2019). Indeed, a study of small microplastics (MP) (32–651 μm) in the North Atlantic water column found a combined mass of 11.6 – 21.1 million tons for polyethylene, polypropylene, and polystyrene suspended in the top 200 m alone (Pabortsava and Lampitt, 2020). It is not well-known how MP are transported into the North Atlantic gyre, but eddies may be an important mechanism (Brach et al., 2018).

Around the SO289 study region, the Azores, Madeira, and Ireland act as anticipated source regions or intermediates for transport to the North Atlantic gyre. Coastal zones around and between the Azores archipelago and Madeira are extensively contaminated with plastic debris (Pieper et al., 2015; Pieper et al., 2016; Chambault et al., 2018). Due to oceanographic circulation structures, the Azores and Madeira act as a retention zone for plastic debris from Europe (Chambault et al., 2018), and the interface between continental sources and the open ocean accumulation zone. Similar plastic debris is present in Ireland coastal and continental shelf waters (Lusher et al., 2014; Martin et al., 2017). Ireland is positioned at the Gulf Stream eastern divergence, and provides the link between southward transport into the North Atlantic gyre. The northern branch carries debris toward high latitudes.

3.2 Aims of the Cruise

3.2.1 Cruise Objectives

NAPTRAM is part of connected research cruises to build an understanding of the transport pathways of plastic and microplastic debris in the North Atlantic, from the input through rivers and air across coastal seas into the accumulation spots in the North Atlantic gyre and the vertical export to its final sink at the seabed.

NAPTRAM builds on a preliminary cruise to the study region (RV Poseidon, POS536; Aug-Sep 2019), expanding its smaller study area and extending into deeper waters. NAPTRAM also complements RV Alkor cruise AL534/2 (March 2020) that focused on microplastic inputs from rivers and estuaries to coastal waters.

Specific objectives of NAPTRAM:

- Assessing the abundance, composition, and size distribution of MP particles at the sea surface from European coastal waters to the open North Atlantic
- Assessing the horizontal, long-distance transport of buoyant MP, including the role of eddy-facilitated transport
- Assessing the abundance, composition, and size distribution of MP particles in the water column using *in situ* pumps

- Assessing the abundance, composition, and size distribution of MP particles in the water column and in pelagic meso- and macrofaunal organisms using multi-net and catamaran trawls
- Measuring the depth distribution of additive compounds that commonly leach from plastic materials in the water column
- Assessing the vertical flux of MP from sea surface to seafloor with naturally-occurring radionuclide tracers
- Assessing the abundance, composition, and size distribution of MP particles accumulating in seafloor sediments, and assessing MP burial rates due to bioturbation
- Assessing ingestion, transfer, and alteration of MP particles across various trophic levels from invertebrates to fish in water column and sediments
- Assessing the abundance, composition, and size distribution of MP particles in benthic epi- and infauna organisms
- Identifying the abundance and composition of bacterial biofilms and eukaryotic biofoulers on plastic particles from the sea surface, water column, and seafloor
- Testing methodologies for controlling MP contamination during sample collection, and comparing analytical methods for determination of MP in environmental samples over the entire size range from <10 µm to 5 mm

3.2.2 Background

Currently, 5 - 13 MT (mega tons, 10^6 tons) of plastic debris are believed to enter the oceans every year (Jambeck et al., 2015), but only about 0.27 - 1.00 MT have been observed in the surface ocean (Eriksen et al., 2014; Lebreton et al., 2018). This discrepancy has been explained by various processes, for instance by the fact that 40% of the introduced plastic debris has negative buoyancy and sinks to the seafloor soon after release. A further, much smaller part with positive buoyancy is deposited along the coastlines, while the remaining material is assumed to reach the open ocean where it fragments into particles too small to be recognized by monitoring and/or gets transferred by vertical transport from the sea surface to deeper water layers and finally to the seafloor. This vertical pathway presumably constitutes the largest sink for plastic debris on the planet. However, no observational data exist on the export of this material to the deep sea and the mechanisms facilitating this transport, including biota-plastics interactions.

Consequently, no quantitative models exist that could help to assess vertical transport rates in the oceanic environment. Furthermore, little knowledge exists on the trophic transfer of plastic debris in open ocean food webs and on the environmental impact it may have on deep sea ecosystems. In summary, we are currently unaware of the ultimate fate of the largest part of the marine plastic debris and of the effects it may have on the world’s largest ecosystem.

The targeted working area for the research cruise is located within the inner accumulation zone of the North Atlantic garbage patch (Fig. 3.1), where debris loads of up to 2500 g per km^2 have been documented at the sea surface (Cózar et al., 2014). On the basis of these data, a permanent and substantial vertical transport of plastic debris from the surface to the seafloor can be expected.

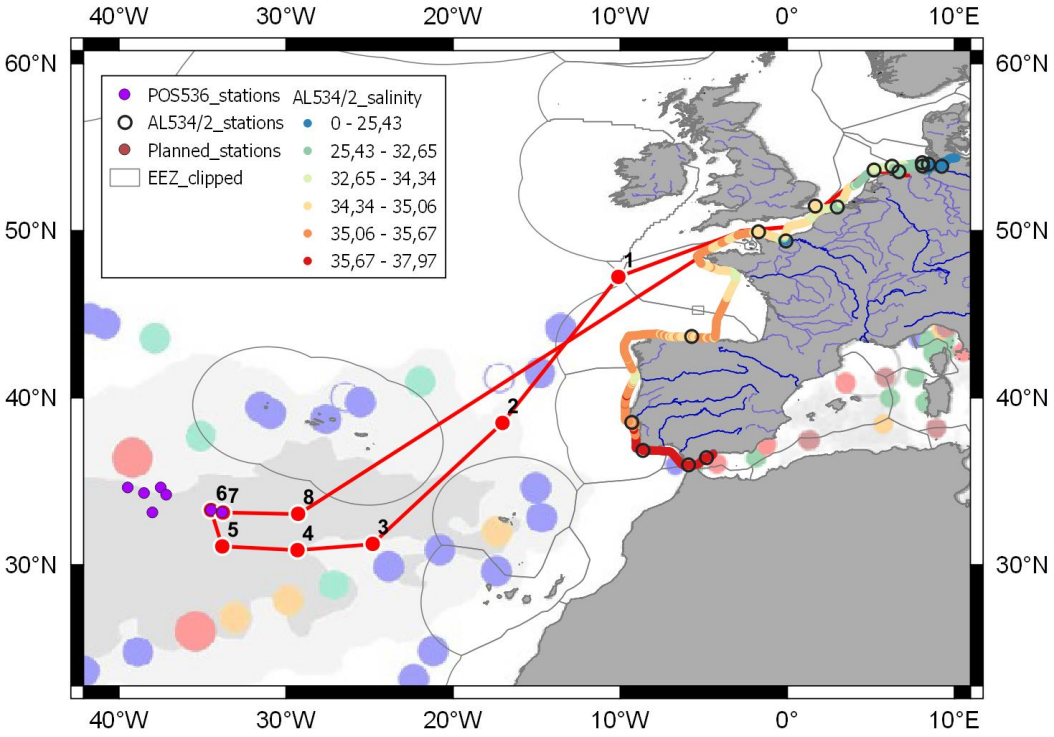

Figure 3.1. Map showing the location of the working area within the inner accumulation zone of the North Atlantic garbage patch. Translucent red dots mark areas where plastic surface loads of up to 2500 g per km^2 were measured (Cózar et al., 2014). Original planned stations and cruise track are indicated by the red dots and line, respectively. The purple dots indicate stations occupied during supporting cruise POS536, and black circles indicate stations sampled during supporting cruise AL534/2. The multicolored line shows surface water salinity in European coastal seas during AL534/2.

SO279 builds on two preliminary cruises (RV Poseidon POS536; Aug-Sep 2019), greatly extending the much smaller study area of POS536, and complementing another cruise (RV Alkor AL534/2; March 2020) that focused on microplastic inputs from rivers and estuaries to coastal waters (Fig. 3.1).

Most of the plastic that is produced is less dense than seawater (Andrady, 2011), and about 60% of the positively buoyant plastic debris that enters the oceans from land is likely transported offshore by surface currents and winds (Maximenko et al., 2012; Lebreton et al., 2012). Floating plastic debris therefore tends to accumulate within oceanic gyres and restricted coastal waters (Lebreton et al., 2012). During the time the debris remains at sea, large plastics items gradually fragment into smaller pieces – so called microplastics (MP; plastic particles <5 mm) – under the combined effects of temperature, UV radiation, and actions by waves and organisms (Andrady, 2011).

Long distance transport of MP from coastal sources to the open ocean is poorly understood, in part, because little is known regarding transport mechanisms from the coast to accumulation areas in the centre of subtropical gyres. Due to potential vorticity constraints, coastal waters have a tendency to spread along the coast, making offshore transport unlikely to occur. Mesoscale eddies which have diameters between 50 and 300 km are frequently generated at eastern boundaries of the oceans (Chelton et al., 2011; Schütte et al., 2016), and may provide an effective mechanism for shore-normal transport. Due to their non-linear characteristics, these eddies trap coastal water inside their core and carry it offshore into the interior ocean (Thomsen et al., 2016). The trapped coastal water masses and MP loads are released only when the eddies decay, which may take up to 5 years after generation and occurs thousands of km west of their generation site (Chelton et al.,

2011). Increased concentrations of MP have been found in anti-cyclonic mesoscale eddies in the North Atlantic subtropical gyre (Brach et al., 2018).

Given current estimates of plastic input to the ocean, at least 1.71 MT should reach the gyres in the North Atlantic, North Pacific, South Atlantic, South Pacific and Indian Oceans per year (Eriksen et al., 2014). Despite these theoretical reflections, it is still not known how much plastic debris actually floats at the ocean surface, or what mechanisms control plastic transport and fate from land to the open ocean. Estimates based on empirical data from field observations suggest 0.27 MT (Eriksen et al., 2014), but more recent measurements in the North Pacific garbage patch found that this number may still underestimate the total amount of plastic debris floating at the sea surface worldwide (Lebreton et al., 2018). However, Lebreton et al. (2018) also concluded that there remains a major discrepancy between the amount of buoyant plastic that enters the oceans every year (i.e., millions of tons) and the amount that can be observed at the ocean surface (i.e., hundred thousands of tons). Furthermore, data from time series revealed no significant increase in plastic debris concentrations in the surface ocean since the 1980s (Law et al., 2010; Law et al., 2014).

This prompts a fundamental question: what has become of the missing plastic? Several, mutually non-exclusive mechanisms have been proposed to explain the apparent loss of plastic debris from surface waters. First, a part of the material could constantly be transferred into the ocean interior by biota-plastic interactions, namely ingestion by invertebrates and vertebrates with subsequent formation of sinking fecal pellets, and colonization by bacteria, protozoans and metazoans which decreases buoyancy. Another part may be fragmented into pieces too small to be captured by current monitoring schemes (Poulain et al., 2019), and/or it could be deposited along the shores of islands or the continents (Andrady, 2011). Furthermore, it is conceivable that MP coagulate with suspended biogenic particles such as phytoplankton cells (Zhao et al., 2017; Michels et al., 2018), increasing particle density of otherwise buoyant MP and accelerating removal by sinking (Galloway et al., 2017). Recent findings also indicate that gelatinous zooplankton could play a significant role in capturing and sinking marine particles including MP through the water column (Katija et al., 2017; Macali et al., 2018), since the mucus that they release during reproduction, defense, or as a response to stress is highly efficient at trapping micro- and nano-sized particles (Patwa et al., 2015). While all of these processes are possible explanations, quantitative data on these mechanisms and their relative contribution to plastic debris loss from ocean surface waters do not exist.

The North Atlantic is estimated to contain approximately 20% of the global amount of floating plastic debris (Cózar et al., 2014; Eriksen et al., 2014). Most of this material is concentrated in an area that Cózar et al. (2014) described as the inner accumulation zone of the North Atlantic subtropical gyre, and which spans from the Azores to Bermuda (Fig. 3.1). Substantially smaller amounts are localized in what the authors identified as the outer accumulation zone and the non-accumulation areas (Cózar et al., 2014). Plastic inventories averaged 400 g km^{-2} within the inner accumulation zone, with maxima as high as 2500 g km^{-2} (Cózar et al., 2014). For the same sea area Eriksen et al. (2014), who did not quantify masses, reported plastic particle densities of up to 10^6 km^{-2}. Plastic particles within the North Atlantic gyre have a wide range of compositions and sizes, including nanoplastics (ter Halle et al., 2017), and small size particles may comprise the major mass fraction in the region (Poulain et al., 2019).

Most of the available data on the abundance and composition of floating plastic debris have been collected by sampling with sea surface trawls developed for the sampling of neuston (e.g., Manta trawl). These devices usually have a small aperture size (0.5 -1 m width, 0.15 – 1 m depth) and can therefore cover only small areas and are restricted to the uppermost water column. Very few

studies have quantified plastic debris at different water depths, which is a major knowledge gap in efforts to monitor and map MP distributions in the ocean. For example, Lattin et al. (2004) sampled near-shore waters in Santa Monica Bay, California, at the surface, 5 m depth, and 30 m depth, and found highest MP (355 - 4750 µm) concentrations in deep waters. Bagaev et al. (2017) analyzed Baltic Sea water samples taken from various water depths and found MP (200 – 3000 µm) concentrations, especially those of fibers, to be 3-5 times higher in near-surface and near-bottom waters than in intermediate layers. Reisser et al. (2015) used a multi-level trawl to sample the uppermost 5 m water column in the North Atlantic subtropical gyre and found highest MP (500 – 5500 µm) concentrations at the sea surface. However, data about the abundance of plastic debris in the open ocean water column between the surface and the seafloor, in particular from beneath known accumulation zones, are missing.

A few studies have investigated the abundance of plastic debris and MP in coastal sediments (e.g., Van Cauwenberghe et al., 2015a), but data from the deep sea (water depths greater than 1000 m) are even scarcer. The lack of information on MP in deep-sea sediments prevents assessment of MP effects on sensitive deep-sea ecosystems, and evaluation of this potential sink for land-sourced plastic debris. Bergmann et al. (2017) analyzed nine sediment samples from water depths between 2340 and 5570 m near Svalbard, Spitzbergen, and found MP (11 – 1000 µm) concentrations between 42 and 6595 particles per kg of dry sediment, most of which were <25 µm in size. Van Cauwenberghe et al. (2013) inspected 11 sediment cores from water depths between 1200 and 4900 m in the North Atlantic, South Atlantic, and Mediterranean Sea, and identified at least one plastic particle in each of these cores. Furthermore, there is increasing evidence of potential transport of microplastics to deeper layers in soft marine sediments by means of bioturbation (Nakki et al., 2017), although field estimates are lacking. Collectively, this suggests that the deep sea is a sink for plastic debris and MP, although the magnitude of this sink and the processes that control it are very poorly constrained. Indeed, models of MP transport and fate in the ocean generally omit vertical fluxes due to sinking or ingestion because there is insufficient data on these vertical transport processes (van Sebille et al., 2015).

3.3 Agenda of the Cruise

The cruise focused on sample collection within the accumulation zone of the North Atlantic gyre. Because of the COVID situation, the cruise departed from and returned to Emden, Germany, which meant nearly a week of transit at the start and end of the cruise. No sample collection was possible within national EEZs during the transits.

The sample collection agenda was identical for all stations. Deployments of net trawls (Catamaran Neuston, Bongo, Multi-net) constituted core activities during SO279 in order to map plastic pollution at the sea surface and throughout the water column. When time allowed, additional catamaran samples were collected between the primary stations. Sediment coring was conducted with a box corer (BC) after unsuccessful attempts with the multiple corer (MUC). Sediment subsamples from the BC were taken for microplastic analyses of the sediment and sediment-dwelling fauna. At each station about 1500 L of water were filtered at 5 different depths using in situ pumps. Vertical CTD profiles complemented the work to collect small-volume water samples and relevant oceanographic data for the investigation of the particle export. Observations of macrolitter on the seafloor were made with the ship's OFOS system.

In addition, water and particle samples were collected along the cruise track from the ship's underway seawater supply, a pump system deployed in the moonpool, and a metal-clean towfish deployed in surface waters. Visual litter surveys were conducted during the few periods when seas were calm enough for reliable observations.

Taken together, the SO279 sampling plan provides a comprehensive investigation of plastic pollution from the surface ocean, through the water column, and into the deep ocean sediments. Station locations focused primarily on the accumulation zone south of the Azores, but intermediate stations on the transit to the primary working area provide a linkage between the continental source of plastic debris and the open ocean accumulation zone.

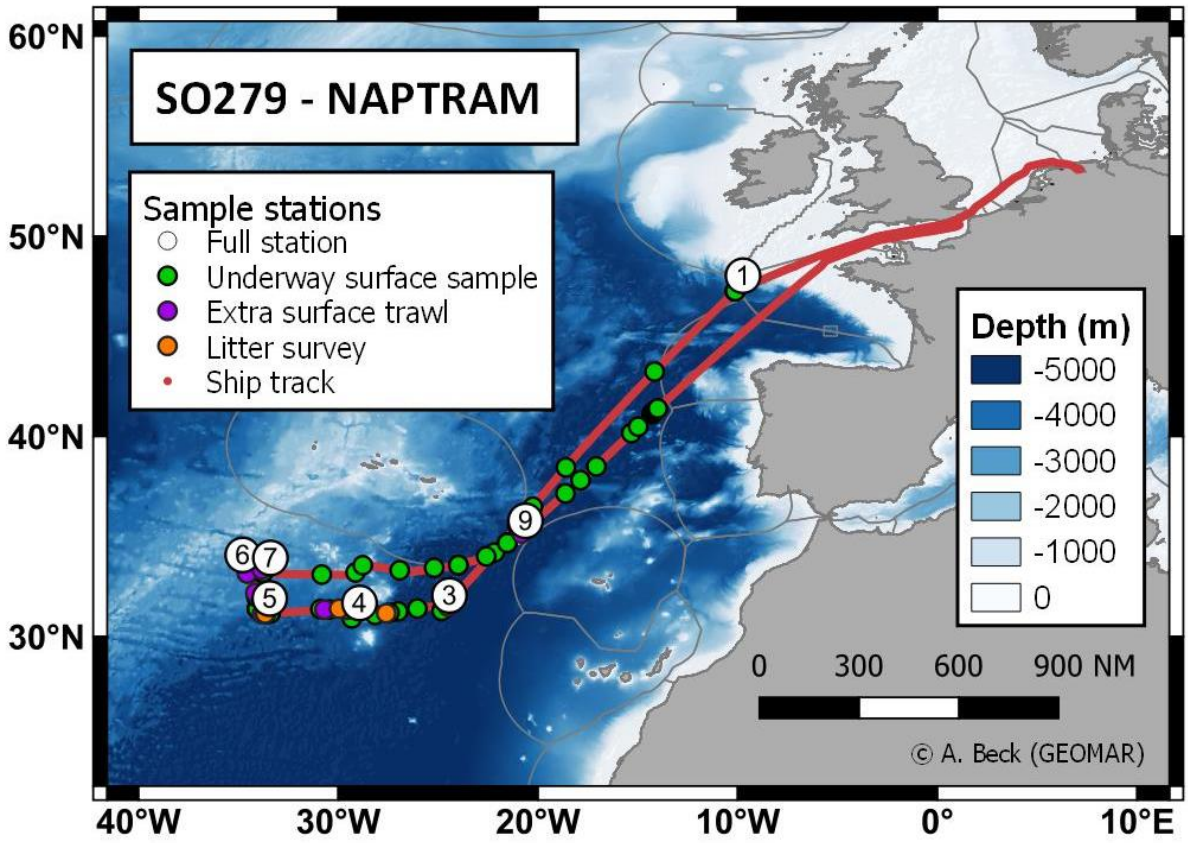

Figure 3.2. Track chart of R/V SONNE cruise SO279. Primary sampling stations and additional sampling locations are indicated. Bathymetry from GEBCO 2019.

4 Narrative of the Cruise

On Friday, 04 December 2020, RV SONNE set sail from port in Emden, Germany, heading for the plastic accumulation zone in the North Atlantic gyre south of the Azores. The scientists and crew spent four lonely days in individual quarantine in Leer before boarding the ship, the monotony of isolation broken only by emails, phone calls, and two early-morning visits from COVID testing professionals. It was a relief when everyone tested negative both times, and we were finally able to board the ship on 03 December.

Most of our equipment was loaded onto SONNE by the ship's crew on 01 December, while we were in quarantine, so we were able on 03 December to immediately begin unloading the shipping containers and unpacking equipment. After a slight delay waiting for delivery of some mis-directed equipment pallets, RV SONNE left dock on 04 December under assistance from a tugboat and entered the North Sea through the lock at Emden. We had smooth sailing over the next days along the Dutch and Belgian coastline, past the cliffs at Dover, and through the Bay of Biscay.

We reached the first station of SO279 outside of national EEZ borders on 08 December in 3-4 m swell and winds above 8 Beaufort. Nonetheless, the CTD rosette was deployed at 8 a.m., approached the seafloor at 4400 m, and returned with samples from throughout the water column. Five in situ pumps were deployed next on a single line down to 300 m depth. The pumps each collected particles from about 1500 L of water before being retrieved.

The first attempts to collect sediments with the multi-core and box core were unsuccessful, so we switched to towing the multi-net while it was still dark. Net operations were usually scheduled at night to capture zooplankton that migrate vertically. The multi-net has nine nets that can be opened and closed remotely, and it collects samples between the surface and 3000 m depth. Weather conditions were too rough to deploy the surface catamaran trawl.

Net operations finished around daybreak, and two subsequent attempts to collect sediment box cores were both successful. The sediment processing team was occupied for the rest of the day collecting sub-cores and surface samples of the sticky carbonate mud. Sediments and porewater will be processed back in home laboratories for microplastic distribution, various geochemical parameters, and benthic biota. No plastic debris was observed in the samples at this first station.

After the station was successfully completed in the afternoon of 09 December, SONNE continued transiting southward. Weather conditions steadily worsened, with swell above 4 m and winds around 10 Bft. We decided to postpone the second planned station and travel directly to our primary working area south of the Azores. A high pressure system in that region promised much better weather, and we hoped to take advantage of the good conditions to complete as much work as possible.

We continued transiting southward on 10 and 11 December with little change in the weather conditions. On 12 December, we awoke to the relative calm of 2-3 m waves and 6-7 Bft winds and were able to deploy the trace-metal clean towfish. The towfish is a stainless-steel torpedo designed to hold clean tubing so that the inlet samples only water untouched by the ship's hull. The towfish travels alongside the ship while we transit for continuous collection of uncontaminated water.

We reached our primary working area south of the Azores in the afternoon of 13 December. The weather was better than we hoped, with 2-4 m swell arriving from storms farther north, but low winds and sunny skies. Favorable conditions meant we could begin Station 3 and deploy the catamaran trawl to sample particles floating at the sea surface. Along with seaweed, shrimp, crabs, and small fish, the first tows returned an enormous number of plastic fragments.

Nearly double cable length is required to operate the multi-net at 3000 m depth as planned. To reach these depths, the SONNE crew switched the ca. 6000 m winch cable for an 8000 m cable. With the help of the ship's scientific-technical support personnel (WTD), we unfortunately learned that the resistivity of the longer cable was too much for the net powering unit. The crew then went through the laborious process of switching back to the shorter cable. The following multi-net deployment would be the first of many unsuccessful attempts, as the equipment was apparently too light and unstable to prevent turning at depth.

We postponed further multi-net tests and continued with water column and sediment sampling through 14 December. Station 3 was our deepest, at 5500 m, and most of our time on station was spent waiting for sampling devices to reach the distant seafloor and return to the surface. Nevertheless, the remaining sampling went smoothly, and we did a first video observation of the seafloor with the SONNE's OFOS (Ocean Floor Observatory System). We saw mostly featureless mud, but occasional red shrimp, purple fish, and sea cucumbers.

After the OFOS profile finished on 15 December, SONNE transited to Station 4. We arrived on 16 December at 4:00 in the morning and immediately began our sampling program. The box cores returned with rather strange sediments—fine grained carbonates that behaved somewhat like a non-Newtonian fluid. The sediment was soft when gently pressed or shaken, but much harder when struck suddenly.

Sampling continued into 17 December, with more multi-net testing. The still unsuccessful multi-net was replaced with a Bongo net to collect particles from the water column down to a depth of 300 m. We then conducted our second OFOS dive, which was similar to the first dive except for a piece of rope or fishing net entangled in Sargassum seaweed. We frequently saw clumps of apparently decaying Sargassum on the seafloor, but this was our first piece of deep-sea litter.

On 18 December, we transited to Station 5, filling two tanks with about 1500 L of clean water from the towfish while traveling. We arrived on station around 11:00, and completed the full program, again relying on bongo nets for sampling zooplankton and suspended particulates. While on station, we also observed large rafts of Sargassum at the sea surface. The floating seaweed aggregates along wind-driven lines, stretching as far as the eye can see. Floating plastic litter accumulates with the Sargassum, and within one patch we saw large pieces of plastic sheets, crates, buckets, bottle caps, and rope. We finished Station 5 on 19 December. The OFOS dive revealed several pieces of macro-litter on the seafloor, including a plastic bag in apparently quite good condition.

Sampling activities started at Station 6 before dawn on 20 December. We finished the station around 8:00 on 21 December, and SONNE immediately traveled to station 7. These stations were separated by only about 50 nmi, but they were sampled in September 2019 during cruise POS536 on RV POSEIDON, and the current cruise will provide a valuable comparison. Stations 6 and 7 were also located over the mid-Atlantic Ridge, a deep-sea mountain range several kilometers high. These were our shallowest stations, at only about 3000 m deep, so the sampling went relatively quickly.

The OFOS deployments at stations 6 and 7 were especially successful, as we saw a variety of plastic debris on the seafloor. OFOS provides valuable information about a wider area of seafloor. The box cores sampled an area of approximately 50 x 50 cm, and the sparse distribution of anthropogenic debris, macrofauna, and Sargassum deposits make it unlikely that they would have

been captured in the cores. The plastic objects we saw ranged in size from a few cm to nearly a meter long and were generally not very overgrown or biofouled.

Sampling activities at Station 7 continued into 22 December and finished in the evening. Unfortunately, a low-pressure system developed over the working area, and the weather began to worsen. High winds and waves forced us to cancel the next few catamaran net deployments, and Station 8 was also not possible. From 23 December to 25 December, SONNE transited slowly eastward against 4-5 m waves. We monitored conditions throughout the North Atlantic, and hoped to add a final station during a brief calm period forecast for the coming days between two major storm systems.

The weather improved noticeably during the evening of 26 December and we arrived at an improvised station between the Azores and Madeira around 6:00 on 27 December. We completed this last full station without any complications in the afternoon of 28 December, and began the long transit back to Emden. RV SONNE transited along a stormy Iberian coast on 29, 30, and 31 December.

We passed through the English Channel from 01 to 03 January. RV SONNE arrived in port in Emden in the afternoon of 04 January, and the scientists disembarked in the morning of 05 January 2021.

5 Preliminary Results

5.1 Net trawls and sample handling

5.1.1 Neuston net trawls

(Thea Anna Hamm[1], Ulrike Christiane Panknin[1], Rebecka Molitor[2], and Erik Borchert[1])

[1] GEOMAR

[2] IMET-FZJ

5.1.1.1 Background and Objectives

Microplastics (> 300 µm) floating at the sea surface within the working area were sampled with a neuston catamaran trawl. The collected material was screened for plastic debris in different size classes, large microplastic pieces (>0.2 mm) were sorted out and preserved for later microbiome analysis or incubated in seawater for enrichment cultures, smaller visible microplastic pieces were counted for abundance estimates and the biological material was preserved for later biodiversity analysis. The large microplastic pieces will be subjected to FTIR analysis at TUTECH GmbH, Hamburg for polymer identification.

The microbiome analysis of the biofilms attached to non-native polymers will give insights into colonization patterns and potential biodegradation potential of these communities, this work will contribute to the Plastisea project (funding reference number 031B0867A). It was shown that some bacteria and fungi are able to produce enzymes/biocatalysts that are able to degrade synthetic polymers. Nonetheless to date only a handful of enzymes that can degrade PET and PU are known and for most other man-made polymers no enzymes have been found. Exploiting environmental sources, such as bacterial enzymes, will be a crucial step in developing strategies for plastic pollution reduction.

Microplastic abundance estimates and biodiversity analysis of eukaryotic organisms will be performed within the framework of the HOTMIC project (BMBF project number 03F0851A) and will supplement data collected on previous cruises (POS536, ALK534-2) and thus generate more up to date distribution data for the Atlantic Ocean.

5.1.1.2 Methods

A neuston catamaran outfitted with a microplastic trawl net (mesh size 300 µm, mouth opening 70 cm x 40 cm, Fig. A2-1) was used to collect microplastics at the sea surface. The net opening was equipped with a flowmeter to measure the volume of water that was filtered by the net during one trawl, a representative sample is shown in Fig A2-2. The catamaran was towed starboard of the ship, with the current wind direction and outside of the ships wake at 3 knots for 20 minutes. If sampling was conducted inside a very dense patch of floating *Sargassum* sp. (Fig. A2-3), trawl time was reduced to minimize the amount debris collected outside of the codend and to reduce the risk of getting the flowmeter entangled in the algal material. The collected samples were then further dissected and large microplastic pieces (>0.2mm) were preserved in RNAlater© (SIGMA Life Sciences) and frozen at -20°C or put in filtered seawater at 4°C for subsequent enrichment cultures or fixed with 4% formaldehyde for microscopic biofilm analysis. Small visible microplastic pieces were sorted out and documented (Fig. A2-4). Furthermore, all biological material was preserved in 4% formaldehyde for later biodiversity analysis.

5.1.1.3 Preliminary results

During the cruise SO279, 27 neuston catamaran deployments were realized at six out of seven stations and two transits (Table 1). Three of 27 deployments needed to be reduced in time due to large patches of *Sargassum* sp., occasional strong winds (three deployments) required the research

vessel to move transversally to allow for gear deployment, this may influence microplastic abundances. All 27 samples will be used for biodiversity and microplastic abundance analysis. Furthermore 158 large microplastic pieces were collected, out of these 39 pieces will be used for bacterial enrichment cultures, to culture novel and potentially plastic degrading microorganisms. 43 pieces will be used for CLASI-FISH (combinatorial labelling and spectral imaging – fluorescence *in situ* hybridization) imaging of the bacterial biofilms that developed on the polymer surface. From 76 samples DNA and RNA will be extracted and sequenced for metagenome and metatranscriptome analysis.

5.1.1.4 Work to be conducted in home laboratory

The 39 microplastic pieces for enrichment culture experiments will be equally distributed between the laboratories of Prof. Wolfgang Streit (University of Hamburg) and Prof. Ruth Schmitz-Streit (Christian-Albrechts University Kiel), collaborators within the framework of Plastisea. The cultures may lead to the isolation of novel and/or potentially plastic degrading microorganisms. The long incubation times at sea may enrich for certain types of bacteria especially equipped for utilizing these non-native polymers. The CLASI-FISH imaging will be done by Dr. Cathleen Schlundt (GEOMAR, Kiel) and the metagenome and metatranscriptome analysis will be performed by Dr. Erik Borchert with the help of the Competence Centre for Genomic Analysis (CCGA) Kiel. Microscopic analysis of the biofilms on plastic pieces enables insights into the structure and layering of these communities. Metagenome sequencing permits gene content analysis to decipher the interplay between different microbial community members, coupled with metatranscriptomic sequencing, the active gene repertoire can be assessed and identification of novel enzymes/biocatalysts, which would be overlooked by metagenomic analysis only, involved in plastic utilization might be possible. All 158 microplastic pieces will be subsequently scanned with an FTIR microscope at the TUTECH GmbH, Hamburg to identify the respective polymer type of each particle. Identification of polymer type is crucial for all analysis as each plastic type possesses different chemical properties and thus displays different challenges for colonization and degradation.

Table 5.1. Stations at which neuston trawls were performed during SO279

Station ID	**Date**	**Time [Ship time]**	**Area**	**Latitude (start)**	**Longitude (start)**
SO279_18-1 NEMICAT-1	13.12.2020	12:19	3	31°39,925'N	24°27,299'W
SO279_18-1 NEMICAT-2	13.12.2020	12:45	3	31°40,463'N	24°28,349'W
SO279_18-1 NEMICAT-3	17.12.2020	13:11	3	31°41,050'N	24°29,404'W
SO279_43-1 NEMICAT-4	17.12.2020	06:06	4	31°19,463'N	29°34,324'W
SO279_43-1 NEMICAT-5	17.12.2020	06:35	4	31°20,457'N	29°35,132'W
SO279_43-1 NEMICAT-6	17.12.2020	07:12	4	31°21,525'N	29°36,005'W
SO279_48-1 NEMICAT-7	17.12.2020	21:01	Transit 4-5	31°19,939'N	30°41,100'W
SO279_48-1 NEMICAT-8	17.12.2020	21:31	Transit 4-5	31°20,671'N	30°42,265'W
SO279_48-1 NEMICAT-9	18.12.2020	22:00	Transit 4-5	31°21,532'N	30°43,211'W
SO279_55-1 NEMICAT-10	18.12.2020	18:06	5	31°07,051'N	33°48,968'W
SO279_55-1 NEMICAT-11	18.12.2020	18:32	5	31°07,902'N	33°49,730'W
SO279_55-1 NEMICAT-12	19.12.2020	18:59	5	31°09,010'N	33°50,491'W
SO279_68-1 NEMICAT-13	19.12.2020	22:10	Transit 5-6	32°10,425'N	34°09,155'W
SO279_68-1 NEMICAT-14	19.12.2020	22:39	Transit 5-6	32°11,406'N	34°09,905'W
SO279_68-1 NEMICAT-15	21.12.2020	23:08	Transit 5-6	32°12,404'N	34°10,631'W
SO279_78-1 NEMICAT-16	21.12.2020	08:20	6	33°08,521'N	34°33,677'W
SO279_78-1 NEMICAT-17	21.12.2020	08:50	6	33°09,562'N	34°34.524'W
SO279_78-1 NEMICAT-18	22.12.2020	09:23	6	33°10,711'N	34°35,535'W
SO279_87-1 NEMICAT-19	22.12.2020	08:46	7	33°20,453'N	33°49,994'W
SO279_87-1 NEMICAT-20	22.12.2020	09:15	7	33°21,639'N	33°49,510'W
SO279_87-1 NEMICAT-21	28.12.2020	09:44	7	33°22,757'N	33°49,088'W
SO279_107-1 NEMICAT-22	28.12.2020	05:17	9	35°08,269'N	20°49,388'W
SO279_107-1 NEMICAT-23	28.12.2020	05:48	9	35°09,293'N	20°48,236'W
SO279_107-1 NEMICAT-24	28.12.2020	06:18	9	35°10,315'N	20°47,905'W
SO279_107-1 NEMICAT-25	28.12.2020	06:48	9	35°11,268'N	20°46,031'W
SO279_107-1 NEMICAT-26	28.12.2020	07:18	9	35°12,198'N	20°44,991'W
SO279_107-1 NEMICAT-27	13.12.2020	07:46	9	35°14,206'N	20°43,88'W

5.1.2 Horizontal sampling of the water column with the Multinet and the Bongo Net

(Thea Anna Hamm[1], Ulrike Christiane Panknin[1], Annalisa Sambolino[2], Sonia Gueron[2], and Erik Borchert[1])

[1] GEOMAR

[2] MARE

5.1.2.1 Background and Objectives

Most data on the abundance and composition of marine plastic debris stem from surface trawls, while little is known about the vertical distribution of microplastics in the open ocean. We similarly know very little about interaction of microplastics with zooplankton. Zooplankton can act as a temporary sink for microplastics by ingesting plastic particles in the surface waters and egesting them later. This process might also influence the transport of microplastics into the deep sea when zooplankton migrate during the day to the mesopelagic zone and egest microplastics there (Choi et al., 2019)

At the same time, zooplankton can also be negatively affected by the ingestion of these plastic particles, and by the absorption of some associated chemicals such as phthalates. Phthalic acid esters (PAEs) or phthalates are a family of plastic additives widely used as plasticizers, in various kinds of polymeric products such as polyvinyl chloride and polyethylene. PAEs are not chemically bounded to the polymeric structure, thus they can easily leach from plastic debris into the marine environment and concentrate in the biological tissue of marine organisms (Net et al., 2015).

The samples collected will be used to investigate (i) the vertical distribution of microplastics, (ii) the biological transport mechanism of microplastics across different depth zones and (iii) the relation between microplastics concentration and PAEs contamination level in zooplankton.

5.1.2.2 Methods

The Multinet was equipped with a v-fin depressor, nine 300µm mesh size nets and cod ends set up for horizontal deployment. An inside flowmeter and outside flowmeter for measuring the volume filtered by the nets are attached to the frame of the Multinet. Flowmeter data and depth are continuously transmitted via the coax cable to the deck unit and are monitored by the scientist. First deployment at Station 1 was conducted at 1.5 knots accelerating to 2 knots at 300 m depth with opening the first net at 3000 m depth. The first net sampled from 3000 to 2000 m depth, the second net from 2000 m to 1000m depth, the third net from 1000m to 300m, the fourth net from 300 m to 100 m, the fifth net from 100 m to 10 m, the sixth and seventh net were towed for 30 min at 10 m, the 8th net from 10 m to 100 m and the 9th net from 100 to 300 m. Lowering and raising speed was adjusted to ensure sampling took place over the course of 30 min. The second deployment and all other following deployments were unsuccessful at the subsequent stations because the net turned in the water column and consequently stopped sampling. Measures for stabilizing the net in the water column included changing the bridle to the second hole in the Multinet frame, shortening the parachute to prevent entanglement with the nets, adding 120kg weight equally to all four sides of the net frame and opening the first net in a opened state without and with cod-end as a second parachute. Despite joint efforts of the Crew, technicians at GEOMAR and the producing company HYDRO-Bios it was not possible to stabilize the Multinet enough for successful sampling. Water currents in the work area are very strong and the current configuration of the Multinet is not suitable for deployment under these conditions. A larger V-fin depressor of at least 1.10 m width and 70 kg weight would have probably been necessary to stabilize the net sufficiently. The first station was 400 sea miles from the main working area and is most likely part

of a different water current regime which allowed successful and easy deployment of the net. As a substitute, the Bongo net was deployed at all other stations.

The bongo net (HYDRO-BIOS Kiel) was deployed with a 22 kg V-fin depressor with a 300 µm mesh size on both net rings at 10m, 100 m and 300 m during the night. Whenever possible, two deployments per each depth were performed, in order to obtain one full net sample per each research group (GEOMAR/IPMA/MARE-Madeira), plus a backup sample. If time or weather conditions did not allow, only one deployment was performed, and one of the net samples was halved with a zoosplitter to be shared by two groups (IPMA/MARE-Madeira). Ship speed during deployment was 2 knots and the net was towed 30 min at the desired depths. The net was equipped with depth loggers (Star Oddi, dst centi) and a mechanical flowmeter with back-run stop (HYDRO-BIOS Kiel) to measure the water volume that passed through the nets during deployment. The nets were rinsed with seawater to collect the sample in the detachable net bucket. Net buckets were washed with 0.5 µm filtered seawater (Knaub Trading GmbH) into a metal pot to avoid contamination with microplastics. The whole sample was washed over a metal sieve (125 µm) and stored for later analysis.

Samples for zooplankton analyses (GEOMAR) were stored in Weck glass jars and initially frozen at -20 °C; then 30% formaldehyde was added for a final concentration of 4% formaldehyde in the sample for conservation. Samples for microplastics abundance analysis (IPMA) were stored in aluminum bowls and dried at 40 °C in the oven. Samples for PAEs analysis (MARE – Madeira) were sieved into aluminum containers and immediately frozen at -80 °C.

5.1.2.3 Preliminary results

The Multinet was deployed successfully at Station 1 until a depth of 3000m . The multinet was further tested at subsequent station with several alterations to the gear but none of the deployments were successful at Station 3, 4 and 5. At station 5 we switched to the Bongo net and at five stations (4,5,6,7,9) it was deployed two times per each depth. In three occasions (10 m and 100 m depth at station 4 and 10m depth at station 6) it was possible to perform only one deployment per depth. On one occasion (station 4) the 300 m depth deployment was not performed.

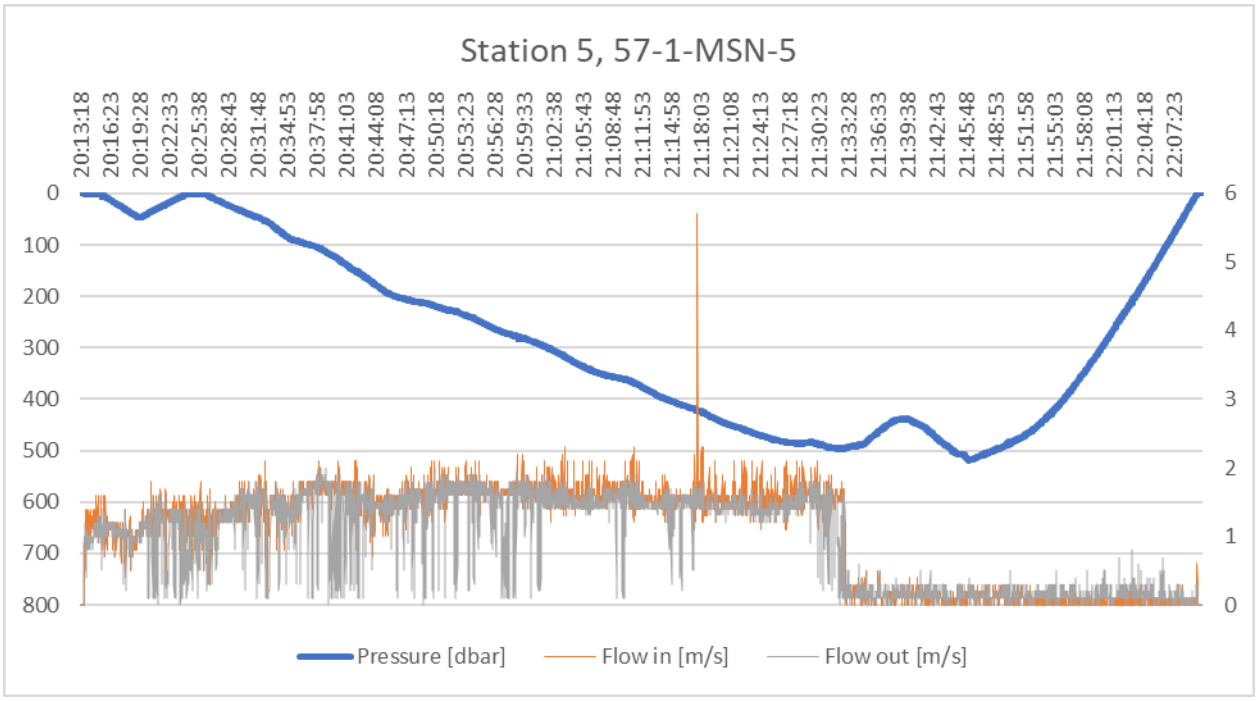

Figure 5.1. Example of a Multinet deployment. X-axis shows time, while the left y-axis is indicating depth [m]. The right y-axis indicates flow [m/s] the inside flowmeter is depicted in orange, the outside flowmeter in grey.

Flowmeter values during lowering for the inside flowmeter (orange) matched the ship speed and stayed continuously around 1.5 m/s (Fig. 5.1). Outside flowmeter values (grey) regularly oscillated indicating that the multinet was not stable in the water column. At 500 m depth the winch was stopped to start heaving which caused the Multinet to turn completely in the water column, which was first indicated by the outside flowmeter's strongly reduced values and subsequently the inside flowmeter to stop measuring.

5.1.2.4 Work to be conducted in home laboratory

Samples for IPMA will be observed under a stereo-microscope for microplastic identification, characterizing shape, size and colour, following the MSFD guidelines. The organic matter will be previously digested with H_2O_2, KOH or similar.

Another part of the sample will be scanned and uploaded into EcoTaxa, an online database for zooplankton, to determine biodiversity and total abundances of taxonomic group per cubic meter seawater. Four exemplary taxonomic groups will be picked at representative numbers for gut analysis. Copepods make up the largest biomass in the north Atlantic while Euphausicae are the second largest group and also represent filter feeders. Chaetognaths are not as abundant but represent a group of predators. Fish larvae are the only vertebrate representative within the zooplankton community and can possibly digest larger pieces. Fish larvae and copepods comprise different modes of feeding.

Samples for MARE-Madeira will be used for PAEs analysis. The samples will be extract following the method described in Baini et al. (2017), with some modifications. Briefly about 100 mg of freeze-dried sample will be extracted with a hexane/dichloromethane mixture, the extract will be injected into a gas chromatograph/mass spectrometer (GC/MS: HP 6890/5973) in Selected Ion Monitoring (SIM) mode and PAEs will be identified and quantified in each sample.

Table 5.2. Stations at which Multinet samples were collected during SO279

DSHIP	No.	Net no.	Date	Time (UTC)	Sta.	Latitude (start)	Longitude (start)	depth
SO279_6-1 MSN	1	1	09.12.2020	02:14	1	47° 16.664' N	010° 14.544' W	3000-2000
SO279_6-1 MSN	1	2	09.12.2020	03:32	1	47° 16.664' N	010° 17.394' W	2000-1000
SO279_6-1 MSN	1	3	09.12.2020	04:13	1	47° 16.664' N	010° 18.902' W	1000-300
SO279_6-1 MSN	1	4	09.12.2020	04:50	1	47° 16.654' N	010° 20.253' W	300-100
SO279_6-1 MSN	1	5	09.12.2020	05:12	1	47° 16.644' N	010° 21.067' W	100-10
SO279_6-1 MSN	1	6	09.12.2020	05:24	1	47° 16.640' N	010° 21.517' W	10
SO279_6-1 MSN	1	7	09.12.2020	05:54	1	47° 16.627' N	010° 22.608' W	10
SO279_6-1 MSN	1	8	09.12.2020	06:24	1	47° 16.540' N	010° 23.695' W	10-100
SO279_6-1 MSN	1	9	09.12.2020	06:40	1	47° 16.423' N	010° 24.258' W	100-300
SO279_19-1 MSN	2	1	13.12.2020	19.20	3	31° 28,049' N	024° 32,419' W	3000-2000
SO279_19-1 MSN	2	2	13.12.2020	20:45	3	-	-	2000-1000
SO279_19-1 MSN	2	3	13.12.2020	21:18	3	-	-	1000-300
SO279_29-1_MSN	3	1	15.12.2020	01:34	3	31° 25.131' N	024° 53.000' W	1000-300
SO279_29-1_MSN	3	2	15.12.2020	03:08	3	31° 29.007' N	024° 56.299' W	300-100
SO279_29-1_MSN	3	3	15.12.2020	03:55	3	31° 30.988' N	024° 57.812' W	100-10
SO279_29-1_MSN	3	4	15.12.2020	04:20	3	31° 31.919' N	024° 58.518' W	10
SO279_41-1 MSN	4	1	17.12.2020	19:17	4	30° 54.504' N	029° 19.424' W	0-2000
SO279_41-1 MSN	4	2	17.12.2020	00:28	5	-	-	2000-1000
SO279_41-1 MSN	4	3	17.12.2020	03:13	5	-	-	1000-10
SO279_56-1_MSN-5-1	5	1	18.12.2020		5	-	-	0-300

Table 5.3. Stations at which bongo net samples were collected during SO279

DSHIP	No.	Date	Time (UTC)	Sta.	Latitude (start)	Longitude (start)	Latitude (end)	Longitude (end)	depth
SO279_42-1 BONGO	1	17.12.2020	05:03	4	31° 16.396' N	029° 32.521' W	31° 17.641' N	029° 33.107' W	10
SO279_42-1 BONGO	2	17.12.2020	05:53	4	31° 17.718' N	31° 17.718' N	31° 19.230' N	029° 34.165' W	100
SO279_58-1 BONGO	3	18.12.2020	23:30	5	31° 14.665' N	033° 55.588' W	31° 15.403' N	033° 56.449' W	10
SO279_58-1 BONGO	4	18.12.2020	00:10	5	31° 15.595' N	033° 56.640' W	31° 17.048' N	033° 58.047' W	100
SO279_58-1 BONGO	5	18.12.2020	01:22	5	31° 17.316' N	033° 58.306' W	31° 18.930' N	033° 59.871' W	100
SO279_58-1 BONGO	6	18.12.2020	03:22	5	31° 19.044' N	034° 00.037' W	31° 21.377' N	034° 02.251' W	300
SO279_75-1 BONGO	7	20.12.2020	18:58	6	33° 17.538' N	034° 29.572' W	33° 14.926' N	034° 28.526' W	300
SO279_75-1 BONGO	8	20.12.2020	21:05	6	33° 14.847' N	034° 28.460' W	33° 13.496' N	034° 28.298' W	100
SO279_75-1 BONGO	9	20.12.2020	22:08	6	33° 13.433' N	034° 28.292' W	33° 12.545' N	034° 28.270' W	10
SO279_75-1 BONGO	10	20.12.2020	22:46	6	33° 12.475' N	034° 28.261' W	33° 09.814' N	034° 29.320' W	300
SO279_75-1 BONGO	11	20.12.2020	00:28	6	33° 09.716' N	034° 29.331' W	33° 08.121' N	034° 30.010' W	100
SO279_75-1 BONGO	12	21.12.2020	01:30	6	33° 08.129' N	034° 30.010' W	33° 08.266' N	034° 30.036' W	10
SO279_86-1 BONGO	13	22.12.2020	02:47	7	33° 08.611' N	033° 46.715' W	33° 11.054' N	033° 47.435' W	300
SO279_86-1 BONGO	14	22.12.2020	04:36	7	33° 11.242' N	033° 47.491' W	33° 12.868' N	033° 48.021' W	100

SO279_86-1 BONGO	15	22.12.2020	05:43	7	33° 12.959' N	033° 48.060' W	33° 13.977' N	033° 48.592' W	10
SO279_86-1 BONGO	16	22.12.2020	06:23	7	33° 14.110' N	033° 48.649' W	33° 17.184' N	033° 49.430' W	300
SO279_86-1 BONGO	17	22.12.2020	08:02	7	33° 17.282' N	033° 49.456' W	33° 18.340' N	033° 49.693' W	10
SO279_86-1 BONGO	18	22.12.2020	08:41	7	33° 18.438' N	033° 49.712' W	33° 20.173' N	033° 50.070' W	100
SO279_106-1 BONGO	19	28.12.2020	23:26	9	35° 00.054' N	020° 59.914' W	35° 00.054' N	020° 59.914' W	300
SO279_106-1 BONGO	20	28.12.2020	00:10	9	35° 02.159' N	020° 57.494' W	35° 03.243' N	020° 56.040' W	100
SO279_106-1 BONGO	21	28.12.2020	01:10	9	35° 03.333' N	020° 55.881' W	35° 04,066' N	020° 54,847' W	10
SO279_106-1 BONGO	22	28.12.2020	01:50	9	35° 04.170' N	020° 54.712' W	35° 05.984' N	020° 52.346' W	300
SO279_106-1 BONGO	23	28.12.2020	03:26	9	35° 06.053' N	020° 52.251' W	35° 07.325' N	020° 50.597' W	100
SO279_106-1 BONGO	24	28.12.2020	04:28	9	35° 07.397' N	020° 50.500' W	35° 08.200' N	020° 49.472' W	10

5.1.3 Shipboard measurement of net-collected microplastics using near-infrared hyperspectral imaging

(Mikael L.A. Kaandorp[1], Thea Hamm[2], Boie Bogner[2], Aaron Beck[2])
[1] Utrecht
[2] GEOMAR

5.1.3.1 Background and Objectives

Plastics are ubiquitous in the ocean surface waters, especially in convergence zones such as the South Atlantic garbage patch. Using for example a catamaran net trawl, many particles end up in the net. It is often not straightforward to say that a particle is a polymer just by visual inspection. On board, we tested a hyperspectral near-infrared (NIR) camera set-up, in order to identify whether particles are really plastic particles, and to identify what kind of polymer the plastic is made of. We developed a methodology to scan a long strip of plastic particles, automatically identify the particles using a image segmentation algorithm, and then classify the particles according to their polymer.

5.1.3.2 Methods

The hyperspectral camera gives a spectrum with wavelengths ranging from 935 to 1720 nm, with a resolution of 224 bands. The hyperspectral images were captured using the Lumo software. The image width is fixed to 640 pixels.

Plastic particles were removed from the catamaran trawls by visual inspection as described in section 5.1.1. Particles were placed on test beds made of metal bars covered with electrical tape. Particles are placed on the sticky side of the electrical tape, so they do not move around. Black electrical tape was chosen, as this simplifies the image segmentation process. The black background does not reflect much radiation and is therefore easily removed during the image processing. The test beds are separated into three strips of approximately 1.2 centimeters wide, which is roughly the camera field of view at the given test bed height.

Multiple image segmentation algorithms were tested during the cruise. At first, the particle pixel locations and their dimensions had to be set by hand. This proved to be a lot of work and not feasible for test beds with larger number of particles. The first algorithm to be tested was the scikit-learn spectral clustering algorithm (Scikit-learn, 2021). This proved to be unreliable for our test case however, and computationally very costly. The second algorithm to be tested was the scikit-image blob detection algorithm (Scikit-image, 2021). While this seemed to work quite well, the downside is that it will not be able to detect all pixels from non-spherical particles. Finally, a combination of an edge-finding algorithm (sobol) and a segmentation algorithm (watershed) from scikit-image (see Scikit-image, 2021b) turned out to be very effective, as long as the particles are not touching. The sobol filter computes an approximation of the pixel intensity

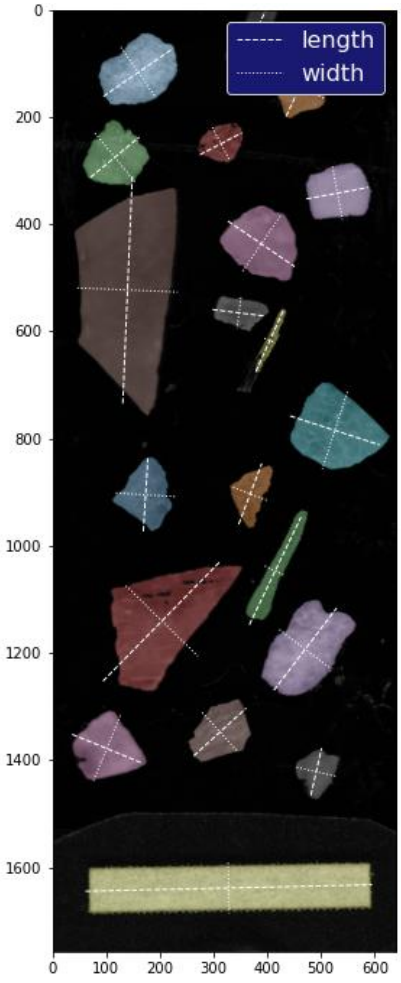

Figure 5.2. Example scan of particles. Each color indicates a separate segment (or particle), particle lengths and widths are represented using the white dashed/dotted lines

gradients. Edges of particles tend to have the highest gradient magnitudes, and can be extracted this way. The detected edges are used to seed the watershed segmentation algorithm. The watershed algorithm fills in the particles, by treating the picture similar to an elevation map, and then 'flooding' the regions.

After running the image segmentation, the user can check the output. Sometimes false particles are detected, or particles are split in multiple segments (which is often the case for darker or translucent particles). The user can select the segments which need to be merged in postprocessing, and can select segments which need to be removed. The script can then be run again in postprocessing mode.

One of the goals is to measure the particle dimensions automatically. In order to do this, the width of the pixels needs to be set. Calibration is achieved by printing out a white bar with a width of 1 cm (Fig. 5.2). The image recognition algorithm is able to detect this bar. The width of the bar in pixels is used to set the amount of millimeters per pixel in the software.

Particle length and width are determined by calculating a singular value decomposition on the particle pixels. This allows us to rotate the particle pixels towards its major axis. The particle length is then calculated by taking the maximum distance in the x-direction, the particle width by taking the maximum distance in the y-direction. Other particle properties, such as particle area and perimeter, are calculated using the scikit-image measure class. Example scanned particles are shown in Fig. 5.2, along with the indicated lengths and widths of the particles.

The particle materials are classified from their spectra (Fig. 5.3) using a decision tree algorithm. This classification algorithm is still at an early stage of development. Peaks are detected in the spectra, and are then compared to eight reference materials (HDPE, LDPE, PP, PA66, PMMA, PET, PS, PC). The decision tree always decides on at least one polymer. This still needs to be extended at a later stage with other materials such as organic materials and paint chips (Fig. 5.3).

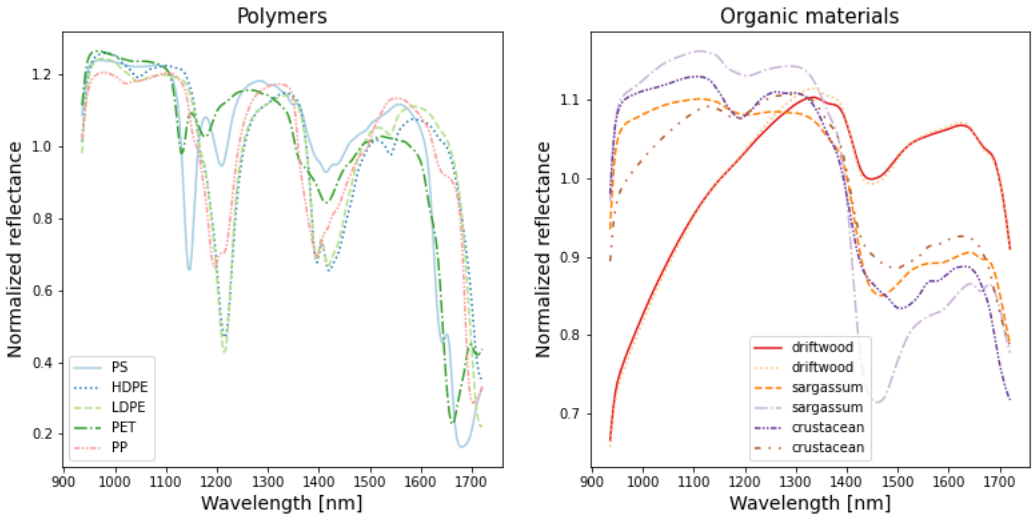

Figure 5.3. Reference spectra of polymers (left) and organic materials (right)

5.1.3.3 Preliminary results

One of the first things to be investigated was whether particles should be completely dry before scanning. In some cases, the particles cannot remain dry for too long, as the biofilm still had to be analyzed. Example results are shown in Fig. 5.4. Multiple liquids were tested, such as RNAlater and seawater, all with the same effects. The liquids absorb the higher wavelengths, making it difficult for the classification algorithm to determine what the polymer material is.

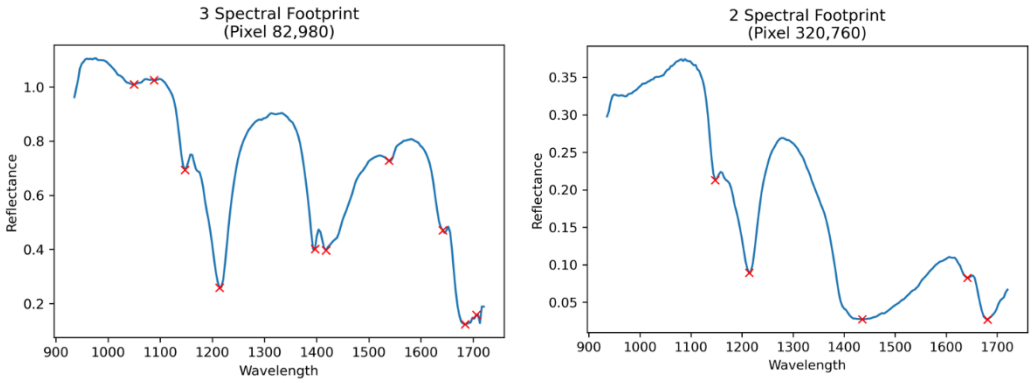

Figure 5.4. (Left) Spectrum of a dry PE particle. (right) Spectrum of a wet (seawater) particle.

Particles from 27 catamaran trawls were put on the test beds, yielding a total of 2368 particles. The particles are still to be analyzed further. The far majority of the particles was determined to be polyethylene. An example output figure for a polyethylene particle is presented in Fig. 5.5. Typical of the polyethylene particles is the peak in the spectrum slightly above 1500 nm.

Preliminary results were calculated regarding the particle dimensions (Fig. 5.6). Polymers still need to be selected out of the dataset. The majority of the particles were around 2 millimeters. The distribution seems to adhere to a log-normal distribution, which becomes clearer after transforming to a log-scale (Fig. 5.6). The slope of the right tail of this distribution could still be compared to e.g. Cozar et al. (2014), to see whether this is similar. Effects of turbulent mixing, see e.g. Poulain et al. (2019), along with a size-detection limit could be used to explain why there is such a strong decrease in abundance for particles smaller than 1 millimeter.

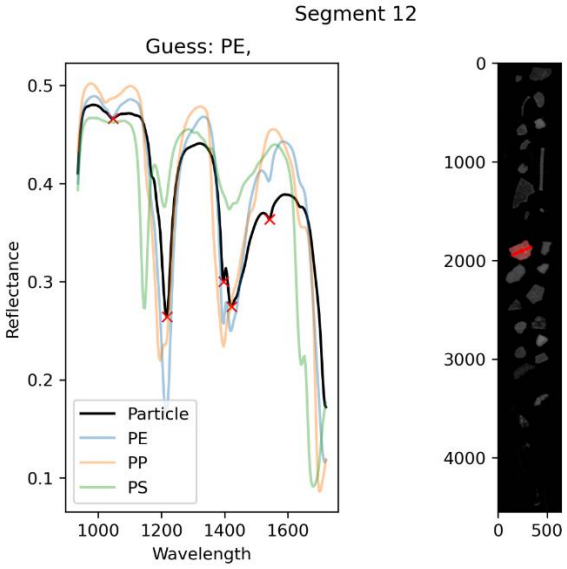

Figure 5.5. Example PE particle: spectrum (left; reference spectra for PE, PP, PS shown in colored lines) and segment (right)

Other useful quantities can be derived from the data. One quantity is the particle perimeter to area ratio (Fig. 5.7). This could be used to separate more spherical particles from for example fibers. Furthermore, it could be used to detect badly imaged particles. The perimeter to area ratio increases for more complex shapes. A particle like to one on the bottom in figure 1 has a very large perimeter to area ratio. Some example fibers which were analyzed had perimeter to area ratios of about 4—5, the badly detected particles had higher ratios, often above 10.

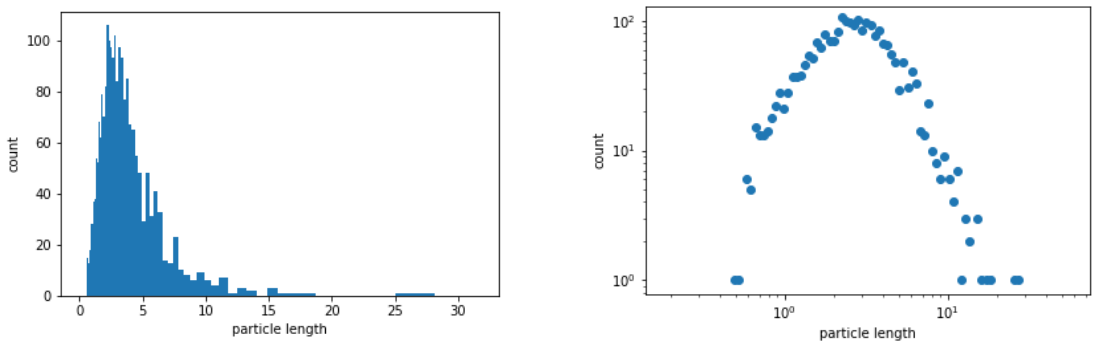

Figure 5.6. (left) Histogram of particle lengths. (right) Log-log transformed particle length distribution.

Some particles were found which look like hard foam. Upon closer inspection it seems likely these are pumice particles. Example output for a spectrum is shown in Fig. 5.8.

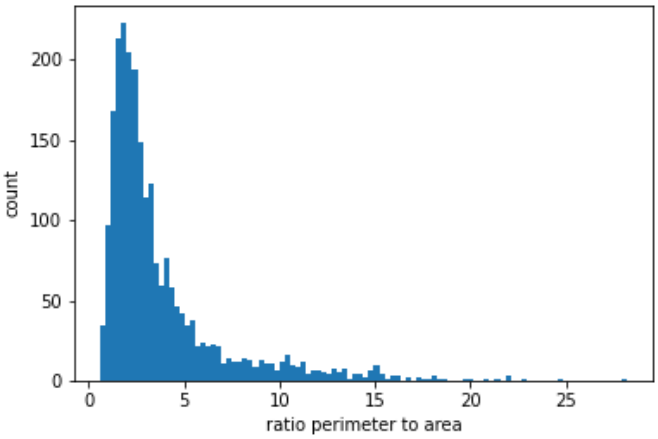

Figure 5.7. Histogram of the particle perimeter to area ratio

Sediment samples

Some particles were detected in sediment samples after sieving the box cores. Some of these originated from the spades (paint chips) used to scoop sediment out of the box core, which was verified by scanning some samples directly taken from the spade. A piece of plastic film was found in one of the box cores, see Fig. 5.9. The decision tree classifies the film as either PE or PP. The signal from the spectrum is relatively weak however, perhaps due to its translucence. Looking at the peaks it seems more likely it is a PS film, but this would need to be verified at a later stage to be certain.

5.1.3.4 Work to be conducted in home laboratory

One of the main things to be done is creating a bigger database with different polymers and other materials which might be found in the marine environment. Example materials might be paint chips, rust, minerals (e.g., pumice), seaweeds, crustaceans, fish, and various types of possible biofilms.

Regarding the classification algorithm, it would be good to explore probabilistic algorithms, which assign a probability to a certain polymer/material. One could for example look into machine learning algorithms such as Gaussian processes (Scikit-learn, 2021b).
A closer look is needed into the features for the classification. Right now, only peaks are used for the classification. It might be useful to look at integrated quantities of the spectrum, or derivative information for more robust classification, and to detect ‘shoulders’ in the spectrum.

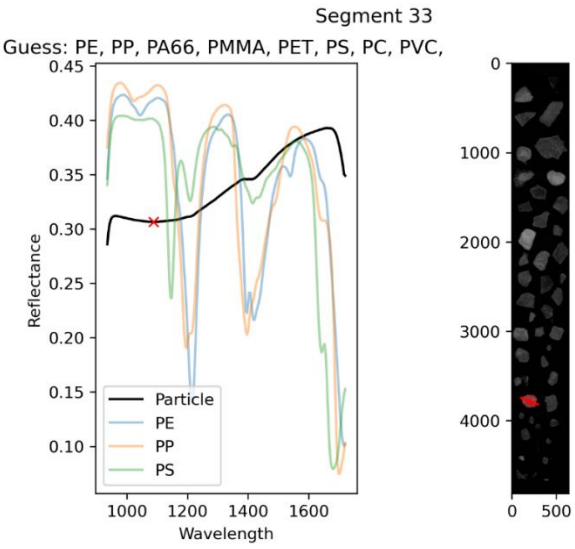

Figure 5.8. Particle with a foam-like structure, likely a piece of pumice

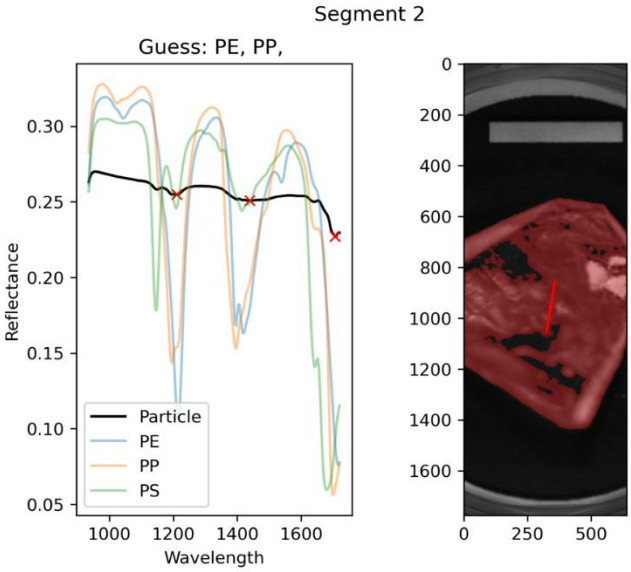

Figure 5.9. Sample film obtained from a box core sample (SO279_104-1)

5.2 Water and particle sampling with CTD/rosette and in situ pumps

5.2.1 Thorium isotope tracer measurements and particle filtration with the Challenger-In-Situ-Pump systems

(Aaron J. Beck, André Mutzberg, Eric Achterberg)
[1]GEOMAR

5.2.1.1 Background

This is a novel application of the naturally-occurring ^{234}Th tracer to quantify the vertical flux of microplastic particles under the North Atlantic garbage patch. Less than approximately 10 % of the plastic entering the ocean can currently be accounted for, likely due to fragmentation into small microplastics that are exported from the surface to the deep ocean. The radionuclide ^{234}Th has a half-life of 24.1 days and is constantly produced by the decay of its parent ^{238}U. While U is highly soluble and mixes conservatively in oxygenated waters, ^{234}Th scavenges strongly to particle surfaces. Export of particulate ^{234}Th from the euphotic zone to the deep ocean produces a ^{234}Th deficit in the upper water column equal to the export flux. With information on the microplastic to ^{234}Th ratio (MP/^{234}Th) in sinking particles, the vertical fluxes of MPs can be quantified. These export fluxes will be used to improve the marine plastic mass balance and determine if a deep ocean sink can account for the missing plastic mass.

5.2.1.2 Methods

During SO279, unfiltered seawater samples along a depth profile in the upper 300 m of the water column were collected with Niskin bottles mounted on a traditional CTD at 7 stations (Fig. 5.10; Table 5.4). Total ^{234}Th activities were determined on 4 l samples. Stations were chosen within the accumulation zone of the North Atlantic garbage patch (Cozar et al., 2014), where the highest MP abundances were expected. High vertical resolution sampling was performed within the upper 300 m, where most of the biological activity occurs. Additional samples were collected as deep as 2000 m. Filtered (0.45 µm PES) seawater (15 ml) for ^{238}U concentrations was sampled from the same Niskin bottles as for ^{234}Th.

At seven in situ pump stations, suspended and sinking particles (>10 µm, on stainless steel mesh) were collected using the Challenger in situ pump systems (Fig. 5.10; Table 5.5) that was deployed on the CTD cable. These in situ pump stations were located within the core of the North Atlantic garbage patch, and two revisited locations occupied during POS536 (Stations 6 and 7; Fig. 3.2).

Figure 5.10. (right) CTD/Niskin rosette deployment for discrete water sample collection. (right) In situ pump deployment for collection of suspended particles**.**

Further samples for particulate ^{234}Th and microplastics (>10 µm) were collected from the underway seawater system along two transects using a stand-alone filtration unit (10 µm stainless steel mesh) that was connected to the RV SONNE membrane pump seawater tap (Table 5.6).

The chemical separation of thorium from seawater on board followed van der Loeff et al. (2006). Thorium was co-precipitated with MnO_2 and filtered onto 25 mm silver filters (3 µm pore size). These precipitates were dried in an oven at 60˚C for several hours before analysis. Filters of both total and particulate ^{234}Th were mounted onto Risø sample holders, and initial activities of ^{234}Th were counted on a Risø low-level beta GM multicounter.

Figure 5.11. In situ pump filter for collection of suspended and sinking particulates. The stainless-steel filter mesh is discolored after ashing at 450°C to remove plastic and carbon contamination.

Silver filters were used to collect particulate material to avoid contamination from plastic filter membranes, and allow detection and identification of MP particles, as well as particulate organic carbon (POC). This method will provide the MP/Th ratio for quantifying MP export fluxes to the deep ocean.

5.2.1.3 Sample processing and analysis at GEOMAR

Filters of both total and particulate ^{234}Th will be re-counted on the Risø low-level beta GM multicounter 5 months after sample collection, at which time ^{234}Th will have decayed to undetectable levels. The original beta activities will be corrected for any residual activity (i.e., from other nuclides with longer half-life). After the final counting, total ^{234}Th samples will be dismounted and dissolved in a mixture of H_2O_2 and HNO_3, and analyzed by ICP-MS to determine chemistry yield (Pike et al., 2005). Particulate ^{234}Th samples will be dismounted for MP analysis by FTIR or Raman spectroscopy, followed by POC analysis in order to determine the MP/^{234}Th and POC/^{234}Th ratios.

Seawater samples for uranium concentrations will be measured on the Element ICP-MS (Owens et al., 2011). We expect all chemical processing and analysis be completed within a year from the end of SO279.

Table 5.4. List of stations at which seawater was collected with the CTD for total ^{234}Th / Uranium / microplastics and particulate ^{234}Th /microplastics during SO279.

Station number	**Latitude**	**Longitude**	**Depths (m)**
SO279_1-1 CTD_1	47° 15.000' N	010° 06.281' W	300,150,75,50,25
SO279_22-1_CTD_2	31° 16.048' N	024° 48.743' W	300,120,80,50,25
SO279_36-1_CTD-3	30° 53.538' N	029° 18.836' W	300,100,75,50,25
SO279_53-1_CTD-4	31° 07.076' N	033° 48.981' W	300,130,75,50,25
SO279_69-1_CTD-5	33° 17.592' N	034° 29.501' W	300,150,75,50,25
SO279_81-1_CTD-6	33° 08.606' N	033° 46.671' W	300,150,75,50,25
SO279_102-1_CTD-7	35° 00.007' N	021° 00.001' W	300,150,75,50,25

Table 5.5. List of stations at which the in situ-pumps were used for sampling particulate ^{234}Th and microplastics during SO279.

Station number	**Latitude**	**Longitude**	**Depths (m)**
SO279_3_1_ISP_1	47° 15.000' N	010° 06.281' W	300,150,75,50,25
SO279_23_1_ISP_2	31° 16.052' N	024° 48.712' W	300,120,80,25 (one Pump failed)
SO279_37_1_ISP_3	30° 53.540' N	029° 18.837' W	300,100,75,50,25
SO279_54_1_ISP_4	31° 07.054' N	033° 48.966' W	300,130,75,50,25
SO279_71_1_ISP_5	33° 17.607' N	034° 29.484' W	300,150,75,50,25
SO279_82_1_ISP_6	33° 08.613' N	033° 46.716' W	300,150,75,50,25
SO279_103_1_ISP_7	35° 00.004' N	020° 59.992' W	300,150,75,50,25

Table 5.6. List of underway water samples for particulate ^{234}Th / microplastics.

Station number	**Latitude**	**Longitude**	**Latitude**	**Longitude**	**Sample depths (m)**
SO279_15-1 UWS	35°14.387´N	021°16.177´W	34°43.961´N	021°41.062´W	Surface
SO279_31-1 UWS	31°23.234´N	026°01.432´W	31°14.466´N	026°59.821´W	Surface

5.2.2 Total Alkalinity, Dissolved Inorganic Carbon, pH and nutrients

(Louise Delaigue)
[1] NIOZ

5.2.2.1 Background and Objectives

Carbon dioxide (CO_2) is a key player in the Earth's climate system. Recent atmospheric CO_2 concentrations have reached record levels due to anthropogenic emissions, exceeding 415 ppm in 2020 – the highest concentration recorded in the past 3 million years (Willeit et al., 2019). The oceans have been acting as a sink of CO_2 emissions, absorbing an estimated 24% of anthropogenic CO_2 since the beginning of the industrial era, thus significantly mitigating the greenhouse effect on global warming (Doney et al., 2009; Feely et al., 2004; Friedlingstein et al., 2019; Orr, 2011; Sabine et al., 2004). Measuring components of the marine carbonate system allows us to assess the state of the carbon cycle in our oceans, with important variables such as total alkalinity (TA), dissolved inorganic carbon (DIC) and pH, giving direct insights on ocean acidification. Furthermore, measuring parameters of the carbonate system not only sheds some light on the absorption of our CO_2 emissions by the oceans, but also on their correlation with other problematic topics such as microplastics.

5.2.2.2 Methods

Table 5.7 summarizes the quantity of samples taken for each parameter.

TA/DIC samples were collected following the protocol by Dickson et al. (2007). Seawater was collected from the Niskin bottles on the CTD rosette through a silicone tube into 250 mL borosilicate glass bottles (Corning, Germany). Each bottle was thoroughly rinsed with excess sample and overflowed by at least a full bottle volume before withdrawing the tube and closing with a stopper. During sampling, special care was taken to avoid any bubble formation in both the tube and the bottles. Samples were processed by removing 1% of the total bottle volume (2.5 mL) and poisoned with 50 µL saturated $HgCl_2$. Samples were then stored at 4°C in a cold room.

Nutrient **s**amples were collected in 60 mL high-density polyethylene syringes connected with a three-way valve via tubing to avoid any air contact when sampling directly from the CTD Niskin bottles. Samples were filtered immediately over a combined 0.8/0.2 µm filter and sub-sampled for Si, and PO_4 NH_4, NO_3 and NO_2 in polyethylene "pony-vials" with a volume of 6 mL. DIC was also sub-sampled into 5 mL glass vials already containing 15 µL saturated $HgCl_2$. All samples were stored at -20°C in a freezer except Si and DIC, which were stored at 4°C in a cold room.

A few samples were collected from the ship's underway seawater supply at the front of the ship (with a delay inferior to 5 seconds from the source), but otherwise following the same protocol as described above. Continuous pH measurements at 30 seconds interval were also achieved using an optode from PyroScience (range 7 – 9, PHROBSCPK8T-SUB) over the entirety of the cruise (outside of any EEZ; Fig. 5.12). The optode was calibrated prior to the start of measurements, using PyroScience buffers (pH 2.0 and pH 10.0) and certified reference material (CRM) seawater obtained from the laboratory of Prof. A. G. Dickson (Scripps Institution of Oceanography, CA, USA).

5.2.2.3 Preliminary results

Because of COVID-19 restrictions and other limitations, results are not available yet. Results should be available by mid-2021.

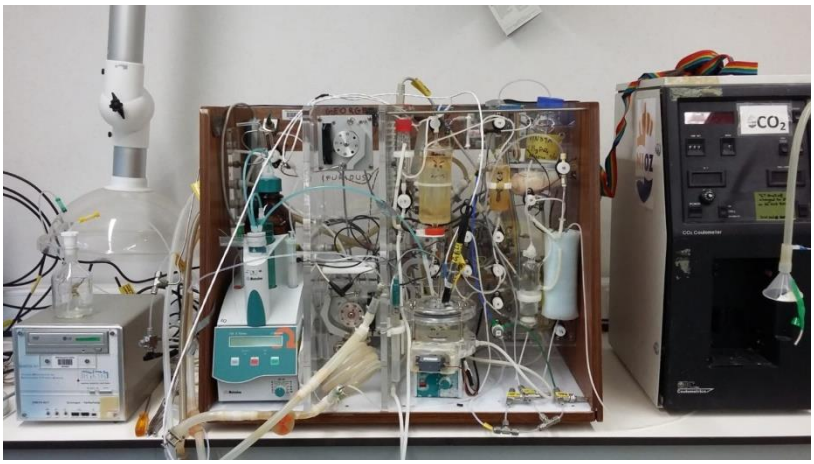

Figure 5.12. VINDTA 3C which will be used to analyze TA and DIC once back at NIOZ.

5.2.2.4 Work to be conducted in the home laboratory

All analyses will be carried out in the NIOZ CO_2 lab. TA and DIC will be measured using a VINDTA 3C (for both DIC and TA). The VINDTA 3C (Versatile INstrument for the Determination of Total inorganic carbon and titration Alkalinity) combines the proven VINDTA alkalinity titration concept with a simplified extraction unit for coulometric dissolved inorganic carbon (DIC) measurement. TA and DIC results will be calibrated using certified reference material (CRM) seawater obtained from the laboratory of Prof. A. G. Dickson (Scripps Institution of Oceanography, CA, USA). TA will be recalculated from the titration data after the cruise, considering the varying nutrient concentrations, using a least-squares fitting approach (e.g., Dickson et al., 2003). Nutrients and DIC will be measured using a Seal QuAAtro, gas-segmented continuous flow auto analyser for Phosphate, Ammonium, Nitrate with Nitrite together, and Nitrite separate.

Data calibration and processing will be achieved once back on land, to assess measurement quality, compare the different instruments and visualize the results. Final values will consider all CRM measurements, and TA results will be recalculated using nutrient analysis. pH will also be calculated for discrete samples from TA and DIC, both to report water column estimates at stations, but also to correct for any potential drift from the optode. pH continuous measurements will also be recalculated at the in-situ temperature from the ship's thermosalinograph to reflect real surface waters' conditions.

Figure 5.13. Setup for continuous pH measurements. The optode is in a closed cell, in the upper left panel, along with a temperature sensor. The cell is located inside a metal box (upper right panel) to isolate the optode from light. The bottom panel shows the setup for the pump and thermosalinograph, which will later be used to recalculate pH at in-situ surface conditions.

Table 5.7. Number of samples taken per station, per parameter, as well as from the underway. Nutrients include sub-samples for Si, and PO_4 NH_4, NO_3 and NO_2 and DIC.

Station	**Max depth**	**TA/DIC**	**Nutrients**
STN 1	~4430 m	24	72
STN 3	~5400 m	22	66
STN 4	~4300 m	19	60
STN 5	~4400 m	22	66
STN 6	~3590 m	22	66
STN 7	~3650 m	22	66
STN 9	~5200 m	22	66
UNDERWAY	Surface	102	306
Total	n/a	255	768

5.2.3 Organic and inorganic carbon and its stable isotopes

(Hashan Niroshana Kokuhennadige[1])

[1] Ocean and Earth Science, National Oceanography Centre Southampton, University of Southampton Waterfront Campus, European Way, Southampton SO14 3ZH, United Kingdom

5.2.3.1 Background and Objectives

Carbon dioxide (CO_2) from the burning of fossil fuel and other anthropogenic activities greatly affects our atmosphere, and leads to global warming and climate change (Keeling, 1979; IPCC, 2007). Since the beginning of the industrial revolution, emission of carbon dioxide from anthropogenic activities have increased the atmospheric partial pressure of CO_2 (Ahn et al., 2012) by ~ 47% from the preindustrial value of about 280 ppm (Snyder et al., 2004) to a monthly average of 412.89 ppm recorded at Mauna Loa Observatory in November 2020 (www.esrl.noaa.gov/gmd/ccgg/trends/mlo.html) and these anthropogenic activities resulted in an increase of about 120 ppmv (Mackensen and Schmiedl, 2019). Thus, without immediate measures being taken, atmospheric CO_2 levels are to be further increased up to a level between 750 ppm and more than 1300 ppm by the end of this century (IPCC, 2014). It has been reported that global ocean has absorbed about 50% of the anthropogenic CO_2 emitted since the late 18th century (Sabine et al., 2004; Khatiwala et al., 2013) and currently absorbs about 25% of annual anthropogenic CO_2 emissions (Le Quéré et al., 2009). Hence, without this uptake of CO_2 by oceans, anthropogenic CO_2 in the atmosphere and its effects for global climate would be significantly greater (Humphreys et al., 2016a). Research on the effects of rising anthropogenic CO_2 levels in the atmosphere on carbon sequestration in the ocean and marine carbon cycle is ongoing. However, the results have been limited by the ability to study all carbon pools in parallel. Using unique methods to measure the isotopes of carbon in marine samples can help in elucidating the carbon cycle in more detail. In this study, marine carbon cycle, carbon fluxes and processes in the North Atlantic Ocean, particularly within the inner accumulation zone of the North Atlantic garbage patch will be studied using stable carbon isotopes in marine samples to understand how the oceanic processes react to increasing CO_2 levels in the atmosphere. Moreover, our study aims to assess the carbon export in this study area using carbon isotopes and to test the utility of carbon isotopes to understand the processes that support surface ocean productivity, and to establish a database with all these $\delta^{13}C$ measurements of dissolved and particulate carbon reservoirs.

5.2.3.2 Methods

A total of 7 stations were sampled along the transect from Emden (Germany) to Azores (Portugal) (Fig. 2.1) during the research cruise RV SONNE SO279. Seawater samples for $\delta^{13}C_{DIC}$ were collected following the best practice standard operating procedure (Dickson et al., 2007; McNichol et al., 2010). At every station seawater samples for $\delta^{13}C_{DIC}$ measurements were collected from most depths directly from the Niskin bottles through a piece of silicone tubing into pre-cleaned sample containers: (1) 40 mL Clean Borosilicate glass vials (with plastic screw caps and PTFE/silicone septa) and (2) pre-cleaned 100 and 250 mL Pyrex Borosilicate glass narrow mouth reagent bottles (with ground glass stoppers) straightaway after arrival of the stainless steel CTD rosette on the deck of the ship and immediately after opening the valves of the Niskin bottles. During sample filling, sample containers were first thoroughly rinsed with seawater, and then slowly filled with seawater by placing the silicone tube at the bottom of the sample container allowing to overflow with excess seawater (by at least a half or a full sample container volume) and care was taken to ensure that no air bubbles generate or trap inside the sample container prior to closure. Before sealing glass bottles, an air headspace of 1% of the bottle volume (i.e., 1 mL for a 100 mL bottle, 2.5 mL for a 250 mL bottle) was left in the bottle by removing 1 mL of seawater

for 100 mL bottle and 2.5 mL of seawater for 250 mL bottle using a 1 mL plastics syringe. This prevents thermal expansion and contraction of seawater when exposing the bottle to different temperatures before analysis (Dickson et al., 2007; Humphreys et al., 2016b). Nevertheless, the flexible septa on the 40 mL vial allowed them to be sealed when full of seawater. Then seawater samples were immediately poisoned by adding 0.02% of the sample container volume of saturated $HgCl_2$ using a 1-100 µL microliter syringe (for 40 mL vials) and a Thermo Scientific 10-100 µL finnipette pipette (for 100- and 250-mL glass bottles). After poisoning, vials were sealed air-tight with screw caps, and glass bottles were sealed air-tight with greased ground glass stoppers (greased with Apiezon® L grease), which were further fastened with duct tape. The sealed seawater sample vials and bottles were then gently inverted for several times to mix the poison and stored at 4 ºC in the dark environment to inhibit further biological activity or photo oxidation (Kroopnick et al., 1972; Shadwick et al., 2011; Cotovicz et al., 2019) until further laboratory analysis.

At every station seawater samples for the measurements of $\delta^{13}C_{DOC}$ collected from most depths directly from the Niskin bottles and DOC samples were also collected at all stations except station 4 and 7. Seawater samples were collected from the Niskin bottles using a silicone tube into 20 mL pre-combusted (at 450°C for 4 hours) glass ampoules by filtering through a polycarbonate inline filter holder in which a pre-combusted (at 450°C for 4 hours) GF/F filter (25 mm diameter, 0.7 µm pore sized) was placed to remove particulate carbon and organisms. Before collecting the samples into glass ampoules, care was taken to wash the filter in place and filter holder with seawater sample. Then samples were immediately preserved by acidifying with HCl (preferably 100 µL of 6M HCL) (Lee et al., 2020) to reduce the pH<2 (Sharp et al., 1993) using a BioHit M200 20-200 µL pipette and were then sealed tightly and stored at 4 ºC in the dark environment.

At every station, samples for the measurements of $\delta^{13}C_{POC}$ and $\delta^{13}C_{PIC}$ were collected from 5 depths onto pre-combusted (at 450 °C,4 hours) GF/B filters (293 mm diameter, 1 µm pore sized, shipped in aluminium foil pouches) by filtering large volume of water (~ 1500 L) using in situ pumps (Stand-Alone Pumps; SAPS). Immediately after filtration, filters were stored again in the same aluminium foil pouches and preserved deep frozen at -80 °C to -20 °C in a freezer until analysis (Liu et al., 2007, Brown et al., 2014).

5.2.3.3 Preliminary results

No preliminary data are available.

5.2.3.4. Work to be conducted in the home laboratory

$\delta^{13}C_{DIC}$ in seawater samples will be measured at the National Oceanography Centre Southampton (NOCS), University of Southampton, using a Thermo Scientific Delta V Advantage Continuous Flow Isotope Ratio Mass Spectrometer (CF-IRMS) attached to a Thermo Scientific GasBench II system and a CTC Analytics PAL Autosampler in a continuous flow condition, following the standard best practice procedures (Torres et al., 2005; Humphreys et al., 2016b).

DOC samples will be analysed at GEOMAR using the high temperature combustion technique using a Shimadzu TOC-TDN instrument and $\delta^{13}C_{DOC}$ in seawater samples will be measured at NOCS, University of Southampton, using the high temperature combustion method using a Thermolax TOC-TN analyzer attached to a Thermo Scientific Delta V Advantage Continuous Flow Isotope Ratio Mass Spectrometer.

$\delta^{13}C_{POC}$ in seawater samples will be measured at NOCS, University of Southampton, using the high temperature combustion method using a Thermo Scientific Flash 2000 Elemental analyzer attached to a Thermo Scientific Delta V Advantage Continuous Flow Isotope Ratio Mass Spectrometer.

5.2.4 Analysis of microplastic particles > 1 µm

(Oliver Jacob[1])

[1]IWC-TUM

5.2.4.1 Objectives

At different stations within the North Atlantic garbage patch, water samples of different depths as well as sediment samples of the top layer of the sediment at the seabed are to be analysed for their microplastic content. Microplastic particles (MPP) shall be analysed regarding number, sizes (maximum Feret diameters > 1 µm are to be considered), and plastic types. An analysis technique using automated Raman microspectroscopy (RM) has already been developed and validated for particle sizes > 10 µm (Esch et al., 2020). The reliable determination of particles down to 1 µm is the aim of further development. The measurements are intended to determine the microplastic pollution of this region, especially by small MPP.

The work is part of the HOTMIC project, work package 4.

5.2.4.2 Methods

Water samples from three or five different depths between 25 m and 300 m were collected at seven stations in total using a CTD rosette water sampler equipped with 10 L Niskin bottles, according to the following table (Table 5.8):

Table 5.8. List of samples for small microplastic analysis

Station #	Depths / m
1	25, 75, 300
22	25, 50, 80, 120, 300
36	25, 50, 75, 100, 300
53	25, 50, 75, 130, 300
69, 81, 102	25, 50, 75, 150, 300

All water subsamples were collected in glass bottles (1 L, Schott AG, Germany), which were thoroughly cleaned in advance of the cruise. Screw caps made from TpCH260 (Schott AG, Germany) were used to avoid contamination with commonly used plastic types. A blank of a Niskin bottle was generated. For this, after thorough rinsing, a Niskin bottle was filled with onboard generated MilliQ water. A sample (1 L) was taken in the same manner as for seawater samples. Additionally, a sample of the MilliQ water (1 L) was collected directly from the MilliQ system to account for possible particulate contamination within.

Sediment samples were collected at each of the above-named stations. Sediments were brought to the surface using a box corer. For subsampling cylindrical corers made from PMMA were used. The top 3 cm of each core (one per station) are stored separately in preserving jars (FloraCura GmbH, Germany), which were thoroughly cleaned in advance of the cruise. At three stations, blanks were additionally generated. During processing of the cylindrical cores, an additional open jar was placed nearby to account for possible airborne contamination.

5.2.4.3 Preliminary results

Preliminary results are not available.

5.2.4.4 Work to be conducted in home laboratory

After development and validation of a method for the determination of MPP (> 1 µm), water and sediment samples will be analysed for their microplastic content (at institute of hydrochemistry, TU München). Water samples are likely to need no additional processing step, since there is no significant amount of (non-plastic) solid matter to be expected. Due to limited laboratory capacities, measurements of water samples should only be conducted if they originate from stations for which corresponding measurements show significant amounts of MPP of the higher size range (> 10 µm).

Sediment samples must be subjected to additional processing to remove organic matter and separate plastic from non-plastic particles (to be done at GEOMAR, Kiel). Afterwards, the analysis of the purified samples for their microplastic content (particle sizes > 1 µm) will be conducted at the institute of hydrochemistry, TU München, as well.

Additional blanks of unused cleaned bottles and jars shall be examined to account for possible contamination after the cleaning step.

5.2.5 Per- and Polyfluoroalkyl Substances (PFASs) in Seawater from the North Atlantic Ocean

(Rui Shen[1])

[1] HZG

5.2.5.1 Background

Per- and polyfluoroalkyl substances (PFASs) embrace a large number of synthetic fluorinated organic chemicals with unique properties such as high surface activity, resistance to thermal and chemical degradation, and strong water and oil repellency. Due to these properties, PFASs have been developed for various industrial and commercial surfactant applications including lubricants, refrigerants, insecticides, adhesives, firefighting foams, repellants, paints, and cosmetics since 1950s. (Kissa, 2001; Lindstrom et al., 2011)

As a consequence of the widespread use of PFASs and their resulting emissions, a broad range of these substances have been detected in the environment,3-5 including locations in the remote polar and Alpine regions (Zhao et al., 2012; Codling et al., 2014; Wang et al., 2015; Xie et al., 2015; Kirchgeorg et al., 2016; Butt et al., 2010; Pickard et al., 2018; Yeung et al., 2017), wildlife (Giesy et al., 2001; Da Silva et al., 2005; Blevin et al., 2017; Butt et al., 2007), and humans (D'Eon et al., 2007; Loi et al., 2013).

Because of their ubiquitous presence, persistence, toxicity, tendency to bioaccumulate and biomagnify in food web as well as capacity for long-range transport (OECD, 2002), PFASs have become a serious concern to regulators and scientists worldwide (Ritscher et a., 2018). Since more than two decades, researcher have been dedicated to elucidate the environmental level, origin, transport, fate and impact of this class of contaminants.

The transport pathways of PFASs to the Arctic have not been conclusively characterized to date. Direct transport of ionic PFASs via oceanic currents is one of the main hypotheses. Inputs of surface waters from the North Atlantic and atmospheric deposition lead to accumulation of PFASs in Arctic surface waters. The majority of seawater inflows to the Arctic occurs from mid depth North Atlantic seawater (20 -200 m), which results in PFASs being present below the polar mixed layer (PML)(Yamashita et al., 2005; Prevedouros et al., 2006). However, measurements of PFASs in the aqueous environment in the N Atlantic is limited, and further research is needed to determine the transport pathways and global fate of PFASs.

The aim of the study is to investigate the source, transport and fate of PFASs from estuaries to the oceanic garbage patches in the North Atlantic. Water and sediment samples will be collected and analyzed from different depth of the water column at eight locations. The main focus is (1) to understand the spatial and vertical transfer of PFASs from the surface and near-surface waters to the deep sea of the N Atlantic gyre and on the processes that mediate this transport; (2) to access the roles of oceanic transport of PFASs into the Arctic Ocean.

5.2.5.2 Materials and Methods

Water samples (1 L/layer of water/location) were collected during expedition SO279 in December 2020 as follows: (1) seven locations in the N Atlantic from surface to bottom (up to 5000 m); and (2) surface water samples were taken onboard during transit via centrifugal pump (Table 5.9). Water samples were stored in 1 L polypropylene (PP) bottles. The sampling bottles were rinsed with seawater from sampling points before sampling. The seawater samples were stored at 4 °C in darkness before extraction. Six sediment samples were taken at six stations (Table 5.9). Sediment

samples were stored in aluminum boxes at -20 °C before extraction. All aluminum boxes were prerinsed with acetone.

Table 5.9. Sampling List

#	Sample ID	Field ID	Sample Type	Depth	Sampling Point	Sampling Date
1	SO279-01-CTD-1	SO279_1-1_CTD-22	CTD	10 m	47°15 N, 10°06 W	12/8/2020
2	SO279-01-CTD-2	SO279_1-1_CTD-20	CTD	25 m	47°15 N, 10°06 W	12/8/2020
3	SO279-01-CTD-3	SO279_1-1_CTD-19	CTD	50 m	47°15 N, 10°06 W	12/8/2020
4	SO279-01-CTD-4	SO279_1-1_CTD-17	CTD	75 m	47°15 N, 10°06 W	12/8/2020
5	SO279-01-CTD-5	SO279_1-1_CTD-14	CTD	150 m	47°15 N, 10°06 W	12/8/2020
6	SO279-01-CTD-6	SO279_1-1_CTD-12	CTD	300 m	47°15 N, 10°06 W	12/8/2020
7	SO279-01-CTD-7	SO279_1-1_CTD-10	CTD	775 m	47°15 N, 10°06 W	12/8/2020
8	SO279-01-CTD-8	SO279_1-1_CTD-9	CTD	1000 m	47°15 N, 10°06 W	12/8/2020
9	SO279-01-CTD-9	SO279_1-1_CTD-8	CTD	2000 m	47°15 N, 10°06 W	12/8/2020
10	SO279-01-CTD-10	SO279_1-1_CTD-7	CTD	3000 m	47°15 N, 10°06 W	12/8/2020
11	SO279-01-CTD-11	SO279_1-1_CTD-6	CTD	4000 m	47°15 N, 10°06 W	12/8/2020
12	SO279-01-CTD-12	SO279_1-1_CTD-1	CTD	bottom, ca. 4300 m	47°15 N, 10°06 W	12/8/2020
13	SO279-02-CTD-1	SO279_22-1_CTD-24	CTD	10 m	31°27 N, 24°81 W	12/13/2020
14	SO279-02-CTD-2	SO279_22-1_CTD-23	CTD	25 m	31°27 N, 24°81 W	12/13/2020
15	SO279-02-CTD-3	SO279_22-1_CTD-21	CTD	50 m	31°27 N, 24°81 W	12/13/2020
16	SO279-02-CTD-4	SO279_22-1_CTD-19	CTD	80 m	31°27 N, 24°81 W	12/13/2020
17	SO279-02-CTD-5	SO279_22-1_CTD-17	CTD	120 m	31°27 N, 24°81 W	12/13/2020
18	SO279-02-CTD-6	SO279_22-1_CTD-14	CTD	500 m	31°27 N, 24°81 W	12/13/2020
19	SO279-02-CTD-7	SO279_22-1_CTD-13	CTD	1000 m	31°27 N, 24°81 W	12/13/2020
20	SO279-02-CTD-8	SO279_22-1_CTD-8	CTD	2000 m	31°27 N, 24°81 W	12/13/2020
21	SO279-02-CTD-9	SO279_22-1_CTD-7	CTD	3000 m	31°27 N, 24°81 W	12/13/2020
22	SO279-02-CTD-10	SO279_22-1_CTD-6	CTD	4000 m	31°27 N, 24°81 W	12/13/2020
23	SO279-02-CTD-11	SO279_22-1_CTD-3	CTD	bottom, ca 5400 m	31°27 N, 24°81 W	12/13/2020
24	SO279-03-CTD-1	SO279_36-1_CTD-24	CTD	10 m	30°53 N, 29°18 W	12/16/2020

25	SO279-03-CTD-2	SO279_36-1_CTD-23	CTD	25 m	30°53 N, 29°18 W	12/16/2020
26	SO279-03-CTD-3	SO279_36-1_CTD-21	CTD	50 m	30°53 N, 29°18 W	12/16/2020
27	SO279-03-CTD-4	SO279_36-1_CTD-19	CTD	75 m	30°53 N, 29°18 W	12/16/2020
28	SO279-03-CTD-5	SO279_36-1_CTD-18	CTD	100 m	30°53 N, 29°18 W	12/16/2020
29	SO279-03-CTD-6	SO279_36-1_CTD-15	CTD	300 m	30°53 N, 29°18 W	12/16/2020
30	SO279-03-CTD-7	SO279_36-1_CTD-14	CTD	500 m	30°53 N, 29°18 W	12/16/2020
31	SO279-03-CTD-8	SO279_36-1_CTD-13	CTD	1000 m	30°53 N, 29°18 W	12/16/2020
32	SO279-03-CTD-9	SO279_36-1_CTD-12	CTD	2000 m	30°53 N, 29°18 W	12/16/2020
33	SO279-03-CTD-10	SO279_36-1_CTD-11	CTD	3000 m	30°53 N, 29°18 W	12/16/2020
34	SO279-03-CTD-11	SO279_36-1_CTD-1	CTD	bottom, ca. 4300 m	30°53 N, 29°18 W	12/16/2020
35	SO279-04-CTD-1	SO279_53-1_CTD-24	CTD	10 m	31°7 N, 33°48 W	12/18/2020
36	SO279-04-CTD-2	SO279_53-1_CTD-23	CTD	25 m	31°7 N, 33°48 W	12/18/2020
37	SO279-04-CTD-3	SO279_53-1_CTD-20	CTD	50 m	31°7 N, 33°48 W	12/18/2020
38	SO279-04-CTD-4	SO279_53-1_CTD-19	CTD	75 m	31°7 N, 33°48 W	12/18/2020
39	SO279-04-CTD-5	SO279_53-1_CTD-16	CTD	130 m	31°7 N, 33°48 W	12/18/2020
40	SO279-04-CTD-6	SO279_53-1_CTD-15	CTD	300 m	31°7 N, 33°48 W	12/18/2020
41	SO279-04-CTD-7	SO279_53-1_CTD-13	CTD	500 m	31°7 N, 33°48 W	12/18/2020
42	SO279-04-CTD-8	SO279_53-1_CTD-12	CTD	1000 m	31°7 N, 33°48 W	12/18/2020
43	SO279-04-CTD-9	SO279_53-1_CTD-11	CTD	2000 m	31°7 N, 33°48 W	12/18/2020
44	SO279-04-CTD-10	SO279_53-1_CTD-7	CTD	3000 m	31°7 N, 33°48 W	12/18/2020
45	SO279-04-CTD-11	SO279_53-1_CTD-1	CTD	bottom, ca. 4400 m	31°7 N, 33°48 W	12/18/2020
46	SO279-05-CTD-1	SO279_69-1_CTD-24	CTD	10 m	33°17 N, 34°29 W	12/20/2020
47	SO279-05-CTD-2	SO279_69-1_CTD-23	CTD	25 m	33°17 N, 34°29 W	12/20/2020
48	SO279-05-CTD-3	SO279_69-1_CTD-20	CTD	50 m	33°17 N, 34°29 W	12/20/2020
49	SO279-05-CTD-4	SO279_69-1_CTD-19	CTD	75 m	33°17 N, 34°29 W	12/20/2020
50	SO279-05-CTD-5	SO279_69-1_CTD-16	CTD	150 m	33°17 N, 34°29 W	12/20/2020
51	SO279-05-CTD-6	SO279_69-1_CTD-14	CTD	500 m	33°17 N, 34°29 W	12/20/2020
52	SO279-05-CTD-7	SO279_69-1_CTD-12	CTD	1000 m	33°17 N, 34°29 W	12/20/2020

53	SO279-05-CTD-8	SO279_69-1_CTD-8	CTD	2000 m	33°17 N, 34°29 W	12/20/2020
54	SO279-05-CTD-9	SO279_69-1_CTD-7	CTD	3000 m	33°17 N, 34°29 W	12/20/2020
55	SO279-05-CTD-10	SO279_69-1_CTD-1	CTD	bottom, ca. 3590 m	33°17 N, 34°29 W	12/20/2020
56	SO279-06-CTD-1	SO279_81-1_CTD-24	CTD	10 m	33°08 N, 33°46 W	12/21/2020
57	SO279-06-CTD-2	SO279_81-1_CTD-22	CTD	25 m	33°08 N, 33°46 W	12/21/2020
58	SO279-06-CTD-3	SO279_81-1_CTD-21	CTD	50 m	33°08 N, 33°46 W	12/21/2020
59	SO279-06-CTD-4	SO279_81-1_CTD-18	CTD	75 m	33°08 N, 33°46 W	12/21/2020
60	SO279-06-CTD-5	SO279_81-1_CTD-17	CTD	100 m	33°08 N, 33°46 W	12/21/2020
61	SO279-06-CTD-6	SO279_81-1_CTD-13	CTD	500 m	33°08 N, 33°46 W	12/21/2020
62	SO279-06-CTD-7	SO279_81-1_CTD-11	CTD	1000 m	33°08 N, 33°46 W	12/21/2020
63	SO279-06-CTD-8	SO279_81-1_CTD-10	CTD	2000 m	33°08 N, 33°46 W	12/21/2020
64	SO279-06-CTD-9	SO279_81-1_CTD-9	CTD	3000 m	33°08 N, 33°46 W	12/21/2020
65	SO279-06-CTD-10	SO279_81-1_CTD-1	CTD	bottom	33°08 N, 33°46 W	12/21/2020
66	SO279-07-CTD-1	SO279_102-1_CTD-24	CTD	10 m	35° N, 21° W	12/27/2020
67	SO279-07-CTD-2	SO279_102-1_CTD-23	CTD	25 m	35° N, 21° W	12/27/2020
68	SO279-07-CTD-3	SO279_102-1_CTD-21	CTD	50 m	35° N, 21° W	12/27/2020
69	SO279-07-CTD-4	SO279_102-1_CTD-18	CTD	75 m	35° N, 21° W	12/27/2020
70	SO279-07-CTD-5	SO279_102-1_CTD-17	CTD	90 m	35° N, 21° W	12/27/2020
71	SO279-07-CTD-6	SO279_102-1_CTD-16	CTD	150 m	35° N, 21° W	12/27/2020
72	SO279-07-CTD-7	SO279_102-1_CTD-13	CTD	500 m	35° N, 21° W	12/27/2020
73	SO279-07-CTD-8	SO279_102-1_CTD-12	CTD	750 m	35° N, 21° W	12/27/2020
74	SO279-07-CTD-9	SO279_102-1_CTD-11	CTD	1000 m	35° N, 21° W	12/27/2020
75	SO279-07-CTD-10	SO279_102-1_CTD-10	CTD	2000 m	35° N, 21° W	12/27/2020
76	SO279-07-CTD-11	SO279_102-1_CTD-9	CTD	3000 m	35° N, 21° W	12/27/2020
77	SO279-07-CTD-12	SO279_102-1_CTD-8	CTD	4000 m	35° N, 21° W	12/27/2020
78	SO279-07-CTD-13	SO279_102-1_CTD-1	CTD	bottom, ca. 5000 m	35° N, 21° W	12/27/2020
79	SO279-UWS-1	*to be extracted from DSHIP*	surface water	6 m	*to be extracted from DSHIP*	12/10/2020
80	SO279-UWS-2	*to be extracted from DSHIP*	surface water	6 m	*to be extracted from DSHIP*	12/11/2020

81	SO279-UWS-3	*to be extracted from DSHIP*	surface water	6 m	*to be extracted from DSHIP*	12/12/2020
82	SO279-UWS-4	SO279_33-1_UWS	surface water	6 m	31°10 N, 27°25 W	12/15/2020
83	SO279-UWS-5	SO279_50-1_UWS	surface water	6 m	31°08 N, 27°25 W	12/18/2020
84	SO279-UWS-6	*to be extracted from DSHIP*	surface water	6 m	*to be extracted from DSHIP*	12/21/2020
85	SO279-UWS-7	*to be extracted from DSHIP*	surface water	6 m	*to be extracted from DSHIP*	12/24/2020
86	SO279-UWS-8	*to be extracted from DSHIP*	surface water	6 m	*to be extracted from DSHIP*	12/25/2020
87	SO279-UWS-9	*to be extracted from DSHIP*	surface water	6 m	*to be extracted from DSHIP*	12/26/2020
88	SO279-UWS-10	SO279_112-1_UWS	surface water	6 m	37°48 N, 17°51 W	12/29/2020
89	SO279-UWS-11	SO279_115-1_UWS	surface water	6 m	40°28 N, 14°58 W	12/30/2020
90	SO279-BC-1	SO279_8-1_BC	box core	4300 m	47°15 N, 10°06 W	12/10/2020
91	SO279-BC-2	SO279_27-1_BC	box core	5400 m	31°16 N, 24°28 W	12/13/2020
92	SO279-BC-3	SO279_39-1_BC	box core	4300 m	30°53 N, 29°18 W	12/16/2020
93	SO279-BC-4	SO279_60-1_BC	box core	4400m	31°21 N, 34°02 W	12/18/2020
94	SO279-BC-5	SO279_83-1_BC	box core	3700 m	33°08 N, 33°46 W	12/20/2020
95	SO279-BC-6	SO279_104-1_BC	box core	5000 m	35°00 N, 21°00 W	12/27/2020

5.3 Underway pump sampling

5.3.1 Application of continuous flow centrifugation and fractionated filtration to sample microplastics

(Tristan Zimmermann[1], Lars Hildebrandt[1], Daniel Pröfrock[1])

[1] HZG

5.3.1.1 Background and Objectives

Research of microplastic contamination in aquatic systems is in great need for methodological standardization. Currently there is no "standard operating procedure" - neither for sampling the water column nor for subsequent analysis of microplastic (MP) particles. The Department Marine Bioanalytical Chemistry at the Helmholtz-Zentrum Geesthacht develops new analytical tools for sampling and analysis of MP in the aquatic environment.

Aim of our experiments conducted on board RV Sonne was a proof of concept for the application of continuous flow centrifugation (CFC) for the extraction of MPs from ocean water. CFC is an alternative volume-reduced sampling technique to sample the entire load of suspended particulate matter including MP in natural waters. Based on first lab-scale experiments, CFC proves a promising technique bearing potential to alleviate drawbacks such as contamination, filter clogging and particle size-discrimination of commonly used volume-reduced MP sampling approaches (Hildebrandt et al. 2019). Furthermore, CFC has proven to be a very promising technique for nanoplastic sampling and enrichment from natural water samples (Hildebrandt et al. 2020).

In addition to CFC we were applying an in-house developed, fully enclosed sieving cascade for extraction of MP from water (Geesthacht Inert Microplastic Fractionator). The system has already been successfully applied for MP sampling during cruise SO270 (RV SONNE) in the Indian Ocean (Gareb et al. in preparation)

5.3.1.2 Methods

Continuous flow centrifugation (CFC)

A continuous flow centrifuge (Contifuge Stratos, Thermo Scientific, Waltham, United States) in conjunction with a titanium rotor with a sedimentation capacity of 300 mL (Continuous Flow Rotor 3049, Thermo Scientific) was used to extract suspended particulate matter (SPM) from the water phase. Water was taken from the ships seawater system (centrifugal pump). For all centrifugal runs a peristaltic pump (Masterflex L/S, Cole-Parmer, Vernon Hills, United States) was applied to pump approx. 5 L/min of water from a 5 L beaker through the rotating centrifuge rotor. After centrifugation, 10% (w/w) SDS solution were added (for stabilization) to the rotor content prior to ultrasonication for 15 min to avoid adhesion to the vessels. The suspension was stored in glass bottles for further analysis.

Geesthacht Inert Microplastic Fractionator (GIMPF)

The system offers two channels, in case one of the two candle filters in one channel is clogged (300 µm and 10 µm stainless steel cfilters (19 ¾ inch) the operator can simply switch to the second sampling channel. The entire system is made of stainless steel and all seals are PFA coated in order to minimize potential blanks. The system is fed with water by a submersible pump located in the ships moon pool. The intake hose feeding the GIMPF with seawater has a corresponding PFTE insert. At each sampling location two samples (each consisting of one > 300 µm and one 10 µm –

300 µm size fraction) were taken. The filtrated volume for each sample was about 2 m³. Particles were rinsed of the filters, the suspension was filtrated via 5 µm PTFE filters. Subsequently filters were stored in SDS solution for further analysis. Because of issues with the used submersible pump, water was taken from the ships seawater system (membrane pump) for selected samples.

5.3.1.3 Preliminary results

No results available yet

5.3.1.4 Work to be conducted in home laboratory

The collected samples have to be subjected to a sample preparation protocol, in order to remove matrix components prior to analysis via LDIR (Laser Direct Infrared) analysis.

Sample preparation will consist of a microwave assisted one-pot approach with in total three steps using proteinase K, Fenton reagent and chitinase, followed by a density separation using $ZnCl_2$ solution. A process that has been fully validated via different in-house reference MPs.

After sample preparation, the collected MPs will be analyzed for their chemical composition and particle number concentrations via LDIR imaging. LDIR imaging is a new analytical method for the identification and quantification of MP and has been introduced very recently (2019).

5.3.2 Trace metal-clean fish and surface water pump system

(Aaron J. Beck[1], André Mutzberg[1], Eric Achterberg[1])

[1] GEOMAR

A trace metal-clean "fish" was deployed first on 13.12.2020, and consisted of a stainless-steel torpedo-shaped holder for metal-free plastic tubing (Fig. 5.14). The fish was deployed from the aft starboard crane (Crane 3) outside the ship's wake, and provided a source of pumped clean water while the ship was underway. Reinforced PVC tubing was secured in the fish so that the tubing inlet extended away from the metal nose and sampled only untouched water. The tubing was connected to a double-diaphragm Teflon pump actuated by the ship's compressed air supply. The pump outlet was arranged under a portable HEPA hood to prevent contamination during sampling.

Waters samples from the fish were primarily used for trace metal analysis (see section 5.4.3), and also for a large-volume reference seawater sample (~1000 L). The large volume sample was filtered through a 0.8/0.2 µm Acropak Supor cartridge filter directly into a clean 1000 L polyethylene tank. The large volume sample was collected during transit between 31° 21.5 N/30° 53.4 W and 31°08.3 N/33° 30.9 W.

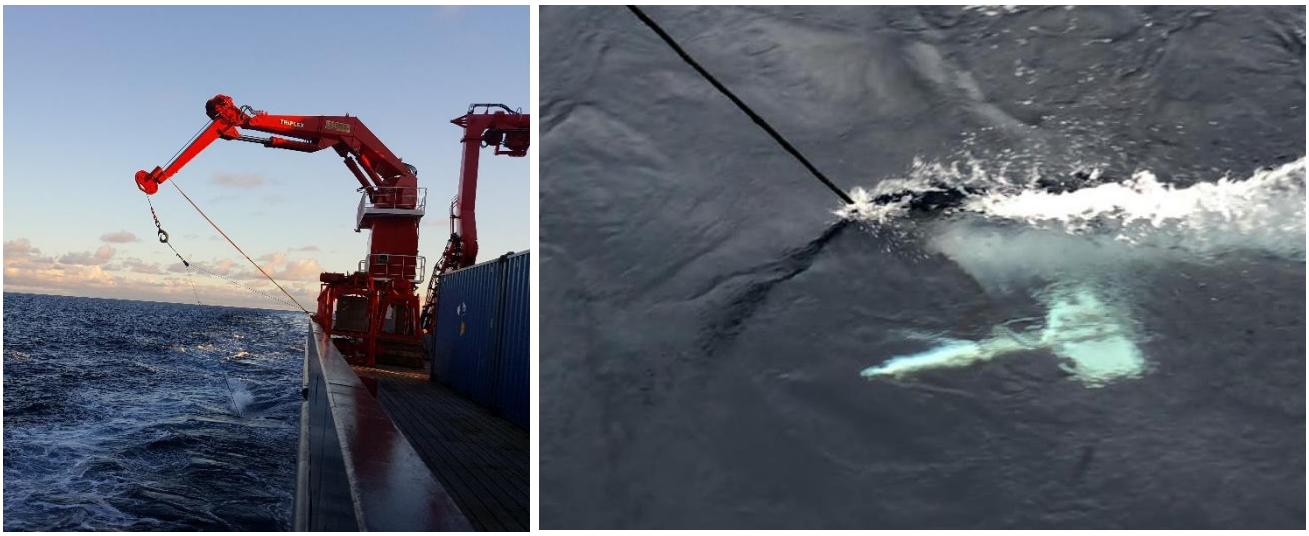

Figure 5.14. Trace metal-clean fish deployed from Crane 3 (left), in the water (right).

5.4 Sediment sampling

5.4.1 Abundance, composition, and size distribution of MP particles in seafloor sediments

(Elke Kossel[1], Gabriella Panto[2], Sarah-Marie Kröger[1], Jannes Hoffmann[1], Ann Vanreusel[2], Matthias Haeckel[1])

[1] GEOMAR
[2] UGent

5.4.1.1 Background and Objectives

GEOMAR

The HOTMIC project aims at the quantification of lateral and vertical transport processes and the distribution of microplastic particles from the coast to the open ocean and from the sea surface to the seafloor. The main focus is on the vertical transfer of plastic debris from the surface and near-surface waters to the deep sea of the North Atlantic gyre and on the processes that mediate this transport. Seafloor sediments are expected to be the final sink of microplastic particles in the marine environment, where they get buried over geological time scales. During the cruise SO279, we collected sediment samples for subsequent microplastics extraction, quantification and spectroscopic identification. One additional core per station was collected for geochemical analyses (major cations and anions, POC, $CaCO_3$, PON, S, porosity, ^{210}Pb). This data will be used for a general biogeochemical characterization of the sediments, including mixing of surface sediments due to bioturbation.

UGent

The presence of microplastics (MPs) in the marine environment is now considered ubiquitous, since they have been recorded from surface waters to sediments, from coastal areas to deep sea bottom, and from fish tissues to zooplankton guts (Andrady 2011; Nelms et al. 2018; Filgueiras 2019; Pohl et al. 2020). The effects of plastics on ecosystem functioning have been investigated in a number of studies, yet there are still gaps in knowledge to be filled, especially concerning the benthic intake of MPs and possible consequences (Fueser et al. 2019). The inevitable destiny of MP particles suspended in the water column is to eventually sink to the sea bottom (even at abyssal depths), where they likely interact with the surrounding environment. Our main objective is to assess MPs distribution within the vertical profile of the seabed and couple it with the burial potential of benthic organisms. Moreover, we intend to identify and analyze the possible effects of MPs on benthos, as well as their potential influence on trophic relationships.

5.4.1.2 Methods

Box corer

The large Box Corer (BC) is used to recover a sediment volume of up to 50 x 50 x 50 cm^3 with an undestroyed sediment surface sample from the ocean floor. It was lowered into the sediment with a rope speed of 0.5 to 0.7 m/s, depending on the sediment hardness. A pinger was attached to the cable at 50 meters above the coring device. The box corer was deployed at all stations (Table 5.9). A total of two box corers came up empty because an entangled steel cable prevented the triggering of the device (BC1 and BC13). These deployments could be successfully repeated. Sediment samples for further processing were either collected from the surface or sub-sampled with MUC liners (Fig. 5.15). Recovered cores had a length of 12 to 40 cm. The cores were sampled on board and the samples were stored for land-based analyses

Multiple corer

The multiple corer (MUC) is equipped with 12 perspex liners with an internal diameter of 9.5 cm and can be used to sample undisturbed sediment cores including the overlying bottom water. Due to the high content of $CaCO_3$ in the seafloor sediments at most stations, the MUC could not be deployed since it does not penetrate into these rather hard sediments. A test deployment at station 1 came back empty from the seafloor and time constraints prevented furthers tests with this device. These observations are consistent with experiences from the HOTMIC cruise POS536, where MUC deployment also failed in this area.

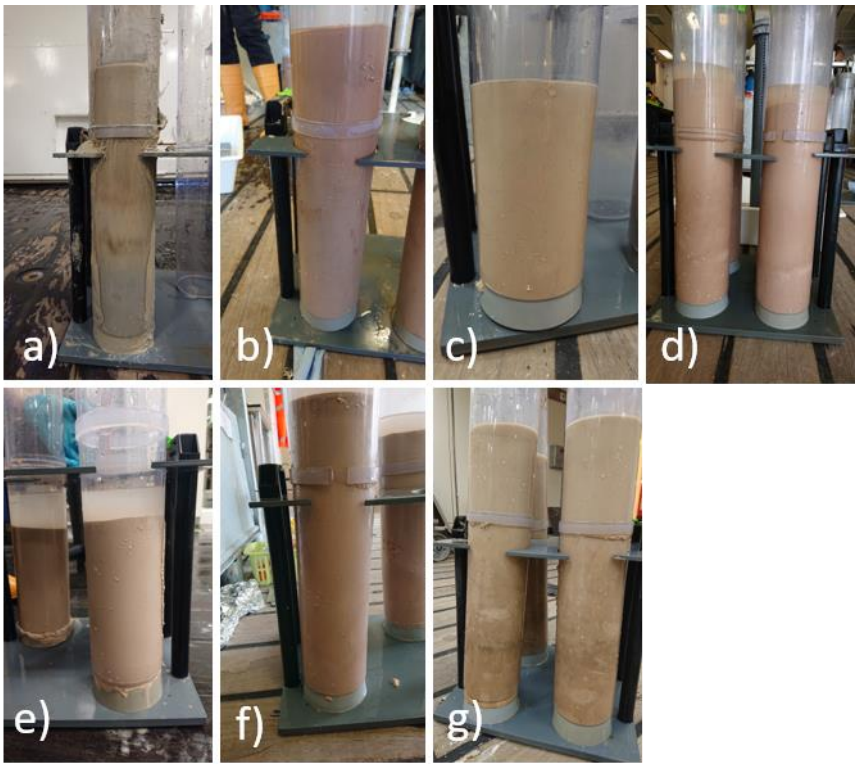

Figure 5.15. Photos of sediment samples that were extracted from box cores: a) 8BC2, b)27BC5, c) 40BC7, d) 60BC9, e) 73BC11, f) 89BC14, g) 105BC16

Sediment sampling: GEOMAR

For geochemical analyses, full MUC liner sub-samples of cores 8BC2, 27BC5, 40BC7, 60BC9, 73BC11, 89BC14 and 105BC16 were sliced. The sectioning had a depth resolution of 1 cm for the top 10 cm of the core and 2 cm for deeper parts. Porewater from the sediments was extracted with rhizones. 1 ml aliquots were mixed with 10 µl suprapure HNO_3 for land based ICP-AES analyses. For microplastics analyses, sub samples from the same box cores were cut into 4 subsequent sections of 3-cm thickness and stored in preservation jars.

Sediment sampling: UGent

A metal plate was used to divide the first Boxcorer into two equal parts. The first half was collected in buckets and sieved on board over a 1 mm sieve, in order to separate bigger macrofauna organisms from finer sediment particles. In the case of detection of microplastics particles, those items were carefully removed and analyzed with a hyperspectral infra-red camera. The remaining content of the sieved sediment was stored in 8% formaldehyde buffered with sea water.

Three cores were inserted in the second half of the Boxcorer, the overlying water was removed and the cores were recovered and processed as follows: All the cores were sliced into 1 cm slices up to 10 cm depth. Overlying water was previously sieved over a 32 µm sieve and was

subsequently added to the first 0-1 cm layer. Each slice was stored in formaldehyde 8% and will be used for the characterization of the meiobenthic community structure at each station.
Three additional cores were inserted in the second Boxcorer, recovered and processed as follows: the first 10 cm of the cores were sliced into 1 cm slices. Each slice was positioned on Aluminum foil to limit contamination and divided into 4 subsamples.

Each subsample was stored according to the relative analysis to be performed. Specifically:

- Subsample 1 & 2: two 4 cm diameter rings were cut out and stored in Aluminum trays at -20 °C. The two metal rings were positioned in the inner portion of the slice to avoid contamination with the outer sediment (in contact with the plastic core during deployment). These subsamples will be each used for i) the quantification and characterization of microplastics (MPs) in the sediment and ii) the potential ingestion of MPs from meiofauna organisms;

- Subsample 3: a small portion of sediment was collected with a metal spatula, stored in scintillation vials and preserved at - 80 °C for the analysis of Chlorophyll *a*.

- Subsample 4: the remaining sediment was stored at - 20 °C in plastic bags for the analysis of other pigments, total organic matter (TOM) and sediment grain size;

Table 5.9. List of stations for sediment corer deployments with date, time, coordinates (ship coordinates and pinger coordinates) and water depth. MUC: multiple corer. BC: box corer.

Ship Station	Date	Area	Latitude Ship (N)	Longitude Ship (E)	Latitude Pinger (N)	Longitude Pinger (E)	Water Depth / m	Device	Comments
SO279_1_4_MUC-1	8.12.2020	Station 1	47°15,008'N	010°06,283'W			4421	MUC	empty
SO279_1_5_BC-1	8.12.2020	Station 1	47°15,006'N	010°06,283'W			4424	BC	empty
SO279_1_8_BC-2	9.12.2020	Station 1	47°15,038`N	010°06,215'W			4427	BC	
SO279_1_9_BC-3	9.12.2020	Station 1	47,15,012'N	010°06,281'W			4677	BC	
SO279_1_25_BC-4	14.12.2020	Station 3	31°16,049'N	024°48,705'W			5499	BC	
SO279_27-1_BC-5	14.12.2020	Station 3	31°16,054'N	024'48,710'W	31°16,052'N	024'48,694,'W	5488	BC	
SO279_39-1_BC-6	16.12.2020	Station 4	30°53,544'N	029°18,837'W	30°53,550'N	029°18,804'W	4332	BC	
SO279_40-1_BC-7	16.12.2020	Station 4	30°53,545'N	029°18,838'W	30°53,538'N	029°18,832'W	4332	BC	
SO279_59-1_BC-8	19.12.2020	Station 5	31°21,398'N	034°02,278'W	31°21,400'N	034°02,258'W	4401	BC	
SO279_60-1_BC-9	19.12.2020	Station 5	31°21,402'N	034°02,268'W	31°21,401'N	034°02,265'W	4398	BC	
SO279 72-1 BC-10	20.12.2020	Station 6	33°17,643'N	034°29,499'W	33°17,635'N	034°29,482'W	3594	BC	
SO279_73-1_BC-11	20.12.2020	Station 6	33°17,607'N	34°29,483'W	33°17,618'N	34°29,472'W	3593	BC	
SO279_83-1_BC-12	21.12.2020	Station 7	33°08,608'N	33°46,719'W	33°08,593'N	33°46,709'W	3675	BC	
SO279_85-1_BC-13	21.12.2020	Station 7	33°08,610'N	33°46,718'W			3673	BC	empty
SO279_89-1_BC-14	22.12.2020	Station 7	33°08,586'N	33°46,707'W	33°08,600'N	33°46,709'W	3675	BC	
SO279 104-1 BC-15	27.12.2020	Station 9	35° 00,010 N	20° 59,991 W	34° 59,986'N	21° 00,010' W	5193	BC	
SO279 105-1 BC-16	27.12.2020	Station 9	35° 00,011 N	21° 00,004 W	35° 00, 015'N	21° 00,006' W	5193	BC	

5.4.1.3 Preliminary results

No further analyses were performed during the cruise SO279 and land-based analyses were not started at the time when this cruise report was compiled. Hence, no preliminary results are available for the time being.

5.4.1.4 Work to be conducted in home laboratory

GEOMAR

Shore-based analyses include geochemical analyses and microplastics quantification. Sediment porosities will be calculated from weight difference before and after freeze-drying. Porewater will be analyzed for major anions and cations using ICP-AES and IC, respectively. Particulate organic carbon and nitrogen, total sulfur and $CaCO_3$ contents of the solid phase will be determined by complete and instantaneous oxidation of the freeze-dried, ground and homogenized sample and subsequent chromatographic identification of the combustion products. Isotope analyses of the solid phase will be used for modeling of the bioturbation process. Geochemical data are expected to be available by July 2021.

Sediment samples for microplastic quantification will be dried to avoid strong microbial degradation and fouling during storage. As a next step, microplastic particles will be extracted by density separation and filtering using an established protocol and Raman spectroscopy will be used for polymer identification. This work is planned for 2022.

UGent

Macrofauna specimens collected from the Boxcorer will be identified at the binocular in the MarBiol laboratory in UGent. Community structure and diversity will be investigated at each station. Coupled with the analysis of the vertical distribution of MPs within the sediment layers, the bioturbation potential of macrofauna organisms will be used to evaluate the possible burial of MPs in the deeper layers of the sediment.

Subsamples from the cores will be used for several analysis:

- Meiofauna extracted from the first three cores will be used to assess the community structure at each station.
- MPs will be extracted from subsamples 1 and 2, respectively from sediment and from meiofauna, counted and identified. These will provide i) the vertical profile of MPs within the sediment layers and i) possible information on meiofauna ingestion of MPs.
- Environmental parameters will be analyzed from subsample 3 (vertical distribution of Chl *a*) and subsample 4 (vertical distribution of other pigments and TOM, sediment grain size information).

All the above-mentioned data will help outlining the characteristics of the benthic ecosystem at each station and understand the interaction of MPs with the benthic habitat in the deep sea, in an area supposedly characterized by high concentration of microplastics.

5.4.2 Plastic degrading enzymes in deep sea environments in the north Atlantic garbage patch

(Rebecka Molitor[1])

[1] IMET-FTJ

5.4.2.1 Background and Objectives

The extensive use of plastics material has led to a dramatic littering problem in our environment which urges the search for novel biocatalysts hoping that appropriate enzymes may be used to degrade and even recycle plastic waste.

Hydrolases capable to attack polyesters represent an example for such biocatalysts. The PETase from the ß-Proteobacteria *Ideonella sakaiensis* (Isa) has been already proven to be such a biocatalyst which developed on a PET waste recycling site (1-4). It is reasonable to assume that novel polyester hydrolases are produced by bacteria which encounter freely floating plastic waste particles. Such particles are a perfect medium for colonization in most marine environments and certain bacterial species may have evolved mechanisms to utilize them as a carbon or nitrogen source. However, not only free-floating plastics but also sedimented plastic at the sea floor might be a breeding ground for new polymer degrading mechanisms in bacteria.

Therefore, we will try to isolate and cultivate marine bacteria from sediment from different stations around the north Atlantic garbage patch to see if we are able to find and identify novel plastic degrading enzymes. In addition, we will try to isolate the environmental DNA and make functional metagenomic libraries for screening.

5.4.2.2 Methods

The sampling took place on the research vessel SONNE between the 4th of December 2020 and the 5th of January 2021 during the cruise SO279. The sampling sites were in the North Atlantic garbage patch as well as two stations on the way to the North Atlantic garbage patch north of the Azores.

At every station two box cores were taken. Samples were taken from the surface of the first box core. A metal spoon cleaned with filtrated water was used for taking three spoons of surface sediments of the first two centimeters from the box core and put into a sterile 50 ml falcon tube. From one box core two samples were taken. One was filled up with filtrated sea water and kept cool at 4 °C for enrichment cultures. The other one was left as it is and frozen at -20 °C for the isolation of environmental DNA in the laboratory. Sample IDs, depth and position dates are listed in Table 5.10.

Table 5.10. Station descriptions and sampling depths of the sampled box cores

Station name	Timestamp	Device	Latitude	Longitude	Depth (m)
SO279_8-1 BC	09.12.2020 09:14	Box Corer	47° 15,035' N	010° 06,216' W	4428.27
SO279_25-1 BC	14.12.2020 08:39	Box Corer	31° 16,048' N	024° 48,707' W	5496.00
SO279_39-1 BC	16.12.2020 12:20	Box Corer	30° 53,545' N	029° 18,836' W	4333.38
SO279_60-1 BC	19.12.2020 09:06	Box Corer	31° 21,398' N	034° 02,274' W	4396.95
SO279_72-1 BC	20.12.2020 13:24	Box Corer	33° 17,647' N	034° 29,505' W	3591.50
SO279_85-1 BC	21.12.2020 23:47	Box Corer	33° 08,612' N	033° 46,715' W	3674.16
SO279_104-1 BC	27.12.2020 15:54	Box Corer	35° 00,002' N	020° 59,980' W	5190.77

5.4.2.3 Preliminary results

No preliminary results are available.

5.4.2.4 Work to be conducted in home laboratory

The sediment will be incubated in different bacterial growth media as well as different temperatures and agitation speeds to higher the chances of enrichment of suitable bacteria. Successfully grown cultures will be isolated and tested with an agar plate based polyester degradation assay with the suitable environmental parameters to screen for degradation activities. The genome of the bacteria will then be sequenced, and the potential gene will be isolated and heterological expressed in Escherichia coli for further biochemical characterization.

The environmental DNA will be isolated using a suitable metagenome isolation kit and a functional metagenomic library will be created with E. coli and the activities will be tested on plate based polyester degradation assays. Successful candidates will be isolated and further tested for their degradation capabilities. The successful enzyme will then be biochemically characterized and analyzed. Further mutagenesis might then be used to further improve the catalytic activities.

Time first results are expected: End 2021.

5.4.3 Metal fluxes at the sediment-bottom water interface

(Feifei Deng[1])

[1] HZG

5.4.3.1 Methods

In the constant temperature laboratory, the core was carefully placed on the core extruder with the bottom bung removed, and the top inserted into a glove bag prepurged with Alphagaz^{TM} 1 N_2 of 99.999% purity through an 'X' cut. The 'X' cut was then sealed with electrical tape before the glove bag was purged another 3 times with N_2 to create an O_2-free environment for extruding and slicing the sediment. Excess overlying core water was removed to waste using a syringe, and the core was extruded at 1 cm resolution for the surface 0-6 cm, then at 2 cm resolution to ~ 20 cm, using polycarbonate sectioning rings and a plastic plate and spatula. Sediment slices were transferred directly to 50 mL HCl-cleaned centrifuge tubes, and capped tightly.

Centrifuge tubes with sediment slices were then transferred to a centrifuge to spin at 4°C, and at a speed of 9,000 rpm for 10 minutes, to separate the pore water from the solid phase of the sediment. Spun sediments were then returned to a clean glove Bag pre-purged with N_2. In the glove bag, centrifuge tubes were reopened and supernatant pore water from each sediment slice was extracted using a Teflon tubing attached to an acid cleaned 20 mL syringe and then filtered through a Whatman® Puradisc 30 syringe filter (Cellulose Acetate, pore size 0.2 µm, diameter 30 mm) into a 15mL acid cleaned DigiTUBE. These porewater samples were then acidified with 6M HCl diluted from ROTIPURAN®Ultra 34 % to pH ~ 1.7, capped, sealed with parafilm and stored at 4^{o}C until return to home laboratory for trace metal and isotope analysis. An aliquot of porewater, between 1 and 3 mL, was transferred into another 50 mL acid cleaned DigiTUBE, sealed and frozen at -20^{o}C until return to home laboratory for analysis of nutrients.

After porewater was transferred to the clean tubes, the sediment residue was stored in the centrifuge tube and stored at 4^{o}C until return to home laboratory for analysis. A summary of the sediment samples is listed in Table 5.11.

Water sampling

Seawater samples were collected from the bottom 2 water depths directly from the stainless steel CTD rosette into acid cleaned sample bottles rinsed 3 times with the seawater. Seawater collected from each depth was then transferred into a Teflon reservoir and pressured by Alphagaz^{TM} 1 N_2 of 99.999% purity through acid cleaned and preweighed Whatman^{TM} nuclepore polycarbonate filter (0.45 µm pore size, 47 mm diameter) housed in an acid cleaned Teflon filter holder. About 500 mL filtered seawater was collected into a LDPE bottle, acidified with 6M HCl diluted from ROTIPURAN®Ultra 34 % to pH~ 1.7, sealed, and double bagged before storage at 4^{o}C. After filtration of 7L of seawater, the filter was gently removed from the filter holder using ceramic tweezers, placed in an acid-cleaned petri dish, and frozen at -20^{o}C until analysis.

Another 7 L of seawater from the bottom 2 depths was filtered through ashed, Milli-Q cleaned, and pre-weighed Whatman® GFF glass fibre filter (0.7 µm pore size, 47 mm diameter) using a 250 mL Millipore filtration apparatus with an applied vacuum. Following filtration, the filter was gently removed from the filter holder using ceramic tweezers, placed in an acid-cleaned petri dish, and frozen at -20^{o}C until analysis.

Surface water samples were collected from the trace metal fish deployed during the transit to the planned stations. 2L of surface water samples were filtered through a AcroPak^{TM} 1500 capsule with Supor membrane (0.8/ 0.2 µm pore size) into acid-cleaned LDPE bottles rinsed 3 times with

the seawater. Filtered samples were acidified with 6M HCl diluted from ROTIPURAN®Ultra 34 % to pH~ 1.7. Samples were then capped and sealed with Parafilm, double-bagged before being stored at 4^{o}C at sea.

Samples collected
In total, sediment was collected from 6 of 7 stations, and were sliced, separated between the solid phase and pore water. Details were summarized in the Table 5.11. Seawater samples from the bottom two depths were collected from 6 of 7 stations. Details are summarized in Table 5.12. A total of 5 surface seawater samples were collected from trace metal fish, and are listed in Table 5.13.

5.4.3.2 Preliminary results
None available.

5.4.3.3 Work to be conducted in the home laboratory
After returning to the home laboratory at Helmholtz Center Geesthacht (HZG), porewater will be analysed for nutrients, metal concentrations, and Fe isotopes. Solid phase will be analysed for metal concentrations and Fe isotopes, as well as sediment compositions, i.e. carbonate, biogenic silica, organic material and lithogenics. Glass fibre filters will be weighed and calculated for the particulate mass. Polycarbonate filters and filtered seawater collected from both the stainless steel CTD and the trace metal fish will be analysed for multi-element concentrations.

Table 5.11. Summary of sediment samples for metals analysis

Sta.	DSHIP code	Lat. (°N)	Long. (°E)	Water depth (m)	Sampling date	Box Core No.	Sample type
1	SO279_8-1 BC	47.25	-10.10	4426.28	09/12/2020	1	1. Solid phase; 2. Pore water (Nutrients); 3. Pore water (Trace Metal); 4. Overlying water
3	SO279_27-1 BC	31.27	-24.81	5503.16	14/12/2020	2	1. Solid phase; 2. Pore water (Nutrients); 3. Pore water (Trace Metal)
4	SO279_40-1 BC	30.89	-29.31	4331.28	16/12/2020	2	1. Solid phase; 2. Pore water (Nutrients); 3. Pore water (Trace Metal)
5	SO279_60-1 BC	31.36	-34.04	4398.26	19/12/2020	2	1. Solid phase; 2. Pore water (Nutrients); 3. Pore water (Trace Metal); 4. Overlying water
7	SO279_83-1 BC	33.14	-33.78	3674.8	21/12/2020	1	1. Solid phase; 2. Pore water (Nutrients); 3. Pore water (Trace Metal) 4. Overlying water
9	SO279_104-1 BC	35.01	-21.01	5190	27/12/2020	1	1. Solid phase; 2. Pore water (Nutrients); 3. Pore water (Trace Metal); 4. Overlying water

Table 5.12. Summary of water samples collected for metals analysis

Sta.	DSHIP code	Lat. (°N)	Long. (°E)	CTD bottle No.	Depth (m)	Sampling date	Sample volume (L)	Sample type
1	SO279_1-1 CTD	47.25	-10.10	2	4300	08/12/2020	7	1. Particulate on polycarbonate filter; 2. ~ 500 mL filtered water
				3	4300	08/12/2020	7	Particulate on glass fibre filter
				4	4000	08/12/2020	7	1. Particulate on polycarbonate filter;

								2. ~ 500 mL filtered water
				5	4000	08/12/2020	7	Particulate on glass fibre filter
3	SO279_22-1 CTD	31.27	-24.81	1	5400	14/12/2020	7	1. Particulate on polycarbonate filter; 2. ~ 500 mL filtered water
				2	5400	14/12/2020	7	Particulate on glass fibre filter
				4	4900	14/12/2020	7	1. Particulate on polycarbonate filter; 2. ~ 500 mL filtered water
				5	4900	14/12/2020	7	Particulate on glass fibre filter
4	SO279_36-1 CTD	30.89	-29.31	2	4300	16/12/2020	7	1. Particulate on polycarbonate filter; 2. ~ 500 mL filtered water
				3	4300	16/12/2020	7	Particulate on glass fibre filter
				4	3800	16/12/2020	7	1. Particulate on polycarbonate filter; 2. ~ 500 mL filtered water
				6	3800	16/12/2020	7	Particulate on glass fibre filter
5	SO279_53-1 CTD	31.12	-33.82	2	4400	18/12/2020	7	1. Particulate on polycarbonate filter; 2. ~ 500 mL filtered water
				3	4400	18/12/2020	7	Particulate on glass fibre filter
				4	3900	18/12/2020	7	1. Particulate on polycarbonate filter; 2. ~ 500 mL filtered water
				6	3900	18/12/2020	7	Particulate on glass fibre filter

7	SO279_81-1 CTD	33.14	-33.78	2	3650	21/12/2020	7	1. Particulate on polycarbonate filter; 2. ~ 500 mL filtered water
				3	3650	21/12/2020	7	Particulate on glass fibre filter
				4	3100	21/12/2020	7	1. Particulate on polycarbonate filter; 2. ~ 500 mL filtered water
				6	3100	21/12/2020	7	Particulate on glass fibre filter
9	SO279_102-1 CTD	35.00	-21.00	2	~5000	27/12/2020	7	1. Particulate on polycarbonate filter; 2. ~ 500 mL filtered water
				3	~5000	27/12/2020	7	Particulate on glass fibre filter
				4	4700	27/12/2020	7	1. Particulate on polycarbonate filter; 2. ~ 500 mL filtered water
				6	4700	27/12/2020	7	Particulate on glass fibre filter

Table 5.13. Summary of surface seawater samples collected from trace metal fish

Dship code	Date	Time	Latitude (ºN)	Longitude (ºE)	Water depth (m)	HZG code	Volume (L)
SO279_14-1 TMF	12/12/2020	15:17:07	35.54	-21.03	5296.82	SO279-FISH-01	2
SO279_14-1 TMF	13/12/2020	11:00:52	32.03	-24.13	5498.91	SO279-FISH-02	2
SO279_30-1 TMF	15/12/2020	10:09:00	31.39	-26.03	5506.75	SO279-FISH-03	2
SO279_49-1 TMF	18/12/2020	00:22:52	31.36	-30.89	4569.14	SO279-FISH-04	2
SO279_49-1 TMF	18/12/2020	10:24:16	31.14	-33.52	4456.73	SO279-FISH-05	2

5.5 Macro-litter observations at sea surface and seafloor

(Sarah-Marie Kröger[1] and the scientific party of SO279)

[1] GEOMAR

5.5.1 Background and Objectives

With approximately 6.4 million tons of plastic litter entering the oceans annually, plastic litter is considered a global threat for the health of marine ecosystems (UNEP 2009). In order to extend information about the distribution of the marine litter in the North-Atlantic garbage patch, a visual litter survey was performed on the cruise of SO279. The data will be later provided to the LITTERBASE data repository maintained by the Alfred-Wegener Institute for Marine and Polar Research (AWI).

5.5.2 Methods

Similar monitoring was already done on the previous cruises POS536 in August 2019 and AL534 in March 2020. As on the previous cruises, we adopted the litter survey protocol developed by the AWI.

The monitoring was conducted during transit time by 2-3 researchers who stood on the foredock of the RV SONNE. At least one scientist observed an area of approximately 10-15 meters on the portside and another scientist did the same on starboard. The monitoring was subdivided into 1-hour shifts. The scientists counted all items down to 5 cm size that were passing by on the sea surface. Spotted items were documented regarding their shape, size, color and material. Additional information about submergence, biofouling, natural origin and aggregation was also recorded.

Figure 5.16. Plastic items entangled in a sargassum patch (photo: A. Mutzberg).

General data about sea state, visibility, animals, was collected as well as the estimated amount of the macroalgae Sargassum as its appearance is suspected to have a positive correlation with plastic items that are entangled in the larger patches (Fig. 5.16).

5.5.3 Preliminary results

Due to unsuitable weather conditions the possibility for monitoring on the cruise of SO279 was limited. The total litter monitoring time conducted on SO279 was 228 min. In total, 30 objects were sighted, with most of them most likely composed of plastic. The mean number of items spotted during one transect was 7.5. The detailed results of the litter monitoring are shown in Table 5.14.

The results of the litter survey will be provided to the LITTERBASE – Dataset.

Table 5.14. Results of litter spotting surveys

	Survey Number	Date	speed	survey dura	sea state, visibility	Name	Animals	Start time	Start Lat/Long	End time	End Lat/Long	Comments	sargassum level
	SO279_20-1_LITTER-1	13.12.2020	1,7 knots		cloudy, windy, rain	Sarah, Stefan	seagulls	17:28 h	31'29,989'N/24°29,572'W	18:15h	31°29,279'N/24°30,709'W	Ended earlie	none

Time	Waypoint Number		Material	Shape	size / cm	colour	submerged?	Aggregated?	Biofouled?	Natural?	Patch: No of Items
					NO ITEMS SPOTTED						

	Survey Number	Date	Survey duration	speed	sea state, visibility	Name	Animals	Start time	Start Lat/Long	End time	End Lat/Long	Comments	sargassum level
	SO279_32-1_LITTER-2	15.12.	1 h	8,5 knots	2-3, clear	Sarah,Jannis, Annalisa		16:15	31°10814'N/27°21,116'W	17:15	31°09,111'N/027°35,451'W		low-medium

Time	Waypoint Number		Material	Shape	size / cm	colour	submerged?	Aggregated?	Biofouled?	Natural?	Patch: No of Items
n.a.	1		styropor box	rectangular/	30x15	white		x	x		
n.a.	2		hardplastic/ cup	cup	10	white					
n.a.	3		?	rectangular	10	brown					
n.a.	4		plastic	round	5	white					
n.a.	5		plastic	round	5	white					
n.a.	6		plastic, piece of b	irregular	22	blue	x				
n.a.	7		plastic	irregular	5	white	x				

	Survey Number	Date	Survey duration/	speed	sea state, visibility	Name	Animals	Start time	Start Lat/Long	End time	End Lat/Long	Comments	sargassum level
	SO279_46-1_LITTER-3	17.12.2020	01:01	13 knots	clear, 2	Louise, Sarah,	Birds, Portuguese Manowar, fish	17:59	31°23,708'N/29°41,304'W	19:00	31°22,499'N/29°57,099'W		medium-high

Time	Waypoint Number		Material	Shape	size / cm	colour	submerged?	Aggregated?	Biofouled?	Natural?	Patch: No of Items
n.a.	1		plastic	round	2	white					
n.a.	2		plastic	irregular	2	white					
n.a.	3		plastic	irregular	3	white					
n.a.	4		plastic	irregular	3	white					
n.a.	5		plastic foil	irregular	15	transparent					
n.a.	6		plastic	rectangular	7	white					

	Survey Number	Date	Survey duration	speed	sea state, visibility	Name	Animals	Start time	Start Lat/Long	End time	End Lat/Long	Comments	sargassum lev
	SO279_51-1_LITTER-4	18.12.	1 h	13 knots	clear	Erik, Sarah	Dolphin, Flying	09:00		10:00			high

Time	Waypoint Number		Material	Shape	size / cm	colour	submerged?	Aggregated?	Biofouled?	Natural?	Patch: No of Items
n.a.	1		plastic (foam)	Boje	20x20	red	x		x		
n.a.	2		plastic	rectangle	2x2	red					
n.a.	3		plastic	rtriangle	5x3	white					
n.a.	4		plastic	oval/round	3x3	white					
09:05	5		plastic	irregular	2						
09:05	6		shoe	shoe	25						
09:10	7		plastic	irregular	15						
09:15	8		plastic can	irregular	10						
09:40	9		plastic	irregular	10						
09:45	10		wood	irregular	200						
09:50	11		plastic	irregular	10						
09:50	12		plastic	irregular	5						
09:50	13		plastic	irregular	5						
09:50	14		plastic rope	irregular	10						
09:50	15		metal barrel	barrel	100						
09:52	16		plastic rope	irregular	100						
09:53	17		plastic	irregular	10						

5.6 Surveys with the Ocean Floor Observation System (OFOS)

(Aaron Beck[1] and the scientific party of SO279)

[1] GEOMAR

5.6.1 Background

Most of the plastic that is produced is less dense than seawater (Andrady, 2011), and about 60% of the positively buoyant plastic debris that enters the oceans from land is likely transported offshore by surface currents and winds (Maximenko et al., 2012; Lebreton et al., 2012). Floating plastic debris therefore tends to accumulate within oceanic gyres and restricted coastal waters (Lebreton et al., 2012). Estimates based on empirical data from field observations suggest that some 0.27 MT of plastic debris is present in the surface ocean (Eriksen et al., 2014), but more recent measurements in the North Pacific garbage patch found that this number may still underestimate the total amount of plastic debris floating at the sea surface worldwide (Lebreton et al., 2018). However, Lebreton et al. (2018) also concluded that there remains a major discrepancy between the amount of buoyant plastic that enters the oceans every year (i.e., millions of tons) and the amount that can be observed at the ocean surface (i.e., hundred thousands of tons).

This implies that a substantial amount of macroplsatic debris may be present and persistent on the seafloor. Indeed, macrolitter had been reported on the depe seafloor from the 4100-m deep Peru Basin after two decades of deposition (Krause et al., 2020). A few studies have investigated the abundance of plastic debris and MP in coastal sediments (e.g., Van Cauwenberghe et al., 2015a), but data from the deep sea (water depths greater than 1000 m) are even scarcer. The lack of information on MP in deep-sea sediments prevents assessment of MP effects on sensitive deep-sea ecosystems, and evaluation of this potential sink for land-sourced plastic debris.

5.6.2 Methods

Given the scarcity and heterogeneity of plastic debris on the deep seafloor, traditional sediment sampling gear (e.g., box coring) cannot provide information appropriate to catalog this debris. To survey seafloor debris, we used the RV SONNE Ocean Floor Observation System (OFOS). This system consists of a towed plastform with high-resolution video and still cameras and illumination (maintained, prepared, and deployed by the SONNE WTD). High-resolution video footage is continuously recorded, and high-resolution still images are recorded very 5-8 seconds, the frequency limited by the recharge time of the flash bulbs.

The OFOS is maintained 1-3 m above the seafloor by the ship’s winch operator, with the help of a heave-compensated winch. Low-resolution video data is streamed live onboard, and annotations recorded by two-person volunteer teams from the scientific party. High-resolution data are downloaded from the OFOS after recovery. OFOS surveys were conducted at the six stations within the primary working area south of the Azores (Table 5.15). Surves were typically 2-4 h in length.

Table 5.15. List of OFOS deployments

Station SO279_	Date/Time (UTC)	Device	Code	Depth (m)	Latitude (N)	Longitude (W)
_28-1	14.12.2020 16:31	OFOS	OFOS	5491.74	31° 16.059'	024° 48.709'
_44-1	17.12.2020 09:00	OFOS	OFOS	4266.77	31° 22.465'	029° 36.764'
_62-1	19.12.2020 12:24	OFOS	OFOS	4398.95	31° 21.398'	034° 02.272'
_77-1	21.12.2020 02:28	OFOS	OFOS	N/A	33° 08.279'	034° 31.114'
_90-1	22.12.2020 15:38	OFOS	OFOS	3674.85	33° 08.609'	033° 46.708'
_108-1	28.12.2020 10:02	OFOS	OFOS	5254.73	35° 14.110'	020° 42.845'

5.6.3 Preliminary results

No macrolitter objects were observed on the first dive (SO279_28-1), but one piece of rope was found on the second dive (SO279_44-1). Several items were observed on each of the subsequent dives. Images of some of the macrolitter objects are shown in Fig. 5.17.

5.6.4 Work to be conducted in the home laboratory

Individual still images from each dive will be compiled into calibrated photomosaics to allow estimation of the macrolitter spatial density. These estimates can then be extrapolated to an inventory of plastic litter within the study area. This work is planned in late 2021/2022. Macrolitter image data are also planned for integration into other databases for outreach and dissemination activities (e.g., https://experience.arcgis.com/experience/8260b2c831de448ea905fb021cacb313/?draft=true).

Figure 5.17. Selected images of macrolitter on the seafloor captured by OFOS.

6 Station List SO279

6.1 Overall Station List

Station SO279_	Date/Time (UTC)	Device	Code	Depth (m)	Latitude (N)	Longitude (W)
_0_UW-1	08.12.2020 06:10	KONGSBERG EM122	EM122	4408.38	47° 21.532'	009° 50.988'
_1-1	08.12.2020 08:00	CTD	CTD	4425.55	47° 15.005'	010° 06.275'
_2-1	08.12.2020 09:30	PUMP	PUMP	4425.48	47° 15.010'	010° 06.293'
_3-1	08.12.2020 11:28	In Situ Pump	ISP	4424.64	47° 15.016'	010° 06.279'
_4-1	08.12.2020 15:33	Multi Corer	MUC	4419.93	47° 15.008'	010° 06.283'
_5-1	08.12.2020 19:09	Box Corer	BC	4420.99	47° 15.006'	010° 06.283'
_6-1	08.12.2020 22:54	Multiple Opening/Closing Net	MSN	4425.71	47° 15.026'	010° 06.318'
_7-1	09.12.2020 08:53	Underway Water Sampling	UWS	4450.44	47° 14.826'	010° 07.768'
_8-1	09.12.2020 09:16	Box Corer	BC	4426.29	47° 15.035'	010° 06.211'
_9-1	09.12.2020 12:21	Box Corer	BC	4426.27	47° 15.012'	010° 06.281'
_10-1	09.12.2020 14:55	Underway Water Sampling	UWS	4422.77	47° 15.021'	010° 06.293'
_11-1	10.12.2020 16:00	Underway Water Sampling	UWS	5358.65	43° 13.835'	014° 08.776'
_12-1	11.12.2020 22:29	Underway Water Sampling	UWS	5061.69	38° 26.323'	018° 35.371'
_13-1	12.12.2020 09:35	Underway Water Sampling	UWS	5171.24	36° 28.560'	020° 14.853'
_14-1	12.12.2020 15:17	Trace Metal Fish	TMF	5296.82	35° 32.147'	021° 01.576'
_15-1	12.12.2020 19:41	Underway Water Sampling	UWS	5260.43	34° 43.961'	021° 41.062'
_16-1	12.12.2020 22:42	Underway Water Sampling	UWS	5197.6	34° 11.276'	022° 09.470'
_0_UW-2	13.12.2020 09:49	Acoustic Doppler Current Profiler	ADCP	5487.23	32° 14.166'	023° 56.477'
_17-1	13.12.2020 10:35	Underway Water Sampling	UWS	5495.3	32° 06.023'	024° 03.818'
_14-1	13.12.2020 11:00	Trace Metal Fish	TMF	5498.91	32° 01.595'	024° 07.817'
_18-1	13.12.2020 13:19	Neuston Microplastics Catamaran	NEMICAT	5502.29	31° 39.920'	024° 27.287'
_20-1	13.12.2020 17:28	Litter Survey	LITTER	5505.35	31° 29.989'	024° 29.572'
_19-1	13.12.2020 21:41	Multiple Opening/Closing Net	MSN	5507.08	31° 25.745'	024° 35.582'
_21-1	13.12.2020 22:16	Underway Water Sampling	UWS	5498.38	31° 24.968'	024° 36.583'
_22-1	14.12.2020 00:24	CTD	CTD	5503.08	31° 16.050'	024° 48.730'
_23-1	14.12.2020 04:39	In Situ Pump	ISP	5493.29	31° 16.054'	024° 48.709'
_24-1	14.12.2020 07:28	Underway Water Sampling	UWS	5501.04	31° 16.057'	024° 48.714'
_25-1	14.12.2020 08:49	Box Corer	BC	5502.25	31° 16.049'	024° 48.705'
_26-1	14.12.2020 09:18	PUMP	PUMP	5493.05	31° 16.046'	024° 48.710'
_27-1	14.12.2020 12:39	Box Corer	BC	5492.39	31° 16.057'	024° 48.710'
_28-1	14.12.2020 16:31	OFOS	OFOS	5491.74	31° 16.059'	024° 48.709'
_29-1	14.12.2020 22:32	Multiple Opening/Closing Net	MSN	5510.49	31° 17.030'	024° 49.526'
_30-1	15.12.2020 10:09	Trace Metal Fish	TMF	5506.75	31° 23.149'	026° 02.009'
_31-1	15.12.2020 14:58	Underway Water Sampling	UWS	4772.41	31° 14.466'	026° 59.821'
_32-1	15.12.2020 17:10	Litter Survey	LITTER	4446.44	31° 10.814'	027° 24.116'
_33-1	15.12.2020 17:17	Underway Water Sampling	UWS	4451.15	31° 10.636'	027° 25.179'
_34-1	15.12.2020 21:42	Underway Water Sampling	UWS	3130.19	31° 04.101'	028° 08.739'
_35-1	15.12.2020 21:43	Underway Water Sampling	UWS	3090.29	31° 04.076'	028° 08.921'
_36-1	16.12.2020 05:17	CTD	CTD	4332.46	30° 53.532'	029° 18.839'
_37-1	16.12.2020 09:04	In Situ Pump	ISP	4330.35	30° 53.549'	029° 18.837'

_38-1	16.12.2020 11:10	Underway Water Sampling	UWS	4331.37	30° 53.545'	029° 18.837'
_39-1	16.12.2020 12:30	Box Corer	BC	4332.35	30° 53.548'	029° 18.838'
_40-1	16.12.2020 15:43	Box Corer	BC	4332.26	30° 53.545'	029° 18.838'
_41-1	16.12.2020 19:04	Multiple Opening/Closing Net	MSN	4330.31	30° 54.072'	029° 19.159'
_42-1	17.12.2020 05:53	Bongo Net	BONGO	4265.88	31° 17.718'	029° 33.157'
_43-1	17.12.2020 08:11	Neuston Microplastics Catamaran	NEMICAT	4260.76	31° 21.472'	029° 35.958'
_44-1	17.12.2020 09:00	OFOS	OFOS	4266.77	31° 22.465'	029° 36.764'
_45-1	17.12.2020 13:49	Underway Water Sampling	UWS	4275.37	31° 23.130'	029° 37.980'
_46-1	17.12.2020 17:59	Litter Survey	LITTER	4298.18	31° 23.708'	029° 41.304'
_47-1	17.12.2020 20:52	Underway Water Sampling	UWS	3991.65	31° 20.550'	030° 26.361'
_48-1	17.12.2020 21:56	Neuston Microplastics Catamaran	NEMICAT	4292.07	31° 19.897'	030° 41.026'
_48-1	17.12.2020 22:00	Neuston Microplastics Catamaran	NEMICAT	4279.34	31° 19.939'	030° 41.100'
_49-1	17.12.2020 23:37	Trace Metal Fish	TMF	4002.55	31° 22.525'	030° 44.457'
_50-1	18.12.2020 09:50	Underway Water Sampling	UWS	4597.51	31° 08.788'	033° 22.939'
_51-1	18.12.2020 09:55	Litter Survey	LITTER	4492.08	31° 08.694'	033° 24.265'
_49-1	18.12.2020 10:21	Trace Metal Fish	TMF	4457.8	31° 08.253'	033° 30.894'
_52-1	18.12.2020 10:52	Underway Water Sampling	UWS	4427.96	31° 07.843'	033° 36.892'
_53-1	18.12.2020 11:50	CTD	CTD	4414.16	31° 07.081'	033° 48.975'
_54-1	18.12.2020 15:22	In Situ Pump	ISP	4412.93	31° 07.050'	033° 48.969'
_55-1	18.12.2020 19:04	Neuston Microplastics Catamaran	NEMICAT	4414.52	31° 07.051'	033° 48.969'
_56-1	18.12.2020 20:34	Multiple Opening/Closing Net	MSN	4272.12	31° 09.810'	033° 51.106'
_57-1	18.12.2020 22:32	Underway Water Sampling	UWS	4314.77	31° 13.594'	033° 54.724'
_58-1	18.12.2020 23:25	Bongo Net	BONGO	4369.81	31° 14.422'	033° 55.515'
_59-1	19.12.2020 05:41	Box Corer	BC	4401	31° 21.398'	034° 02.278'
_60-1	19.12.2020 09:12	Box Corer	BC	4397.21	31° 21.402'	034° 02.268'
_61-1	19.12.2020 10:22	Underway Water Sampling	UWS	4398.98	31° 21.400'	034° 02.274'
_62-1	19.12.2020 12:24	OFOS	OFOS	4398.95	31° 21.398'	034° 02.272'
_63-1	19.12.2020 16:22	Underway Water Sampling	UWS	4396	31° 22.224'	034° 03.153'
_64-1	19.12.2020 16:52	Underway Water Sampling	UWS	4387.31	31° 22.412'	034° 03.341'
_65-1	19.12.2020 17:20	Underway Water Sampling	UWS	4252.67	31° 22.596'	034° 03.524'
_66-1	19.12.2020 17:52	Underway Water Sampling	UWS	4195.53	31° 22.712'	034° 03.623'
_67-1	19.12.2020 22:01	Underway Water Sampling	UWS	4099.88	31° 57.489'	034° 05.995'
_68-1	19.12.2020 23:10	Neuston Microplastics Catamaran	NEMICAT	4121.32	32° 10.424'	034° 09.152'
_69-1	20.12.2020 06:36	CTD	CTD	3594.05	33° 17.589'	034° 29.494'
_70-1	20.12.2020 09:04	Underway Water Sampling	UWS	3593.38	33° 17.607'	034° 29.493'
_71-1	20.12.2020 09:47	In Situ Pump	ISP	3591.91	33° 17.609'	034° 29.483'
_72-1	20.12.2020 13:29	Box Corer	BC	3591.73	33° 17.643'	034° 29.499'
_73-1	20.12.2020 16:03	Box Corer	BC	3592.8	33° 17.607'	034° 29.483'
_74-1	20.12.2020 16:50	Underway Water Sampling	UWS	3593.53	33° 17.603'	034° 29.486'
_75-1	20.12.2020 18:58	Bongo Net	BONGO	0	33° 17.535'	034° 29.571'
_76-1	20.12.2020 22:08	Underway Water Sampling	UWS	0	33° 13.439'	034° 28.291'
_75-1	20.12.2020 22:48	Bongo Net	BONGO	0	33° 12.471'	034° 28.260'
_77-1	21.12.2020 02:28	OFOS	OFOS	0	33° 08.279'	034° 31.114'
_78-1	21.12.2020 09:20	Neuston Microplastics Catamaran	NEMICAT	3412.55	33° 08.520'	034° 33.673'
_79-1	21.12.2020 09:25	Underway Water Sampling	UWS	3373.4	33° 08.689'	034° 33.832'
_80-1	21.12.2020 11:31	Underway Water Sampling	UWS	3083.13	33° 11.404'	034° 26.349'

_81-1	21.12.2020 14:07	CTD	CTD	3675.36	33° 08.608'	033° 46.670'
_82-1	21.12.2020 17:14	In Situ Pump	ISP	3676.83	33° 08.606'	033° 46.719'
_83-1	21.12.2020 21:27	Box Corer	BC	3675.62	33° 08.612'	033° 46.713'
_84-1	21.12.2020 21:40	Underway Water Sampling	UWS	3674.73	33° 08.604'	033° 46.718'
_85-1	22.12.2020 00:03	Box Corer	BC	3673.18	33° 08.606'	033° 46.715'
_86-1	22.12.2020 02:59	Bongo Net	BONGO	3677.48	33° 08.635'	033° 46.720'
_87-1	22.12.2020 09:48	Neuston Microplastics Catamaran	NEMICAT	3485.56	33° 20.447'	033° 49.999'
_88-1	22.12.2020 10:47	Underway Water Sampling	UWS	3374.2	33° 22.915'	033° 49.047'
_89-1	22.12.2020 12:56	Box Corer	BC	3677.74	33° 08.597'	033° 46.716'
_90-1	22.12.2020 15:38	OFOS	OFOS	3674.85	33° 08.609'	033° 46.708'
_91-1	22.12.2020 21:17	Underway Water Sampling	UWS	3570.05	33° 11.075'	033° 45.900'
_92-1	23.12.2020 11:33	Underway Water Sampling	UWS	3551.28	33° 05.052'	030° 49.229'
_93-1	23.12.2020 21:52	Underway Water Sampling	UWS	1323.03	33° 11.395'	029° 07.605'
_94-1	24.12.2020 10:19	Underway Water Sampling	UWS	3056.43	33° 33.037'	028° 45.909'
_95-1	24.12.2020 23:05	Underway Water Sampling	UWS	4241.21	33° 17.926'	026° 55.054'
_96-1	25.12.2020 11:15	Underway Water Sampling	UWS	0	33° 25.366'	025° 11.337'
_97-1	25.12.2020 21:39	Underway Water Sampling	UWS	0	33° 33.664'	023° 58.812'
_98-1	25.12.2020 21:40	Underway Water Sampling	UWS	0	33° 33.676'	023° 58.733'
_99-1	26.12.2020 10:55	Underway Water Sampling	UWS	5378.09	33° 59.635'	022° 34.858'
_100-1	26.12.2020 22:42	Underway Water Sampling	UWS	5210.2	34° 39.806'	021° 31.804'
_101-1	26.12.2020 22:43	Underway Water Sampling	UWS	5213.95	34° 39.838'	021° 31.762'
_102-1	27.12.2020 07:51	CTD	CTD	5190.75	35° 00.002'	020° 59.996'
_103-1	27.12.2020 12:15	In Situ Pump	ISP	5193.33	35° 00.000'	020° 59.985'
_104-1	27.12.2020 15:58	Box Corer	BC	5189.47	34° 59.998'	020° 59.989'
_105-1	27.12.2020 19:38	Box Corer	BC	5190.52	35° 00.006'	020° 59.998'
_106-1	27.12.2020 23:26	Bongo Net	BONGO	5192.34	35° 00.064'	020° 59.906'
_107-1	28.12.2020 06:18	Neuston Microplastics Catamaran	NEMICAT	5245.09	35° 08.367'	020° 49.280'
_108-1	28.12.2020 10:02	OFOS	OFOS	5254.73	35° 14.110'	020° 42.845'
_109-1	28.12.2020 15:16	Underway Water Sampling	UWS	5253.01	35° 15.492'	020° 41.893'
_110-1	28.12.2020 21:39	Underway Water Sampling	UWS	5134.39	35° 32.486'	020° 24.091'
_111-1	29.12.2020 10:58	Underway Water Sampling	UWS	4984.75	37° 08.291'	018° 36.721'
_112-1	29.12.2020 16:40	Underway Water Sampling	UWS	5118.74	37° 48.030'	017° 51.511'
_113-1	29.12.2020 22:44	Underway Water Sampling	UWS	5485.88	38° 29.568'	017° 03.838'
_114-1	30.12.2020 12:04	Underway Water Sampling	UWS	4296.95	40° 09.355'	015° 18.733'
_115-1	30.12.2020 14:37	Underway Water Sampling	UWS	5031.63	40° 28.656'	014° 58.124'
_116-1	30.12.2020 19:26	Underway Water Sampling	UWS	5359.08	41° 06.173'	014° 17.797'
_117-1	30.12.2020 19:48	Underway Water Sampling	UWS	5356.86	41° 08.956'	014° 14.772'
_118-1	30.12.2020 20:01	Underway Water Sampling	UWS	5354.7	41° 10.706'	014° 12.893'
_119-1	30.12.2020 20:14	Underway Water Sampling	UWS	5357.38	41° 12.402'	014° 11.050'
_120-1	30.12.2020 20:30	Underway Water Sampling	UWS	5603.24	41° 14.515'	014° 08.774'
_121-1	30.12.2020 20:47	Underway Water Sampling	UWS	5354.84	41° 16.697'	014° 06.401'
_122-1	30.12.2020 21:05	Underway Water Sampling	UWS	5352.46	41° 19.098'	014° 03.810'
_123-1	30.12.2020 21:23	Underway Water Sampling	UWS	5352.44	41° 21.434'	014° 01.260'
_124-1	30.12.2020 21:36	Underway Water Sampling	UWS	5348.44	41° 23.080'	013° 59.488'

7 Data and Sample Storage and Availability

The Kiel Data Management Team (KDMT) provides an information and data archival system where metadata of the onboard DSHIP-System is collected and publicly available. This Ocean Science Information System (OSIS-Kiel) is accessible for all project participants and can be used to share and edit field information and to provide scientific data, as they become available. The central system OSIS provides information on granted ship time with information on the scientific program and the general details down to the availability of data files from SO279 (https://portal.geomar.de/metadata/leg/show/357846). The transparency on the research activities is regarded as an invitation to external scientists to start communication on collaboration on behalf of the newly available data.

The KDMT will take care as data curators to fulfil the proposed data publication in a World Data Centre (e.g., PANGAEA; https://www.pangaea.de/?q=so279) which will then provide long-term archival and access to the data. The data publication process will be based on the available files in OSIS and is therefore transparent to all reviewers and scientists. This cooperation with a world data center will make the data globally searchable, and links to the data owners will provide points of contact to project-external scientists. OSIS provides contact information for large data files. Where samples are not completely sacrificed for analysis, sample storage such as sediment cores will be stored in the GEOMAR Lithothek and core repository and OSIS serves as a catalogue to the defined storage locations. The samples from this cruise will be available to other researchers if they have not been consumed during the analysis process. Other data generated in laboratory work, e.g. from sedimentological and geotechnical analyses, will be stored in OSIS-Kiel until publication.

Insofar as possible given unexpected delays due to the COVID pandemic, the chief scientist and all principal investigators involved in this cruise will comply with the time schedule below regulating the availability of all information and all research data and where applicable also of physical samples resulting from this cruise. Following the cruise, the KDMT will support and assist researchers in their data management activities.

Table 7.1 Overview of data availability

Type	**Database**	**Available**	**Free Access**	**Contact**
		Date	Date	E-Mail
CTD data	OSIS	June 2021	June 2024	ajbeck@geomar.de
raw data Multinet (depth, flowmeter volume)	OSIS	Jan. 2022	Jan 2025	thamm@geomar.de
Depth logger data Bongo	OSIS	Jan 2022	Jan 2025	thamm@geomar.de
geochemical data	PANGAEA	June 2021	Jan. 2024	mhaeckel@geomar.de
MPs distribution, ecological setting, meiofauna community	UGent	Jan. 2022	Jan. 2025	Gabriella.Panto@UGent.be
OFOS imagery	n.d. (BIIGLE?)	June 2021	June 2024	ajbeck@geomar.de
Microplastic, PFAS data	coastMap	n.d.	n.d.	Tristan.Zimmermann@hzg.de, rui.shen@hzg.de

8 Acknowledgements

Cruise SO279 was planned, coordinated, and conducted by GEOMAR Helmholtz Centre for Ocean Research Kiel, with participation of colleagues from seven additional institutes from Germany and the European Union. The cruise was funded by the Deutsche Forschungsgemeinschaft (DFG) through the GPF review process (GPF 20-3_089). Additional support was provided by the GEOMAR Helmholtz Centre for Ocean Research Kiel and the Bundesministerium für Bildung und Forschung (BMBF) through projects HOTMIC (project number 03F0851A) and PLASTISEA (project number 031B0867A). We especially thank Captain Lutz Mallon and the crew of RV SONNE for their expertise and support to make SO279 a successful and enjoyable expedition. We also want to acknowledge the work and logistical support of the shipping company Briese Schiffahrt GmbH and the German Research Fleet Coordination Centre to make such expeditions possible despite COVID-pandemic challenges. Finally, we gratefully acknowledge logistical support from our colleagues at the GEOMAR Technik- und Logistik Zentrum (TLZ).

9 References

Ahn, J., Brook, E.J., Mitchell, L., Rosen, J., McConnell, J.R., Taylor, K., Etheridge, D. and Rubino, M., 2012. Atmospheric CO2 over the last 1000 years: A high-resolution record from the West Antarctic Ice Sheet (WAIS) Divide ice core. Global Biogeochemical Cycles, 26(2).

Ahrens, L.; Bundschuh, M., Fate and effects of poly- and perfluoroalkyl substances in the aquatic environment: A review. Environ. Toxicol. Chem. 2014, 33 (9), 1921-1929.

Andrady, A. L. (2011). Microplastics in the marine environment. Marine pollution bulletin, 62(8), 1596-1605.

Austin, H. P. et al. Characterization and engineering of a plastic-degrading aromatic polyesterase. Proc. Natl. Acad. Sci. 115, E4350–E4357 (2018).

AWI - Litterbase data repository. Available online at: https://litterbase.awi.de (last accessed: 04.01.2021).

Bagaev, A., Mizyuk, A., Khatmullina, L., Isachenko, I., Chubarenko, I. (2017) Anthropogenic fibres in the Baltic Sea water column: Field data, laboratory and numerical testing of their motion. Science of the Total Environment 599-600, 560-571.

Baini, M., Martellini, T., Cincinelli, A., Campani, T., Minutoli, R., Panti, C., Finoia, M.G. and Fossi, M.C., 2017. First detection of seven phthalate esters (PAEs) as plastic tracers in superficial neustonic/planktonic samples and cetacean blubber. Analytical Methods, 9(9), pp.1512-1520.

Bergmann, M., Wirzberger, V., Krumpen, T., Lorenz, C., Primpke, S., Tekman, M.B., Gerdts, G. (2017) High quantities of microplastic in Artic deep-sea sediments from the HAUSGARTEN observatory. Environmental Science & Technology 51, 11000–11010

Blévin, P.; Angelier, F.; Tartu, S.; Bustamante, P.; Herzke, D.; Moe, B.; Bech, C.; Gabrielsen, G. W.; Bustnes, J. O.; Chastel, O., Perfluorinated substances and telomeres in an Arctic seabird: Cross-sectional and longitudinal approaches. Environ. Pollut. 2017, 230, 360-367.

Brach, L., Deixonne, P., Bernard, M.-F., Durand, E., Desjeand, M.-C., Pereza, E., van Sebille, E., ter Halle, A., (2018) Anticyclonic eddies increase accumulation of microplastic in the North Atlantic subtropical gyre, Marine Pollution Bulletin 126, 191-196.

Brown, K.A., McLaughlin, F., Tortell, P.D., Varela, D.E., Yamamoto-Kawai, M., Hunt, B. and Francois, R., 2014. Determination of particulate organic carbon sources to the surface mixed layer of the Canada Basin, Arctic Ocean. Journal of Geophysical Research: Oceans, 119(2), pp.1084-1102.

Butt, C. M.; Berger, U.; Bossi, R.; Tomy, G. T., Levels and trends of poly- and perfluorinated compounds in the arctic environment. Sci. Total Environ. 2010, 408 (15), 2936-2965.

Butt, C. M.; Muir, D. C. G.; Stirling, I.; Kwan, M.; Mabury, S. A., Rapid Response of Arctic Ringed Seals to Changes in Perfluoroalkyl Production. Environ. Sci. Technol. 2007, 41 (1), 42-49.

Chambault, P., Vandeperre, F., Machete, M., Lagoa, J. C., & Pham, C. K. (2018). Distribution and composition of floating macro litter off the Azores archipelago and Madeira (NE Atlantic) using opportunistic surveys. Marine environmental research, 141, 225-232.

Chelton, D. B., Schlax, M. G., & Samelson, R. M. (2011). Global observations of nonlinear mesoscale eddies. Progress in oceanography, 91(2), 167-216.

Choy, C.A., Robison, B.H., Gagne, T.O., Erwin, B., Firl, E., Halden, R.U., Hamilton, J.A., Katija, K., Lisin, S.E., Rolsky, C. and Van Houtan, K.S., 2019. The vertical distribution and biological transport of marine microplastics across the epipelagic and mesopelagic water column. Scientific reports, 9(1), pp.1-9.

Codling, G.; Halsall, C.; Ahrens, L.; Del Vento, S.; Wiberg, K.; Bergknut, M.; Laudon, H.; Ebinghaus, R., The fate of per- and polyfluoroalkyl substances within a melting snowpack of a boreal forest. Environ. Pollut. 2014, 191, 190-198.

Cotovicz Jr, L.C., Knoppers, B.A., Deirmendjian, L. and Abril, G., 2019. Sources and sinks of dissolved inorganic carbon in an urban tropical coastal bay revealed by δ13C-DIC signals. Estuarine, Coastal and Shelf Science, 220, pp.185-195.

Cózar, A., Echevarría, F., González-Gordillo, J. I., Irigoien, X., Úbeda, B., Hernández-León, S., ... & Duarte, C. M. (2014). Plastic debris in the open ocean. Proceedings of the National Academy of Sciences, 111(28), 10239-10244.

De Silva, A. O.; Mabury, S. A., Isolating Isomers of Perfluorocarboxylates in Polar Bears (Ursus maritimus) from Two Geographical Locations. Environ. Sci. Technol. 2004, 38 (24), 6538-6545.

D'Eon, J. C.; Mabury, S. A., Production of Perfluorinated Carboxylic Acids (PFCAs) from the Biotransformation of Polyfluoroalkyl Phosphate Surfactants (PAPS): Exploring Routes of Human Contamination. Environ. Sci. Technol. 2007, 41 (13), 4799-4805.

Dickson, A. G., Afghan, J. D., and Anderson, G. C. (2003). Reference materials for oceanic CO2 analysis: a method for the certification of total alkalinity. Mar. Chem. 80, 185–197. doi:10.1016/S0304-4203(02)00133-0.

Dickson, A. G., Sabine, C. L., and Christian, J. R. eds. (2007). "SOP 1: Water sampling for the parameters of the oceanic carbon dioxide system," in Guide to Best Practices for Ocean CO2 Measurements, PICES Special Publication 3 (North Pacific Marine Science Organization, Sidney, BC, Canada), Chapter 4.

Dickson, A.G., Sabine, C.L. and Christian, J.R., 2007. Guide to best practices for ocean CO2 measurements. North Pacific Marine Science Organization.

Doney, S.C., Fabry, V.J., Feely, R.A. and Kleypas, J.A. (2009) Ocean Acidification: The Other CO2 Problem. Annual Review of Marine Science 1, 169-192.

Elrod, V.A., Berelson, W.M., Coale, K.H., Johnson, K.S., 2004. The flux of iron from continental shelf sediments: A missing source for global budgets. Geophysical Research Letters 31.

Eriksen, M., Lebreton, L.C.M., Carson H.S., Thiel, M., Moore, C.J., Borerro J.C., Galgani, F., Ryan, P.G., Reisser, J. (2014) Plastic pollution in the world's oceans: more than 5 trillion plastic pieces weighing over 250,000 tons afloat at sea. PLoS ONE 9, e111913.

Esch, E. von der; Kohles, A. J.; Anger, P. M.; Hoppe, R.; Nießner, R.; Elsner, M.; Ivleva, N. P., TUM-ParticleTyper: A detection and quantification tool for automated analysis of (Microplastic) particles and fibers, PLOS One, 15, 6, e0234766, 2020, DOI: 10.1371/journal.pone.0234766.

Feely, R.A., Sabine, C.L., Lee, K., Berelson, W., Kleypas, J., Fabry, V.J. and Millero, F.J. (2004) Impact of anthropogenic CO2 on the CaCO3 system in the oceans. Science 305, 362-366.

Filgueiras, A. V., Gago, J., Campillo, J. A., & León, V. M. (2019). Microplastic distribution in surface sediments along the Spanish Mediterranean continental shelf. Environmental Science and Pollution Research, 26(21), 21264-21273.

Friedlingstein, P., Jones, M.W., Sullivan, M., Andrew, R.M., Hauck, J., Peters, G.P., Peters, W., Pongratz, J., Sitch, S., Le Quéré, C., Bakker, D.C.E., Canadell, J.G., Ciais, P., Jackson, R.B., Anthoni, P., Barbero, L., Bastos, A., Bastrikov, V., Becker, M., Bopp, L., Buitenhuis, E., Chandra, N., Chevallier, F., Chini, L.P., Currie, K.I., Feely, R.A., Gehlen, M., Gilfillan, D., Gkritzalis, T., Goll, D.S., Gruber, N., Gutekunst, S., Harris, I., Haverd, V., Houghton, R.A., Hurtt, G., Ilyina, T., Jain, A.K., Joetzjer, E., Kaplan, J.O., Kato, E., Klein Goldewijk, K., Korsbakken, J.I., Landschützer, P., Lauvset, S.K., Lefèvre, N., Lenton, A., Lienert, S., Lombardozzi, D., Marland, G., McGuire, P.C., Melton, J.R., Metzl, N., Munro, D.R., Nabel, J.E.M.S., Nakaoka, S.-I., Neill, C., Omar, A.M., Ono, T., Peregon, A., Pierrot, D., Poulter, B., Rehder, G., Resplandy, L., Robertson, E., Rödenbeck, C., Séférian, R., Schwinger, J., Smith, N., Tans, P.P., Tian, H., Tilbrook, B., Tubiello, F.N., van der Werf, G.R., Wiltshire, A.J. and Zaehle, S. (2019) Global Carbon Budget 2019. Earth System Science Data 11, 1783-1838.

Fueser, H., Mueller, M. T., Weiss, L., Höss, S., & Traunspurger, W. (2019). Ingestion of microplastics by nematodes depends on feeding strategy and buccal cavity size. Environmental Pollution, 255, 113227.

Galloway, T.S., Cole, M., Lewis, C. (2017) Interactions of microplastic debris throughout the marine ecosystem. Nature Ecology & Evolution 1: 1-8.

GEBCO Compilation Group (2019) GEBCO 2019. doi:10.5285/836f016a-33be-6ddc-e053-6c86abc0788e

Giesy, J. P.; Kannan, K., Global Distribution of Perfluorooctane Sulfonate in Wildlife. Environ. Sci. Technol. 2001, 35 (7), 1339-1342.

Hildebrandt, L.; Voigt, N.; Zimmermann, T.; Reese, A.; Proefrock, D., Evaluation of continuous flow centrifugation as an alternative technique to sample microplastic from water bodies. Marine Environmental Research 2019, 151, 104768.

Hildebrandt, L.; Mitrano, D. M.; Zimmermann, T.; Pröfrock, D., A Nanoplastic Sampling and Enrichment Approach by Continuous Flow Centrifugation. Frontiers in Environmental Science 2020, 8, (89).

Homoky, W.B., John, S.G., Conway, T.M., Mills, R.A., 2013. Distinct iron isotopic signatures and supply from marine sediment dissolution. Nature Communications 4, 2143.

Humphreys, M.P., Greatrix, F.M., Tynan, E., Achterberg, E.P., Griffiths, A.M., Fry, C.H., Garley, R., McDonald, A. and Boyce, A.J., 2016b. Stable carbon isotopes of dissolved inorganic carbon for a zonal transect across the subpolar North Atlantic Ocean in summer 2014. Earth System Science Data, 8(1), pp.221-233.

Humphreys, M.P., Griffiths, A.M., Achterberg, E.P., Holliday, N.P., Rérolle, V.M., Menzel Barraqueta, J.L., Couldrey, M.P., Oliver, K.I., Hartman, S.E., Esposito, M. and Boyce, A.J., 2016a. Multidecadal accumulation of anthropogenic and remineralized dissolved inorganic carbon along the Extended Ellett Line in the northeast Atlantic Ocean. Global Biogeochemical Cycles, 30(2), pp.293-310.

IPCC. (2007) Climate change (2007). The physical science basis. Summary for policymakers. Contribution of working group 1 to the fourth assessment report. The intergovernmental Panel on Climate Change, http://www.ipcc.ch/pdf/assessment-report/ar4/wg1/ar4-wg1-spm.pdf

IPCC. (2014). Summary for Policymakers. In Climate Change 2014 Mitigation of Climate Change (pp. 1–30). Cambridge: Cambridge University Press. https://doi.org/10.1017/CBO9781107415416.005

Jambeck, J.R., Geyer, R., Wilcox, C., Siegler, T.R., Perryman, M., Andrady, A., Narayan, R., Law, K.L. (2015) Plastic waste inputs from land into the ocean. Science 347, 768–77.

Joo, S. et al. Structural insight into molecular mechanism of poly(ethylene terephthalate) degradation. Nat. Commun. 9, 382 (2018).

Katija, K., Choy, C.A., Sherlock, R.E., Sherman, A.D., Robison, B.H. (2017) From the surface to the seafloor: How giant larvaceans transport microplastics into the deep sea. Science Advances 3, e170715.

Keeling, C.D., 1979. The Suess effect: 13Carbon-14Carbon interrelations. Environment International, 2(4-6), pp.229-300. doi:10.1016/0160-4120(79)90005-9.

Khatiwala, S.P., Tanhua, T., Mikaloff Fletcher, S.E., Gerber, M., Doney, S.C., Graven, H.D., Gruber, N., McKinley, G.A., Murata, A., Ríos, A.F. and Sabine, C.L., 2013. Global ocean storage of anthropogenic carbon. Biogeosciences, 10(4), pp.2169-2191.

Kirchgeorg, T.; Dreyer, A.; Gabrielli, P.; Gabrieli, J.; Thompson, L. G.; Barbante, C.; Ebinghaus, R., Seasonal accumulation of persistent organic pollutants on a high altitude glacier in the Eastern Alps. Environ. Pollut. 2016, 218, 804-812.

Kissa, E., Fluorinated Surfactants and Repellents. 2nd ed.; Marcel Dekker, Inc.: New York, 2001; Vol. 97.

Krause, S., Molari, M., Gorb, E. V., Gorb, S. N., Kossel, E., & Haeckel, M. (2020). Persistence of plastic debris and its colonization by bacterial communities after two decades on the abyssal seafloor. Scientific reports, 10(1), 1-15.

Kroopnick, P., Weiss, R.F. and Craig, H., 1972. Total CO2, 13C, and dissolved oxygen-18O at Geosecs II in the North Atlantic. Earth and Planetary Science Letters, 16(1), pp.103-110.

Lattin, G. L., Moore, C. J., Zellers, A. F., Moore, S. L., Weisberg, S. B. (2004) A comparison of neustonic plastic and zooplankton at different depths near the southern California shore. Marine Pollution Bulletin 49, 291–294.

Law KL, et al. (2014) Distribution of surface plastic debris in the eastern pacific ocean from an 11-year data set. Environ Sci Technol 48(9):4732–4738.

Law, K.L., et al. (2010) Plastic accumulation in the North Atlantic subtropical gyre. Science 329(5996):1185–1188.

Le Quéré, C., Raupach, M.R., Canadell, J.G., Marland, G., Bopp, L., Ciais, P., Conway, T.J., Doney, S.C., Feely, R.A., Foster, P. and Friedlingstein, P., 2009. Trends in the sources and sinks of carbon dioxide. Nature geoscience, 2(12), pp.831-836.

Lebreton, L.C.M., Greer, S.D., Borrero, J.C. (2012) Numerical modelling of floating debris in the world's oceans. Marine Pollution Bulletin 64, 653–661.

Lebreton, L.C.M., Slat, B., Ferrari, F., Sainte-Rose, B., Aitken, J., Marthouse, R., Hajbane, S., Cunsolo, S., Schwarz, A., Levivier, A., Noble, K., Debeljak, P., Maral, H., Schoeneich-Argent, R., Brambini, R., Reisser, J. (2018) Evidence that the Great Pacific Garbage Patch is rapidly accumulating plastic. Nature 8, 4666.

Lee, S.A., Kim, T.H. and Kim, G., 2020. Tracing terrestrial versus marine sources of dissolved organic carbon in a coastal bay using stable carbon isotopes. Biogeosciences, 17(1).

Letcher, R. J.; Morris, A. D.; Dyck, M.; Sverko, E.; Reiner, E. J.; Blair, D. A. D.; Chu, S. G.; Shen, L., Legacy and new halogenated persistent organic pollutants in polar bears from a contamination hotspot in the Arctic, Hudson Bay Canada. Sci. Total Environ. 2018, 610-611, 121-136.

Lindstrom, A. B.; Strynar, M. J.; Libelo, E. L., Polyfluorinated Compounds: Past, Present, and Future. Environ. Sci. Technol. 2011, 45 (19), 7954-7961.

Liu, B. et al. Protein Crystallography and Site-Direct Mutagenesis Analysis of the Poly(ethylene terephthalate) Hydrolase PETase from Ideonella sakaiensis. ChemBioChem 19, 1471–1475 (2018).

Liu, K.K., Kao, S.J., Hu, H.C., Chou, W.C., Hung, G.W. and Tseng, C.M., 2007. Carbon isotopic composition of suspended and sinking particulate organic matter in the northern South China Sea—from production to deposition. Deep Sea Research Part II: Topical Studies in Oceanography, 54(14-15), pp.1504-1527.

Loi, E. I. H.; Yeung, L. W. Y.; Mabury, S. A.; Lam, P. K. S., Detections of Commercial Fluorosurfactants in Hong Kong Marine Environment and Human Blood: A Pilot Study. Environ. Sci. Technol. 2013, 47 (9), 4677-4685.

Lusher, A.L., Welden, N.A., Sobral, P., Cole, M. (2017) Sampling, isolating and identifying microplastics ingested by fish and invertebrates. Analytical Methods 9, 1346-1360.

Macali, A., Semenov, A., Venuti, V., Crupi, V., D'Amico, F., Rossi, B., Corsi, I. and Bergami, E., 2018. Episodic records of jellyfish ingestion of plastic items reveal a novel pathway for trophic transference of marine litter. Scientific reports, 8(1), p.6105.

Mackensen, A. and Schmiedl, G., 2019. Stable carbon isotopes in paleoceanography: atmosphere, oceans, and sediments. Earth-Science Reviews, 197, p.102893.

Martin, J., Lusher, A., Thompson, R. C., & Morley, A. (2017). The deposition and accumulation of microplastics in marine sediments and bottom water from the Irish continental shelf. Scientific Reports, 7(1), 1-9.

Maximenko, M., Hafner, J., Niiler, P. (2012) Pathways of marine debris derived from trajectories of Lagrangian drifters. Marine Pollution Bulletin 65, 51–62.

McNichol, A. P., Quay, P. D., Gagnon, A. R., and Burton, J. R. 2010. Collection and Measurement of Carbon Isotopes in Seawater DIC. IOCCP Report No. 14, ICPO Publication Series No. 134, Version.

Michels, J., Stippkugel, A., Lenz, M., Wirtz, K., Engel, A. (2018) Rapid aggregation of biofilm-covered microplastics with marine biogenic particles. Proceedings of the Royal Society B 285: 20181203

Näkki, P., Setälä, O., Lehtiniemi, M., 2017.Bioturbation transports secondary microplastics to deeper layers in soft marine sediments of the northern Baltic Sea. Mar. Pollut. Bull. 119 (1), 255–261

Nelms, S. E., Galloway, T. S., Godley, B. J., Jarvis, D. S., & Lindeque, P. K. (2018). Investigating microplastic trophic transfer in marine top predators. Environmental pollution, 238, 999-1007.

Net, S., Sempéré, R., Delmont, A., Paluselli, A. and Ouddane, B., 2015. Occurrence, fate, behavior and ecotoxicological state of phthalates in different environmental matrices. Environmental Science & Technology, 49(7), pp.4019-4035.

OECD Hazard Assessment of Perfluooctane Sulfonate (PFOS) and Its Salt; Organization for Economic Co-operation and Development: Pairs, 2002.

Orr, J.C. (2011) Recent and future changes in ocean carbonate chemistry. 26.

Owens, S. A., Buesseler, K. O., & Sims, K. W. W. (2011). Re-evaluating the 238U-salinity relationship in seawater: Implications for the 238U–234Th disequilibrium method. Marine Chemistry, 127(1-4), 31-39.

Pabortsava, K., & Lampitt, R. S. (2020). High concentrations of plastic hidden beneath the surface of the Atlantic Ocean. Nature communications, 11(1), 1-11.

Patwa, A., Thiery, A., Lombard, F., Lilley, M.K.S., Bosset, C., Bramard, J.F., Bottero, J.Y., Barthelemy, P. (2015) Accumulation of nanoparticles in "jellyfish" mucus: a bio-inspired route to decontamination of nano-waste. Scientific Reports 2015. 11387.

Pickard, H. M.; Criscitiello, A. S.; Spencer, C.; Sharp, M. J.; Muir, D. C. G.; De Silva, A. O.; Young, C. J., Continuous non-marine inputs of per- and polyfluoroalkyl substances to the High Arctic: a multi-decadal temporal record. Atmos. Chem. Phys. 2018, 18 (7), 5045-5058.

Pieper, C., Ventura, M. A., Martins, A., & Cunha, R. T. (2015). Beach debris in the Azores (NE Atlantic): Faial Island as a first case study. Marine pollution bulletin, 101(2), 575-582.

Pieper C, Ventura MA, Cunha RT and Martins A (2016). Marine Debris Time and Space Variability in a Remote Island: Faial (Azores, NE Atlantic). Front. Mar. Sci. Conference Abstract: IMMR | International Meeting on Marine Research 2016.doi: 10.3389/conf.FMARS.2016.04.00077

Pike, S. M., Buesseler, K. O., Andrews, J., & Savoye, N. (2005). Quantification of 234 Th recovery in small volume sea water samples by inductively coupled plasma-mass spectrometry. Journal of Radioanalytical and Nuclear Chemistry, 263(2), 355-360.

Pohl, F., Eggenhuisen, J. T., Kane, I. A., & Clare, M. A. (2020). Transport and burial of microplastics in deep-marine sediments by turbidity currents. Environmental science & technology, 54(7), 4180-4189.

Poulain M, Mercier MJ, Brach L, Martignac M, Routaboul C, Perez E, Desjean MC and ter Halle A. Small microplastics as a main contributor to plastic mass balance in the north atlantic subtropical gyre Environ. Sci. Technol. 2019, 53 1157–64 DOI: 10.1021/acs.est.8b05458

Prevedouros, K.; Cousins, I. T.; Buck, R. C.; Korzeniowski, S. H., Sources, Fate and Transport of Perfluorocarboxylates. Environ. Sci. Technol. 2006, 40 (1), 32-44.

Reisser, J., Slat, B., Noble, K., du Plessis, K., Epp, M., Proietti, M., de Sonneville, J., Becker, T., Pattiaratchi, C. (2015) The vertical distribution of buoyant plastics at sea: an observational study in the North Atlantic Gyre. Biogeosciences 12, 1249-1256.

Ritscher, A.; Wang, Z.; Scheringer, M.; Boucher, J. M.; Ahrens, L.; Berger, U.; Bintein, S.; Bopp, S. K.; Borg, D.; Buser, A. M.; Cousins, I.; DeWitt, J.; Fletcher, T.; Green, C.; Herzke, D.; Higgins, C.; Huang, J.; Hung, H.; Knepper, T.; Lau, C. S.; Leinala, E.; Lindstrom, A. B.; Liu, J.; Miller, M.; Ohno, K.; Perkola, N.; Shi, Y.; Haug, L. S.; Trier, X.; Valsecchi, S.; Jagt, K. v. d.; Vierke, L., Zürich Statement on Future Actions on Per- and Polyfluoroalkyl Substances (PFASs). Environ. Health Perspect. 2018, 126 (8), 084502.

Sabine, C.L., Feely, R.A., Gruber, N., Key, R.M., Lee, K., Bullister, J.L., Wanninkhof, R., Wong, C.S.L., Wallace, D.W., Tilbrook, B. and Millero, F.J., 2004. The oceanic sink for anthropogenic CO2. science, 305(5682), pp.367-371.

Schütte, F., Brandt, P., & Karstensen, J. (2016). Occurrence and characteristics of mesoscale eddies in the tropical northeastern Atlantic Ocean. Ocean Science, 12(3), 663-685.

Scikit-image. 2021. Blob detection. Website, retrieved Jan 2021. url: https://scikit-image.org/docs/dev/auto_examples/features_detection/plot_blob.html

Scikit-image. 2021b. Expand segmentation labels without overlap. Website, retrieved Jan 2021. url: https://scikit-

image.org/docs/dev/auto_examples/segmentation/plot_expand_labels.html#sphx-glr-auto-examples-segmentation-plot-expand-labels-py

Scikit-learn. 2021. Spectral clustering. Website, retrieved Jan 2021. url: https://scikit-learn.org/stable/modules/generated/sklearn.cluster.SpectralClustering.html

Scikit-learn. 2021b. Gaussian Processes. Website, retrieved Jan 2021. url: https://scikit-learn.org/stable/modules/gaussian_process.html

Shadwick, E.H., Thomas, H., Chierici, M., Else, B., Fransson, A., Michel, C., Miller, L.A., Mucci, A., Niemi, A., Papakyriakou, T.N. and Tremblay, J.É., 2011. Seasonal variability of the inorganic carbon system in the Amundsen Gulf region of the southeastern Beaufort Sea. Limnology and Oceanography, 56(1), pp.303-322.

Sharp, J.H., Peltzer, E.T., Alperin, M.J., Cauwet, G., Farrington, J.W., Fry, B., Karl, D.M., Martin, J.H., Spitzy, A., Tugrul, S. and Carlson, C.A., 1993. Procedures subgroup report. Marine Chemistry, 41(1-3), pp.37-49.

Snyder, M.A., Sloan, L.C. and Bell, J.L., 2004. Modeled Regional Climate Change In The Hydrologic Regions Of California: A CO2 Sensitivity Study 1. JAWRA Journal of the American Water Resources Association, 40(3), pp.591-601.

Ter Halle, A., Ladirat, L., Martignac, M., Mingotaud, A. F., Boyron, O., & Perez, E. (2017). To what extent are microplastics from the open ocean weathered?. Environmental pollution, 227, 167-174.

Thompson, R. C. (2016). Sources, distribution, and fate of microscopic plastics in marine environments. In Hazardous Chemicals Associated with Plastics in the Marine Environment (pp. 121-133). Springer, Cham.

Torres, M.E., Mix, A.C. and Rugh, W.D., 2005. Precise δ13C analysis of dissolved inorganic carbon in natural waters using automated headspace sampling and continuous-flow mass spectrometry. Limnology and Oceanography: Methods, 3(8), pp.349-360.

UNEP (2009): Marine Litter: A Global Challenge. Nairobi.

Van Cauwenberghe, L., A. Vanreusel, J. Mees, Colin Janssens. Microplastic Pollution in Deep-sea Sediments. Environmental Pollution 182 (2013): 495–499.

Van Cauwenberghe, L., Devriese, L., Galgani, F., Robbens, J., Janssen, C.R. (2015) Microplastics in sediments: A review of techniques, occurrence and effects. Marine Environmental Research 11, 5-17.

Van Sebille, Wilcox, Lebreton, Maximenko, Hardesty, Van Franeker, Eriksen, Siegel, Galgani, and Law (2015), A Global Inventory of Small Floating Plastic Debris Environmental Research Letters, 10.

Wang, Z.; Cousins, I. T.; Scheringer, M.; Buck, R. C.; Hungerbühler, K., Global emission inventories for C4–C14 perfluoroalkyl carboxylic acid (PFCA) homologues from 1951 to 2030, Part I: production and emissions from quantifiable sources. Environ. Int. 2014, 70, 62-75.

Wang, Z.; Xie, Z.; Mi, W.; Möller, A.; Wolschke, H.; Ebinghaus, R., Neutral Poly/Per-Fluoroalkyl Substances in Air from the Atlantic to the Southern Ocean and in Antarctic Snow. Environ. Sci. Technol. 2015, 49 (13), 7770-7775.

Willeit, M., Ganopolski, A., Calov, R. and Brovkin, V. (2019) Mid-Pleistocene transition in glacial cycles explained by declining CO2 and regolith removal. Science Advances 5, eaav7337.
www.esrl.noaa.gov/gmd/ccgg/trends/mlo.html

Xie, Z.; Wang, Z.; Mi, W.; Möller, A.; Wolschke, H.; Ebinghaus, R., Neutral Poly-/perfluoroalkyl Substances in Air and Snow from the Arctic. Sci. Rep. 2015, 5, 8912.

Yamashita, N.; Kannan, K.; Taniyasu, S.; Horii, Y.; Petrick, G.; Gamo, T., A global survey of perfluorinated acids in oceans. Marine Pollution Bulletin 2005, 51 (8), 658-668.

Yeung, L. W. Y.; Dassuncao, C.; Mabury, S.; Sunderland, E. M.; Zhang, X.; Lohmann, R., Vertical Profiles, Sources, and Transport of PFASs in the Arctic Ocean. Environ. Sci. Technol. 2017, 51 (12), 6735-6744.

Yoshida, S. et al. A bacterium that degrades and assimilates poly(ethylene terephthalate). Science (80-.). 351, 1196–1199 (2016).

Zareitalabad, P.; Siemens, J.; Hamer, M.; Amelung, W., Perfluorooctanoic acid (PFOA) and perfluorooctanesulfonic acid (PFOS) in surface waters, sediments, soils and wastewater – A review on concentrations and distribution coefficients. Chemosphere 2013, 91 (6), 725-732.

Zhao, Z.; Xie, Z.; Möller, A.; Sturm, R.; Tang, J.; Zhang, G.; Ebinghaus, R., Distribution and long-range transport of polyfluoroalkyl substances in the Arctic, Atlantic Ocean and Antarctic coast. Environ. Pollut. 2012, 170, 71-77.

10 Abbreviations

AWI	Alfred-Wegener Institute for Marine and Polar Research
BC	box corer
BMBF	Bundesministerium für Bildung und Forschung
CFC	Continuous Flow Centrifugation
CF-IRMS	Continuous Flow Isotope Ratio Mass Spectrometer
CLASI-FISH	combinatorial labelling and spectral imaging – fluorescence *in situ* hybridization
CO_2	Carbon dioxide
CRM	certified reference material
DFG	Deutsche Forschungsgemeinschaft
DIC	dissolved inorganic carbon
EEZ	Exclusive Economic Zone
FTIR	Fourier Transform Infrared Spectroscopy
GEOMAR	GEOMAR Helmholtz Zentrum für Ozeanforschung Kiel
GFF	glass fibre filter
GIMPF	Geesthacht Inert Microplastic Fractionator
HDPE	high-density polyethylene
HEPA	high efficiency particle absorbing filter
HOTMIC	HOrizontal and vertical oceanic distribution, Transport, and impact of MICroplastics
HZG	Helmholtz-Zentrum Geesthacht – Zentrum für Material- und Küstenforschung
IC	ion chromatography
ICP-AES	atomic emission spectroscopy with inductively coupled plasma
IMET - FZJ	Molekulare Enzymtechnologie (IMET), Heinrich Heine Universität Düsseldorf, Forschungszentrum Juelich GmbH (FZJ)
IWC - TUM	Institute of Hydrochemistry (IWC), Technical University of Munich (TUM)
KDMT	Kiel Data Management Team
LDIR	Laser Direct Infrared
LDPE	low-density polyethylene
MARE	Marine and Environmental Sciences Centre (MARE), Agência Regional para o Desenvolvimento da Investigação Tecnologia e Inovação (ARDITI)
MP	Microplastic
MPP	Microplastic particles
MT	mega tons, 10^6 tons
MUC	multiple corer
NIOZ	Royal Netherlands Institute for Sea Research
NIR	hyperspectral near-infrared
NOCS	National Oceanography Centre Southampton
OFOS	Ocean Floor Observation System
OSIS-Kiel	Ocean Science Information System
PA66	Polyamide, acrylic
PAE	Phthalic acid esters
PC	polycarbonate
PE	polyethylene
PES	Polyethersulfone
PET	Polyethylene terephthalate
PFASs	Per- and polyfluoroalkyl substances
PLASTISEA	Harvesting the marine Plastisphere for novel cleaning concepts
PML	polar mixed layer
PMMA	polymethyl methacrylate
POC	particulate organic carbon

PP	polypropylene
PS	polystyrene
PTFE	Polytetrafluoroethylene
PU	polyurethane
SAPS	In situ Stand-Alone Pumps
SIM	Selected Ion Monitoring
TA	total alkalinity
TLZ	Technik- und Logistik Zentrum
TOM	total organic matter
UGent	Ghent University
Utrecht	Utrecht University
VINDTA 3C	Versatile INstrument for the Determination of Total inorganic carbon and titration Alkalinity

11 Appendices

11.1 Cruise participants on SO279

Birds-eye science party photo on the bow of RV SONNE, in front of the bridge. (Photo: S. Meinecke)

11.2 Selected Pictures of Shipboard Operations

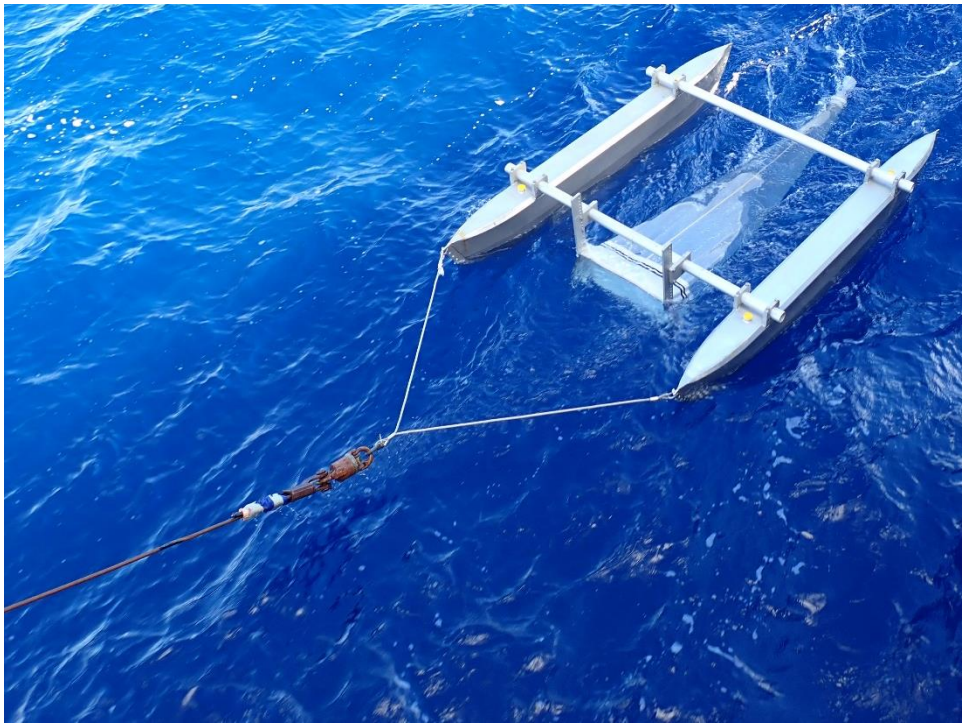

Figure A2-1. Catamaran neuston trawl deployment. (Photo: S. Gueroun)

Figure A2-2. Neuston net sample composition after 20 min towing. (Photo: E. Borchert)

Figure A2-3. Large *Sargassum* sp. patch. (Photo: T.A. Hamm)

Figure A2-4. Small plastic particles retrieved from different catamaran (neuston) trawls, mounted for polymer analysis by near-infrared hyperspectral imaging (section 5.1.3). (Photo: S. Gueroun)

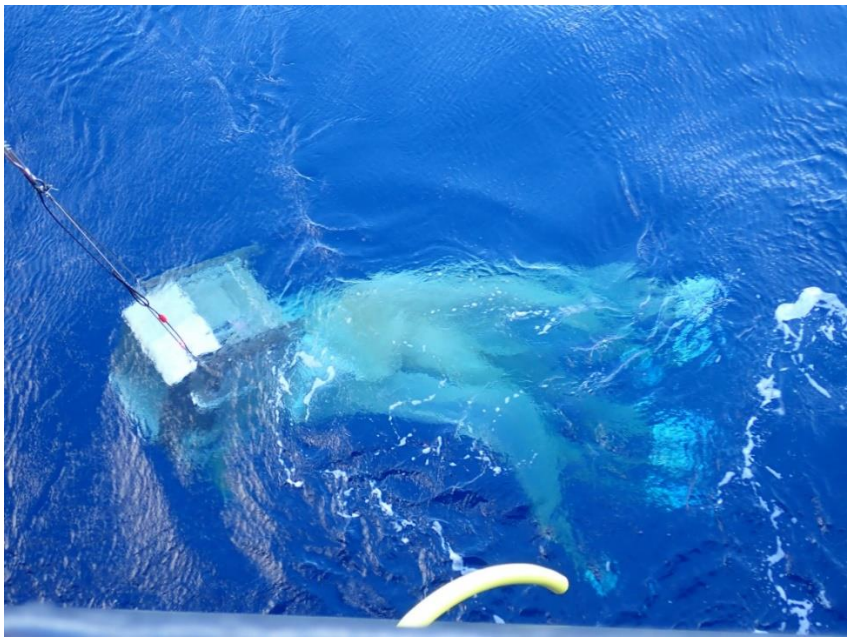

Figure A2-5. Deployment of the Multi Net at 2 knots (Photo: S. Gueron)

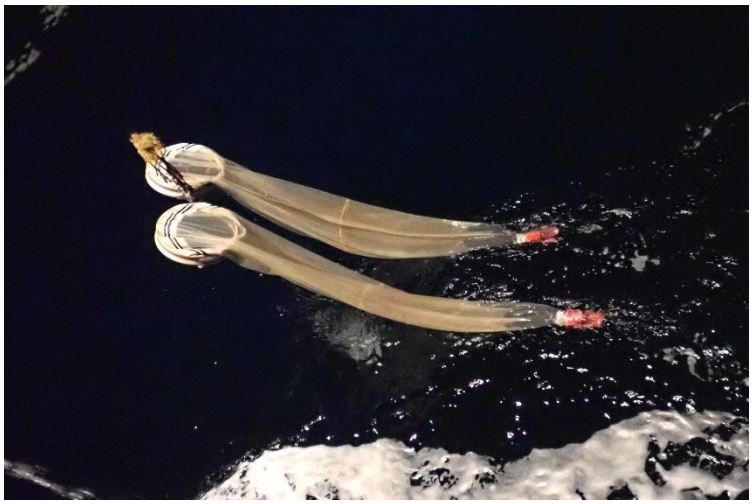

Figure A2-6. Retrieving the Bongo net after successful deployment (Photo: S. Gueron)

Figure A2-7. Sieving a Bongo net sample over 125 µm metal sieve (Photo: S. Gueron)

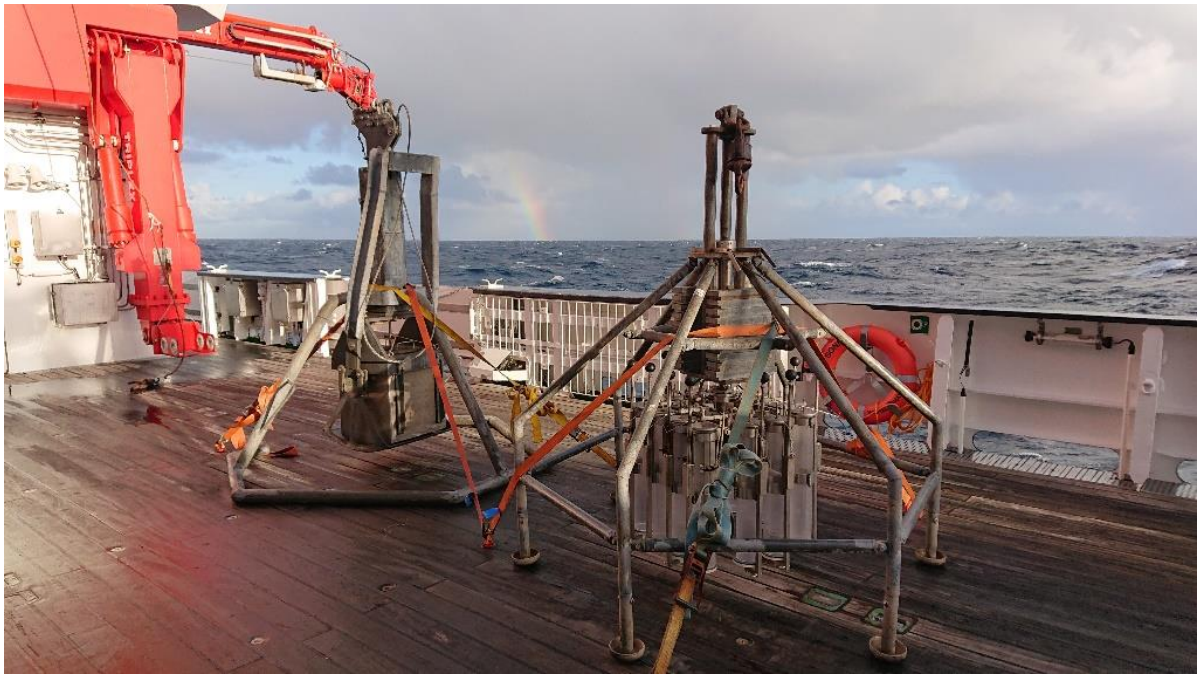

Figure A2-8. Box corer (left) and multiple corer (right) on deck of RV Sonne.

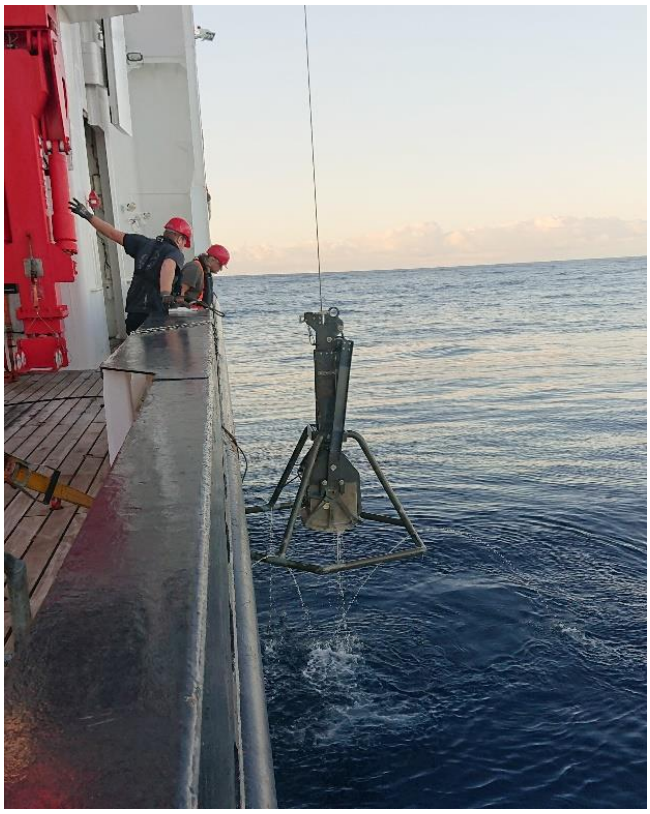

Figure A2-9. Box corer returning from the ocean floor.

Figure A2-10. Laboratory set-up to sample MP via CFC.

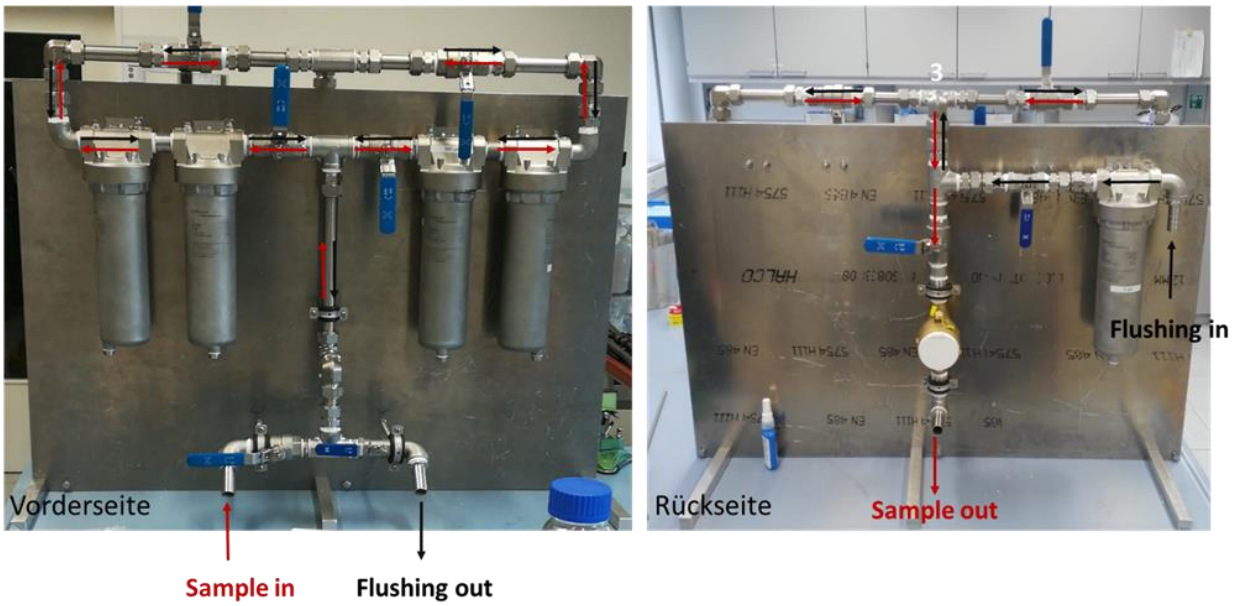

Figure A2-11. Front and back views of the GIMPF